[UNIVERSITÀ DEGLI STUDI DI PADOVA

DEPARTMENT OF CARDIAC, THORACIC, VASCULAR SCIENCES AND PUBLIC HEALTH
Director: Prof. FEDERICO REA

PhD COURSE IN: Translational Specialistic Medicine "G.B. Morgagni"
Coordinator: Prof.ssa Annalisa Angelini

CURRICULUM: Thoracic and Pulmonary Sciences
SERIES XXXVI

Clinical, molecular, and radiological features in the pathogenesis and progression of interstitial lung diseases (ILDs).

Supervisor:

Prof. Paolo Spagnolo

Ph.D. Student:

Dott.ssa Nicol Bernardinello

Co-tutor:

Prof.ssa Fiorella Calabrese

Anno accademico: 2021-2022

INDEX

ABSTRACT

Interstitial lung diseases (ILDs) represent a broad and heterogeneous group of respiratory disorders characterized by various degrees of inflammation and fibrosis. More than 200 entities have been described; some are rare and "orphans." Moreover, the prevalence, incidence, and mortality rates are still unknown for specific entities. Some patients may remain stable or improve over time. Conversely, about one-third of all ILDs may display progressive scarring of the lung parenchyma, thus becoming debilitating, showing poor response to conventional treatment, and leading to early mortality (these forms are called progressive ILD [PF-ILD]). An update of the guideline document on ''Idiopathic Pulmonary Fibrosis and Progressive Pulmonary Fibrosis in Adults" was published in May 2022. This guideline provides clinicians with evidence-based recommendations on diagnosing and managing IPF and PF-ILD. The new guideline highlights the importance of identifying factors that may predict the evolution toward a "progressive" phenotype. So far, several potential predictive biomarkers for PF-ILD have been studied. Nintedanib, an intracellular tyrosine kinase inhibitor (TKI) with antifibrotic properties, was one of the first drugs approved for the treatment of idiopathic pulmonary fibrosis (IPF) and more recently has also been approved for use in PF-ILD and in ILD secondary to systemic scleroderma (SSc). The availability of efficacious therapy has exponentially increased the interest of the respiratory community in these forms of ILD. It has made more urgent the need for reliable predictors of disease outcomes.

My Ph.D. project focused on three lines of research: firstly, I investigated the role of monocytes in predicting disease course in patients with fibrotic ILD. I have shown that serum levels of monocytes may identify a subset of patients more likely to progress. As part of this project, I also focused on the histology of fibrotic ILD and suggested a possible predictive role of micro honeycombing in predicting patient survival. Secondly, I looked at the role of the diaphragm and spinal muscle mass in disease progression and survival in ILD. I found that the prevalence of loss of muscle mass was around 40% at diagnosis in patients with IPF and about 30% in those with ILD secondary to connective tissue disease. The last part of my project focused on basic science. I focused on the role of Hyaluronic Acid (HA) in reducing the production of galectin-3 (Gal-3), transforming growth factor (TGFb), and collagen (Col-I) in a cellular in vitro model of pulmonary fibrosis. HA, a component of the extracellular matrix with water-retaining properties, acts as a regulator of fluid balance in the lung and has been widely used to treat eye, joint, and skin disorders. We have shown that HA might prevent and treat lung fibrosis by reducing Gal-3 production by stimulated fibroblasts.

Finally, I performed one study, with others still ongoing, on Covid-19 pneumonia. Specifically, I looked at serum eosinophil levels as a marker of pulmonary sequelae following SARS CoV2 infection. Notably, we found persistent lung abnormalities in

only a small minority of patients with COVID-19 pneumonia at the 6- and 12-month follow-up. These patients are more frequently older males and active smokers at the time of hospitalization. The role of eosinophils as predictors of persistent disease following COVID-19 pneumonia needs to be further investigated.

RIASSUNTO

Le malattie polmonari interstiziali (ILD) sono un gruppo eterogeneo di patologie del parenchima polmonare. Sono state descritte più di 200 entità diverse e molte di esse vengono ancora considerate malattie rare o "orfane". Per alcune, la prevalenza, l'incidenza e i tassi di mortalità rimangono ancora sconosciuti. In circa un 35% di queste patologie, si può evidenziare una progressiva cicatrizzazione del tessuto polmonare (ILD progressiva, PF-ILD). Questo fenotipo di malattia può risultare estremamente debilitanti e provocare la morte del malato in poco tempo. Le ultime linee guida aggiornate sulla "Fibrosi polmonare idiopatica e fibrosi polmonare progressiva negli adulti" sono state pubblicata nel febbraio 2022. Nel complesso, questo documento ha lo scopo di guidare i medici di tutto il mondo con raccomandazioni basate sull'evidenza per la diagnosi e la gestione dell'IPF e PF-ILD. L'uscita di queste nuove linee guida hanno aumentato la mia curiosità riguardo al potenziale dei diversi biomarcatori esistenti che potrebbero predire l'evoluzione verso un "fenotipo" progressivo. Ad oggi sono stati studiati diversi potenziali biomarcatori predittivi della malattia polmonare interstiziale progressiva fibrosante (PF-ILD).
D'altra parte, c'è sempre più interesse da parte della comunità scientifica per queste forme, in quanto recentemente, la terapia antifibrotica (nintedanib) è stato approvata , oltre che per l'IPF e la sclerodermia, anche per l'uso in altre ILD fibrosanti croniche con fenotipo progressivo. Grazie a questa nuova possibilità, l'interesse generale per queste forme è in aumento. Inoltre, nuovi biomarcatori in grado di prevedere la progressione nel corso della malattia sono necessari. Il mio progetto di dottorato si è concentrato su tre linee principali di ricerca: in primo luogo, ho cercato di studiare il ruolo dei monociti nel predire il decorso della malattia nei pazienti sia con ILD che con IPF. Con questo studio ho dimostrato che il livello di monociti sugli esami del sangue nei pazienti con ILD può aiutare a identificare il fenotipo di interstiziopatia più aggressivo, nella fase precoce della malattia. Una parte del mio progetto si è concentrata anche sulle caratteristiche istologiche delle ILD, mostrando un possibile valore predittivo del micro honeycombing.
In secondo luogo, cercando di guardare oltre il parenchima polmonare, ho valutato il ruolo del diaframma e dei muscoli spinali nella progressione della malattia e nella sopravvivenza. La prevalenza della perdita di massa muscolare nei muscoli spinali al momento della diagnosi nei pazienti con IPF era del 42%, e la disfunzione del diaframma nei pazienti con IPF e CTD-ILD è vicina al 30%. Questo dato sembra suggerire che i pazienti con interstiziopatia possano beneficiare già al momento della diagnosi di una riabilitazione muscolare e respiratoria. L'ultima parte del mio progetto si è incentrata sul ruolo dell'acido ialuronico (HA) nel ridurre la produzione di galectina-3, TGFb e Col-I in un modello cellulare in vitro.
L'acido ialuronico (HA) potrebbe avere un ruolo nella prevenzione e nel trattamento delle malattie polmonari fibrotiche, riducendo la produzione di Gal-3 da parte dei fibroblasti stimolati. Come parte collaterale, a causa della pandemia di COVID-19, il

mio dottorato di ricerca si è arricchito anche di diversi progetti riguardanti l'infezione da SARS-CoV2. Ho cercato di valutare se gli eosinofili potrebbero avere un ruolo nelle sequele polmonari e potrebbero essere implicati nell'ultima parte della risposta infiammatoria. Inoltre, abbiamo evidenziato che solo in una minoranza di pazienti con polmonite COVID-19 persisteva in anomalie polmonari al 6 mese di follow-up e solo il 7% al follow-up a 12 mesi.
Valutandone le varie caratteristiche demografiche, questi pazienti erano più frequentemente maschi anziani e fumatori attivi al momento del ricovero.

INTRODUCTION

Interstitial lung diseases (ILDs) refer to a broad group of acute and chronic disorders characterized by a similar clinical presentation [1][2]. "Interstitial" is closely connected to the pathological process in the interstitial space. However, these disorders could also be connected with a distortion of alveolar architecture and irreversible airway alterations [3-7]. More than 200 different etiologists are now recognized in the ILD group [6-7]. The incidence of ILD has been reported in the literature between 1 and 31.5 per 100,000 person-years, with a prevalence between 6.3 and 71 per 100,000 people. The disease burden appears heterogeneous among countries, probably due to the various diagnostic approaches. In Europe, idiopathic pulmonary fibrosis (IPF) and sarcoidosis are the most prevalent ILDs [6]. The clear definition of these diseases can be helpful in the management and clinical decisions [8]. However, ILD identification and categorizing still need to be improved for clinicians [9]. The pathogenesis of ILD is variable and, at some points, still unknown. However, both inflammation and fibrosis play a fundamental role in developing ILD.

Classification of Interstitial Lung Diseases

Diffuse parenchymal lung diseases are usually divided into known causes and unknown causes. In this figure, I reported the most recent schematic classification of ILD adapted from Cottin V. et al. [6].

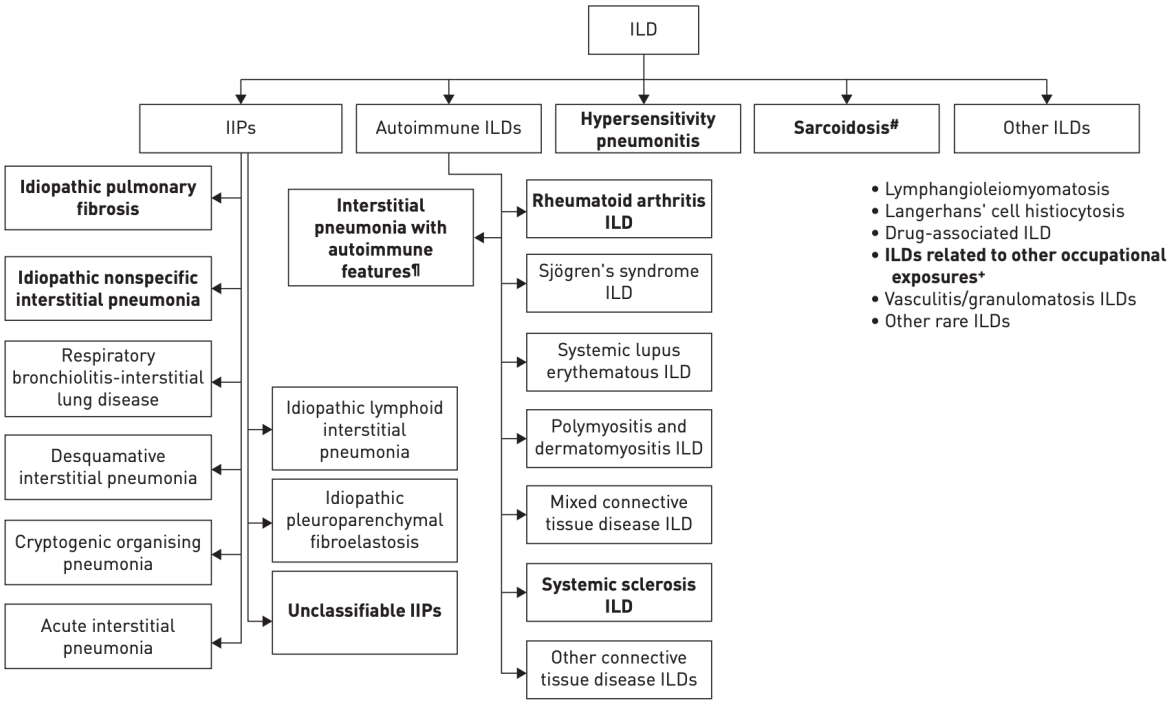

Figure 1: ILD classification adapted from Cottin et al.

ILD of known cause

Occupational exposures are the most frequent cause of ILD of known origin. [3] Asbestosis, silicosis, berylliosis, and other interstitial disease secondary to organic and inorganic dust are part of this category. Moreover, other frequent causes of ILD of known agents are drugs, such as methotrexate, amiodarone, nonsteroidal anti-inflammatory drugs (NSAIDs), biological agents, growth factors (e.g., colony-stimulating factors and interferons) and many different types of proteins (e.g., plasma fraction, intra-venous immunoglobulins and anti-thymocyte globulin). Moreover, cannabinoids and other illegal substances can provoke acute lung damage and interstitial lung disease if not recognized and treated [10]. In oncological patients, chemo and radiotherapy can also induce interstitial lung disease [11]. Finally, a very large and huge sub-category is represented by those related to an underlying systemic illness: not rarely does a pulmonary involvement complicate the course of connective tissue diseases (e.g., polymyositis, dermatomyositis, rheumatoid arthritis, systemic lupus erythematosus, scleroderma, and mixed connective tissue disease) [3].

ILD of unknown cause

The idiopathic interstitial pneumonia (IIPs) group comprises different entities, for some aspects very different from each other. In order of frequency, in the group of ILD of unknown cause, the most common is idiopathic pulmonary fibrosis (IPF). Nonspecific interstitial pneumonia (NSIP), cryptogenic organizing pneumonia (COP), and acute interstitial pneumonia (AIP) are also included [12]. Other rare interstitial pneumonia without a specific etiology are pleural parenchymal fibroelastosis (PPFE) and some cases of lymphoid interstitial pneumonia (LIP) [13]. In the IIPs group, desquamative interstitial pneumonia (DIP) and respiratory bronchiolitis associated with interstitial lung disease (RB-ILD) are considered together in the term smoking-related idiopathic interstitial pneumonia (SR-IIP) [13]. In 2015, the term interstitial pneumonia with autoimmune features (IPAF) was also coined to identify individuals with IIP and features suggestive of, but not definitive for, a connective tissue disease (CTD) [8]. However, in a good percentage of cases, ILDs remain unclassifiable [12].

Other ILDs

Other ILDs are separate because they cannot enter in previous categories. For example, Langerhans cell histiocytosis (LCH) and lymphangioleiomyomatosis (LAM) are rare diseases characterized by cystic patterns on CT scans. LCH is due to cigarette smoking, whereas LAM is exclusive to women. Sarcoidosis is a separate group in the granulomatous lung disorder [1]. Another granulomatous interstitial lung disease is hypersensitivity pneumonitis (HP) [14], which can develop after exposure to a large variety of inhaled antigens found in the environment, which can determine an immune-mediated response [15].

Clinical overview

Dyspnoea on effort and dry cough are the first symptoms that bring patients to clinical evaluation. However, these symptoms can be different according to the specific disease; for example, chest pain is more frequent in some types of sarcoidosis, and fever in case of the acute form of hypersensitivity pneumonitis. The global complexity of clinical diagnosis and management of ILDs justifies the role of multidisciplinary team discussion (MDD), which is globally considered the gold standard [16-17]. The lack of robust diagnostic criteria and the strict ability to differentiate specific ILD entities delay diagnosis and postpone specific prescriptions [18]. The diagnostic process for patients with ILD is often characterized by important delays, exposure to invasive diagnostic exams, and frequent misdiagnosis [19]. A deep and meticulous anamnesis is essential: the investigation of previous or current occupational risk factors, cigarette exposures, radiotherapy, and the list of current and past medications must be investigated, and the evaluation if there is a history of inhalations of pneumotoxic substances and dust is equally essential.

The clinical presentation of ILD can overlap with more common respiratory conditions (such as asthma or COPD)[20]. Moreover, emerging symptoms (like cough and shortness of breath) could be generally attributed to the patients' aging or smoking habits. Another critical issue is the lack of knowledge of ILD among primary care physicians and non-ILD experts. The results of the INTENSITY survey, conducted in 2018 that enrolled 600 patients with ILD show that 55% reported ≥ 1 misdiagnosis and 38% reported ≥ 2 misdiagnoses before the correct diagnosis, and the most common misdiagnoses were asthma (13.5%), pneumonia (13.0%), and bronchitis (12.3%) [18]. The median time from the onset of the symptoms to achieving the correct diagnosis was seven months (range, 0-252 months).

Dyspnea is the sensation of breathing discomfort, one of the most common and distressing symptoms experienced by patients with respiratory disease[21]. The mMRC (Modified Medical Research Council) Dyspnea Scale is used to assess the degree of functional disability due to dyspnea, and it is recommended by guidelines and used as an inclusion criterion or endpoint for clinical trials [22]. Cough is the symptom responsible for almost one in ten primary care consultations [23]. Many patients with interstitial lung disease have a dry and persistent cough, and evidence suggests this symptom may be due to an increased cough reflex sensitivity. Still, cough could also result from more common disorders, such as gastroesophageal reflux disease or asthma, which need to be investigated [24]. Fatigue in interstitial lung disease (ILD) is a common and debilitating symptom that dramatically impacts the quality of life, social relations, and work [25]. It is also essential to recognize extrapulmonary symptoms such as low-grade fever and arthralgia, which may be related to sarcoidosis, hematuria, eye dryness, and weight loss, which may be related to rheumatological diseases.

Suppose the suspicion of ILD arises after the physical examination. In that case, it is essential to direct the patient to the most appropriate diagnostic path to assess the severity of the disease and provide clues to the underlying cause [26].

Medical history

Demographic characteristics can help physicians in the correct identification of the disease. For example, some ILDs are more common in females rather than males. The same is true for age because certain age groups are more at risk of developing certain diseases [27]. The mean age of IPF, which affects males more than females, is around 65–70 years, and the incidence is constantly increasing. In contrast, the majority of patients with sarcoidosis, connective tissue disease-associated ILD, lymphangioleiomyomatosis (LAM), and inherited forms of ILD (e.g., familial IPF) are between the ages of 20 and 40 and seem more frequent in a woman. Two examples regarding the different gender prevalence are LAM, which primarily affects women, and exposure-related ILDs, which are more common among men. Many occupational and environmental exposures are associated with an increased risk of ILD; however, the risk is higher among individuals with a family history of the disease [28]. Data regarding smoking history and quantifying smoking exposure is important. For example, in terms of pack/years or cigarettes/die, a history of tobacco use can be related to interstitial and air space inflammation and fibrosis [29].

Furthermore, a family history of almost any type of ILD is essential because there is a genetic basis for the development of pulmonary fibrosis, and this explains the importance of supervising families with two or more members with pulmonary fibrosis [30]. In connective tissue disease, patients should be evaluated for ILD at the time of the diagnosis and then periodically because it is known that some of them may develop lung involvement. However, precise data on method and time interval are scarce [31].

Laboratory studies and functional test

Laboratory analyses are used frequently during workup diagnosis because they may be helpful but rarely specific in defining it. The laboratory evaluation of suspected ILD includes both simple tests and, in selected cases, more specific ones [32]: complete blood count with leukocyte formula; serum protein electrophoresis; hepatic and renal function; markers of inflammation; precipitating antibodies; ACE; ANCA, ANA, ENA, RF, and other rheumatological titles, urine analysis.

Laboratory studies can be constructive for an underlying CTD-associated ILD or in the suspect of hypersensitive pneumonitis. Pulmonary function tests are a proper investigation in managing patients with previously diagnosed or suspected respiratory disease; they are helpful in diagnosis, assessing response to treatment, and monitoring disease progression. In functional tests, most ILDs present a restrictive pattern, with moderate-severe reduction of DLCO. However, in certain ILDs, such as smoking-related ILD or sarcoidosis, a mixed pattern or only an obstructive one could be present.

Progressor and non-progressor patients

In the last six years, clinicians have highlighted the existence of a percentage of patients with ILD, presenting a clinical progressive behavior similar to IPF despite reasonable adherence to specific treatments (including corticosteroids and/or immunosuppressive

therapy). This new phenotype, called progressive-fibrosing ILD (PF-ILD), includes a subgroup of patients with ILD who show a rapid course of the underlying diagnosis [7]. Besides the IPF, which is the perfect example of progressive phenotype, this pathological behavior can also be found in many types of ILD patients, such as hypersensitivity pneumonitis (HP), idiopathic nonspecific interstitial pneumonia (NSIP), ILD associated with connective tissue diseases (CTD-ILD such as myositis associated ILD, systemic sclerosis-associated ILD, and rheumatoid arthritis associated ILD), and unclassifiable ILD (u-ILD). On the other hand, organizing pneumonia (OP) and lymphoid interstitial pneumonia (LIP) seem to have a limited number of patients with a progressive phenotype [33-34]. Multiple injuries, including inflammation, organic and inorganic dust exposure, and autoimmunity, can trigger lung fibrosis [35]. These triggers induce vascular and epithelial damage that stimulates the inflammatory response and, consequently, the activation of fibroblasts of the lung and the recruitment of those circulating in the blood. Thus, after the stimulation of many pro-fibrotic factors, fibroblasts differentiate into myofibroblasts, leading to excessive extracellular matrix deposition and the subsequent fibrotic remodeling of the interstitium. The inflammatory response stimulates the production of further fibrosis mediators by lymphocytes and macrophages, generating an abnormal proliferative stimulus for fibroblasts; overall, this mechanism degenerates into progressive and uncontrolled lung fibrosis. Pro-fibrotic factors involved in the disease pathogenesis and progression include tumor necrosis factor-alpha (TNF-α), galectin-3 (Gal-3), transforming growth factor beta (TGF-β), platelet-derived growth factor (PDGF), and matrix metalloproteinases (MMPs). It is necessary to underline that regardless of the initial cause, the aging processes and the genetic predisposition affect the fibrogenic response in the lung.

To define PF-ILD, it is necessary to satisfy at least two of the following three criteria occurring within the last year with no alternative explanation [36]:

1) Worsening of respiratory symptoms;

2) Physiological evidence of disease progression (either of the following):
    - Absolute decline in FVC ≥ 5% predicted within one year of follow-up;
    - The total decline of DLCO (corrected for Hb) ≥ 10% in one year of follow-up;

3) Radiological evidence of disease progression (one or more of the following):
    - Increased extent or severity of traction bronchiectasis and bronchiolectasis;
    - New ground-glass opacity with traction bronchiectasis;
    - New fine reticulation;
    - The increased extent or increased coarseness of reticular abnormality;

- New or expanded honeycombing;
- Increased lobar volume loss.

Patients who require lung transplantation or die from ILD's evolution are also considered progressive [36]. In Figure 2, a typical case of progressive interstitial lung disease is shown. Regarding pulmonary function, a decline in the diffusion capacity for carbon monoxide (DLCO) has been proposed as a progression criterion of ILD. Still, it has a controversial role since this parameter is also reduced in the case of pulmonary hypertension and emphysema. DLCO may be considered a sign of progression when associated with FVC decline or worsening of fibrosis at HRCT [37]. The progression of fibrosis can also be suggested by a decrease in the 6-minute walk distance (6MWD). Many factors have been investigated and seem to be connected with an increased risk of progression, including UIP pattern, older age, gastroesophageal reflux, extensive traction bronchiectasis on HRCT, and short telomere syndrome. Patients with IPF and PF-ILD have comparable outcomes: progressive decline in lung function, symptoms' worsening, end-stage fibrosis, and early mortality.
Idiopathic pulmonary fibrosis (IPF) is a classic example of unstoppable disease progression and worse prognosis. Still, progressive fibrosing phenotype has been recently extended to various underlying ILD diagnoses. This development about PF-ILD other than IPF opens the discussion on the importance of an appropriate diagnostic process according to the international guidelines and the need for an accurate definition of disease progression to have the possibility of undertaking antifibrotic therapy, as a second-line treatment in progressor patients [38-39]. In some progressive ILDs, the monocyte count has been reported as an emerging biomarker [40]. Still, it is necessary to consider that it may be affected by ongoing infections or medications. Focusing on systemic sclerosis (SSc) [41], it has been found that the white blood cells and the monocyte and neutrophil counts are higher in patients with lung involvement (ILD) than in patients without it, and also that the monocyte count is higher in patients with progressive lung fibrosis than nonprogressors.

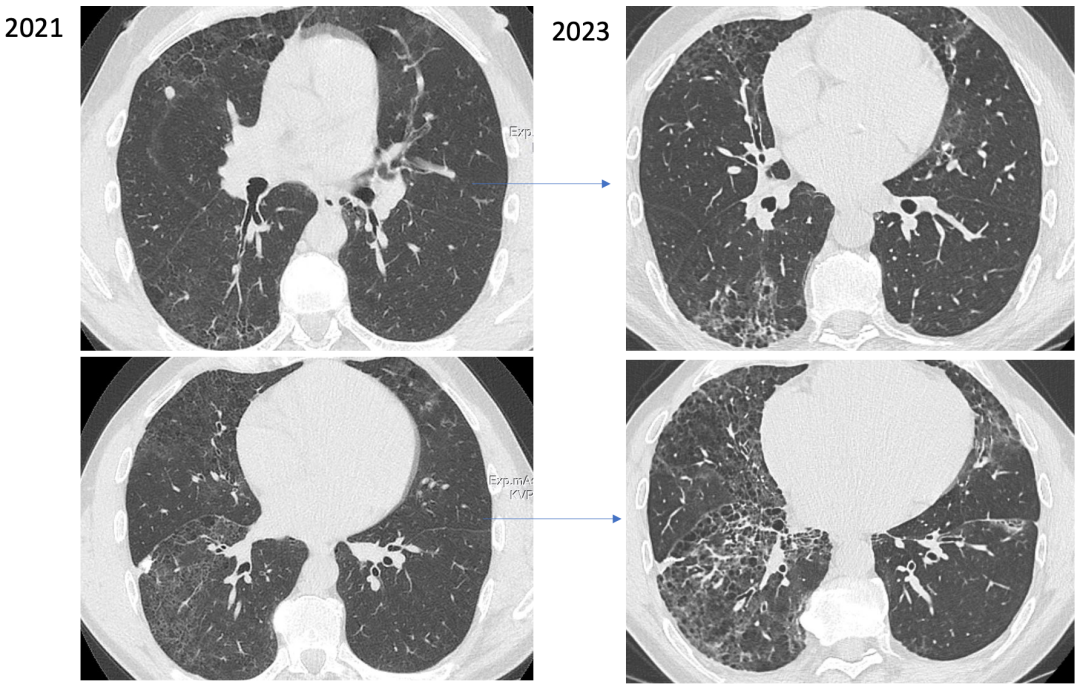

Figure 2: a progressive interstitial lung disease due to amiodarone exposure.

Idiopathic pulmonary fibrosis

Idiopathic pulmonary fibrosis (IPF) is the most common form of idiopathic interstitial pneumonia [42]. IPF Is progressive by definition, and without treatment, the mean survival is around 3-5 years after diagnosis. In a correct clinical context, the diagnosis of IPF requires specific combinations of the radiologic and histopathologic pattern of probable/definite Usual Interstitial Pneumonia (UIP) [43]. IPF is more frequent in male patients and with an age of 60-65 years. The incidence of IPF appears to be higher in North America and Europe (3 to 9 cases per 100,000 person-years) than in South America and East Asia (fewer than 4 cases per 100,000 person-years) [44]. Many risk factors are recognized, such as cigarette smoking, environmental exposures (dust, metals) [45], microbial agents (EBV, CMV, HH-7, etc.) [46], and gastrointestinal reflux [47]. Moreover, some genetic features are correlated with a higher risk of IPF. Familial forms of IPF (when more than two subjects are affected in the same family) are present in 20% of cases. So, it's believed that genetics and environmental exposures contribute to disease pathogenesis and progression. A single nucleotide polymorphism (SNP) (rs35705950) located in the promoter region of MUC5B on chromosome 11p15.5 was strongly associated both with sporadic IPF and familial form of IPF [48].

AIM OF THE THESIS

Interstitial lung diseases are a heterogeneous group of diseases. Among these, idiopathic pulmonary fibrosis (IPF) and sarcoidosis are the most frequent in Europe. However, IPF represents the most frequent form of unknown etiology. IPF is a chronic disease characterized by a progressive and uncontrolled accumulation of extracellular matrix in the pulmonary interstitium, which causes an irreversible subversion of the organ's architecture. The prognosis is generally poor, with a 5-year survival of approximately 20%. However, its course is, in some ways, unpredictable. In some patients, the deterioration is rapid and associated with higher mortality. Several possible phenotypes have so far been studied in a predominantly retrospective manner, and at present, it is not possible to predict the clinical course of each individual.

Furthermore, among all interstitial lung diseases, both in the forms with a known cause and those with an unknown cause, there is a percentage that is not yet well defined, which presents the same clinical trend as IPF, i.e. progressive (progressive fibrotic-ILD). Although this progression's causes are unknown, exposure to gastric microaspirations, organic and inorganic dust, and a UIP pattern are risk factors. Although significant progress has been made in understanding these diseases in recent years, the natural history and clinical course still need to be discovered. A better definition of the pathogenetic mechanisms is of fundamental importance at this time when, after several years of therapeutic failures, only two drugs are available capable of slowing down the progression of IPF (nintedanib and pirfenidone), while only one has been approved for other progressive interstitial diseases (nintedanib).

With this background, the aim of my project during the three-year Ph.D. course was to investigate which variables may be used to predict the clinical course of patients with ILD. Specifically, I developed three main research topics:

I focused on three main topics:

1. To investigate the role of monocyte count at baseline in predicting the clinical course of ILD and IPF patients

2. To investigate the prevalence of muscle mass to predict progression and survival in patients with IPF and the prevalence of diaphragm dysfunction in patients with IPF and CTD-ILD

3. To quantify and describe the role of Hyaluronic Acid (HA) in reducing the production of galectin-3, TGFb, and Col-I in a cellular vitro model.

I was also involved, with my research group, in the analysis of MUC5B Polymorphism and the correlation with radiological assessment in Idiopathic Pulmonary Fibrosis (IPF)

Finally, in the meantime of the pandemic burden, my research activities on Coronavirus disease 2019 (COVID-19) wanted:

- to analyze the relationship between eosinophil count and radiological severity score of patients hospitalized for COVID-19 and the level of medical care;
- to investigate the predictor of pulmonary sequelae after COVID-19 pneumonia (at 6 and 12 months follow-up).

METHODS AND RESULTS

Study 1) ***The clinical relevance of lymphocyte to monocyte ratio in patients with Idiopathic Pulmonary Fibrosis (IPF).***
Bernardinello N*, ...et al. Respiratory Medicine (2022).*

This study aimed to investigate the role of complete blood count, LMR, and NLR in patients with IPF at diagnosis and after one year of antifibrotic therapy (i.e., pirfenidone or nintedanib). Moreover, we explored the prognostic significance of blood count, LMR, and NLR in different patient subsets, namely patients with end-stage disease and patients with lung cancer.

Study population

This retrospective cohort study included three distinct groups of patients: 77 consecutive newly diagnosed patients with IPF, 40 patients with end-stage IPF, and 17 patients with IPF and concomitant lung cancer. Demographics and clinical and lung function data were collected between December 2014 and December 2020. Only newly diagnosed patients with IPF with two blood tests available at diagnosis and at least one year follow-up following antifibrotic therapy were included for the study. Newly diagnosed IPF patients (n = 77) were then divided based on their annual rate of decline in absolute FVC% pred. after the first year of antifibrotic therapy in progressors (FVC decline ≥5%pred.) or stable (FVC decline<5%pred.) [49]. In the end-stage IPF group, the blood sample was obtained at the time of evaluation for lung transplant, while in patients with IPF and lung cancer, it was collected at cancer diagnosis.

Hematological evaluation

White blood cell (WBC), neutrophil, lymphocyte, and monocyte counts were assessed for all three groups. Blood cell counts were performed by a technician blinded to clinical data and outcomes using an automated and certified blood count machine. The lymphocyte-to-monocyte ratio (LMR) was obtained by dividing the absolute number of lymphocytes by the total value of monocytes; similarly, the neutrophil-to-lymphocyte ratio (NLR) was obtained by dividing the absolute number of neutrophils by the absolute number of lymphocytes. Patients with concomitant infection, steroid therapy, or hematologic diseases were excluded.

Statistical analyses

Descriptive statistics were used to summarize the characteristics of patients; categorical variables were described as absolute (n) and relative values (%), whereas continuous variables were used as median and range. For categorical variables, comparisons between groups of patients were performed using Fisher's exact test. The cut-off value for LMR and NLR was obtained by ROC analysis. Survival was evaluated via Kaplan-Meier analysis and Log-rank test. Due to the fewer events, we combined death and transplantation for Kaplan-Meier analysis. The overall survival was calculated from diagnosis to death or lung transplantation, and all data was censored in December 2020. We used the term "not evaluable" in the Kaplan-Meier analysis when the median survival could not be computed. Univariate and multivariate analyses were performed with Cox proportional hazard regression. For quantitative variables, the Mann-Whitney U test compared the median values of the two groups.

Comparisons between the three groups were made using the Kruskal-Wallis test. Correlation coefficients between data were calculated using the nonparametric Spearman's rank method. Finally, only to perform univariate and multivariate logistic regression, the absolute number of monocyte and lymphocyte measuring units were changed in cellular/mm3. All data were analyzed using SPSS Software version 25.0 (New York, NY, US: IBM Corp. USA). All graphs were created using GraphPad Prism 5 (GraphPad Software Inc., la Jolla, California, USA). P-values < 0.05 were considered statistically significant. Survival was considered until lung transplantation, death, or end of follow-up (December 2020).

Results

Clinical, demographics, and functional evaluation in all study Subgroups

The demographics of the three groups are summarized in Table 1. The three groups had a similar history of smoking (i.e., pack/years; $p = 0.39$), whereas differences were observed for age at the time of blood sample ($p < 0.0001$), with patients with newly diagnosed IPF being significantly older than IPF patients with lung cancer and end-stage disease. The type of antifibrotic treatment (pirfenidone or nintedanib) was equally distributed among the three groups. IPF patients with lung cancer showed a lower body mass index (BMI) than newly diagnosed IPF patients and patients with end-stage disease (24 vs. 28 and 27, respectively, $p = 0.006$). In patients with end-stage IPF and IPF with lung cancer, lung function parameters were significantly lower compared with patients with newly diagnosed IPF [FVC (L): 1.94 vs. 2.1 vs 2.77, respectively; $p < 0.0001$; FVC (%): 51 vs. 64 vs. 80, respectively; $p < 0.0001$; and diffusing capacity of the lung for carbon monoxide (DLCO) (%): 26 vs. 40 vs. 57, respectively; $p < 0.0001$].

Table 1: demographics, functional and clinical characteristics of patients with newly-diagnosed IPF, IPF End-stage, IPF with lung cancer at the time of blood sample.

	Newly-diagnosed IPF (77)	End-stage IPF (40)	IPF with LC (17)	p
Age (years)	70 (53 – 81)	60 (36 – 68)	64 (34 – 82)	**<0.0001**
Male (%)	64 (83%)	33 (82%)	16 (94%)	0.49
Smoke history (yes - %)	57 (74%)	31 (77%)	13 (76%)	0.91
- **Current**	7 (9%)	3 (7%)	5 (29%)	
- **Ex-smokers**	50 (65%)	28 (70%)	8 (47%)	0.14
- **Non-smokers**	20 (26%)	9 (23%)	4 (24%)	
Pack/years	15 (0 – 100)	11 (0 – 60)	24 (0 – 80)	0.39
BMI (Kg/m^2)	28 (20 – 37)	27 (17 – 38)	24 (22 – 33)	**0.006**
FVC (L)	2.77 (1.2 – 4.6)	1.94 (0.4 – 3.6)	2.1 (0.7 – 3.9)	**<0.0001**
FVC (%)	80 (50 – 125)	51 (15 – 89)	64 (13 – 100)	**<0.0001**
DLCO (%)	57 (30 – 106)	26 (11 – 55)	40 (13 – 65)	**<0.0001**
Antifibrotic (yes)	77 (100%)	38 (95%)	14 (82%)	**0.002**
- **Nintedanib**	40 (52%)	17 (42%)	7 (41%)	0.52
- **Pirfenidone**	37 (48%)	21 (53%)	7 (41%)	0.73
Comorbidities				
- **Cardiovascular**	48 (62%)	26 (65%)	6 (35%)	0.09
- **GERD**	27 (35%)	29 (72%)	7 (41%)	**0.0005**
- **Metabolic**	36 (47%)	21 (52%)	2 (12%)	**0.014**
Months from IPF diagnosis to BS	0 (1 – -12)	32 (2 – 163)	13 (0 – 54)	**<0.0001**
Type of cancer				
Squamous	-	-	4 (23%)	
Adenocarcinoma	-	-	11 (65%)	
SCLC	-	-	2 (12%)	
Death (n - %)	17 (22%)	18 (45%)	4 (23%)	**0.03**
Transplant (n - %)	3 (4%)	12 (30%)	6 (35%)	**<0.0001**

IPF: idiopathic pulmonary fibrosis, LC: lung cancer, SCLC: small cells lung cancer, GERD: gastroesophageal reflux disease, BMI: body mass index, FVC: forced vital capacity, DLCO: diffusing capacity of the lung for carbon monoxide, BS: blood sample. Value are express as no. (%) or median (range), as appropriate. Comparisons between groups ware made using the Kruskal-Wallis and Mann-Whitney U tests for continuous variables. The Chi-square test was used for categorical variables.

Gastroesophageal reflux disease (GERD) ($p = 0.0005$) and metabolic diseases ($p = 0.014$) were significantly more common in the end-stage IPF group. Among patients with lung cancer, four had squamous cell carcinoma (23%), 11 patients had adenocarcinoma (65%) and two small-cell lung cancer (12%) (Table 1). At the end of the study period, the number of patients who died or were transplanted was higher in the end-stage IPF group and IPF with lung cancer compared to newly diagnosed patients (18, 4, and 17, respectively, among patients who died, $p = 0.03$; and 12, 6 and 3 in those who were transplanted, $p < 0.0001$).

Blood test evaluation in the group of patients with newly diagnosed IPF

In the newly diagnosed IPF patients group, no differences were observed in white blood cells, neutrophils, lymphocytes, LMR, and NLR when comparing blood tests at diagnosis and after one year of antifibrotic treatment (Table 2, A). When considering the pulmonary function test at diagnosis, we observed a negative correlation between FVC%pred and white blood cells (r = - 0.24; p = 0.04), and between FVC%pred and monocyte count (r = - 0.27; p = 0.01), as shown in Fig. 1.

Table 2: Blood count values, LMR and NLR in patients with newly-diagnosed IPF at diagnosis and after 1 year of therapy (A), in patients with End-stage IPF compared with newly-diagnosed IPF group (B), in patients with IPF and Lung cancer compared to newly-diagnosed IPF group (C) and in End-stage IPF compared with IPF with lung cancer (D).

A	**Newly-diagnosed IPF (77)**	**Newly-diagnosed IPF during therapy (77)**	**p**
WBC (n*10^9/L)	7.8 (4.1 – 13.3)	7.5 (3.9 – 13.1)	0.22
Neutrophils (n*10^9/L)	4.4 (2.0 – 9.4)	4.2 (1.7 – 10.2)	0.29
Lymphocytes (n*10^9/L)	2.2 (1.1 – 4.9)	2.3 (0.7 – 3.7)	0.94
Monocytes (n*10^9/L)	0.7 (0.3 – 1.3)	0.6 (0.3 – 4.6)	0.59
LMR	3.5 (0.8 – 8.8)	3.3 (0.7 – 9.5)	0.66
NLR	2.0 (0.7 – 8.8)	1.9 (0.7 – 8.2)	0.53
B	**Newly-diagnosed IPF (77)**	**End-stage IPF (40)**	**p**
WBC (n*10^9/L)	7.8 (4.1 – 13.3)	8.2 (3.7 – 18.6)	0.81
Neutrophils (n*10^9/L)	4.4 (2.0 – 9.4)	4.5 (1.8 – 11.5)	0.91
Lymphocytes (n*10^9/L)	2.2 (1.1 – 4.9)	2.3 (1.1 – 5.2)	0.46
Monocytes (n*10^9/L)	0.7 (0.3 – 1.3)	0.7 (0.4 – 1.4)	0.49
LMR	3.5 (0.8 – 8.8)	3.6 (2.0 – 6.5)	0.97
NLR	2.0 (0.7 – 8.8)	1.9 (0.8 – 5.5)	0.58
C	**Newly-diagnosed IPF (77)**	**IPF with LC (17)**	**p**
WBC (n*10^9/L)	7.8 (4.1 – 13.3)	9.3 (4.9 – 11.7)	0.06
Neutrophils (n*10^9/L)	4.4 (2.0 – 9.4)	5.7 (3.2 – 8.9)	**0.03**
Lymphocytes (n*10^9/L)	2.2 (1.1 – 4.9)	1.9 (0.5 – 3.5)	0.11
Monocytes (n*10^9/L)	0.7 (0.3 – 1.3)	1.0 (0.4 – 1.4)	**0.0007**
LMR	3.5 (0.8 – 8.8)	2.2 (0.8 – 4.4)	**<0.0001**
NLR	2.0 (0.7 – 8.8)	2.5 (1.4 – 9.4)	**0.01**
D	**End-stage IPF (40)**	**IPF with LC (17)**	**p**

WBC (n*10^9/L)	8.2 (3.7 – 18.6)	9.3 (4.9 – 11.7)	0.1
Neutrophils (n*10^9/L)	4.5 (1.8 – 11.5)	5.7 (3.2 – 8.9)	0.05
Lymphocytes (n*10^9/L)	2.3 (1.1 – 5.2)	1.9 (0.5 – 3.5)	0.06
Monocytes (n*10^9/L)	0.7 (0.4 – 1.4)	1.0 (0.4 – 1.4)	**0.006**
LMR	3.6 (2.0 – 6.5)	2.2 (0.8 – 4.4)	**<0.0001**
NLR	1.9 (0.8 – 5.5)	2.5 (1.4 – 9.4)	**0.005**

IPF: idiopathic pulmonary fibrosis; WBC: white blood count; LMR: lymphocyte-to-monocyte ratio; NLR: neutrophil-to-lymphocyte ratio. LC: lung cancer. Values are express as no. (%), media (DS) or median (range), as appropriate. Comparisons between groups were made using the Mann-Whitney U test.

Conversely, no correlation was observed between the pulmonary function test and neutrophil count (r = 0.13; p = 0.25), lymphocyte count (r = 0.13; p = 0.26), LMR (r = 0.12; p = 0.28) and NLR (r = 0.01; p = 0.89). To investigate the prognostic role of lymphocyte-to-monocyte ratio (LMR) in newly diagnosed IPF patients, a cut-off of 4.18 was determined by ROC analysis with an AUC of 0.67 (95%CI 0.5417–0.7960; p = 0.025). Patients were also categorized based on whether they had an LMR above or below 4.18 (Table 3). In the subset of patients with an LMR <4.18, we observed a significantly higher percentage of males (89% vs. 67%, p = 0.036) and individuals who died or were transplanted (19 vs. 1, p = 0.009) as compared to the group with an LMR ≥4.18. Moreover, the overall survival of patients with an LMR <4.18 was significantly lower compared to that of patients with an LMR ≥4.18 [hazard ratio (HR) 6.88; 95% confidence interval (CI): 2.55–18.5; p = 0.027; months: 65 vs. not evaluable] (Fig. 2).

Table 3: demographics, functional and clinical characteristics of newly-diagnosed IPF patients with LMR ≥ 4.18 and IPF patients with LMR < 4.18 at diagnosis.

	Newly-diagnosed IPF (77)	**LMR ≥ 4.18 (21)**	**LMR < 4.18 (56)**	**p**
Age at diagnosis (years)	70 (53 – 81)	71 (53 – 81)	70 (55 – 81)	0.55
Male (% - n)	64 (83%)	14 (67%)	50 (89%)	**0.036**
Smoke history (yes - %)	57 (74%)	14 (67%)	43 (77%)	0.39
- **Current**	7 (9%)	2 (10%)	5 (9%)	0.99
- **Ex-smokers**	50 (65%)	12 (57%)	38 (68%)	
Pack/years	15 (0 – 100)	9 (0 – 100)	20 (0 – 100)	0.21
BMI (Kg/m^2)	28 (20 – 37)	28 (22 – 37)	28 (20 – 37)	0.35
FVC (L)	2.8 (1.2 – 4.6)	2.6 (1.6 – 4.6)	2.7 (1.2 – 4.3)	0.35
FVC (%)	80 (50 – 125)	87 (50 – 125)	76 (54 – 124)	**0.023**
DLCO (%)	57 (30 – 106)	56 (30 – 106)	58 (30 – 79)	0.77
Antifibrotic (yes)	77 (100%)	21 (100%)	56 (100%)	
- **Nintedanib (n - %)**	40 (52%)	10 (48%)	30 (54%)	0.79

- **Pirfenidone (n - %)**	37 (48%)	11 (52%)	26 (46%)	
Comorbidities				
- **Cardiovascular (n - %)**	48 (62%)	15 (71%)	33 (59%)	0.43
- **GERD (n -%)**	27 (35%)	8 (38%)	19 (34%)	0.79
- **Metabolic (n -%)**	36 (47%)	10 (48%)	26 (46%)	0.99
Death - transplant/ (n - %)	20 (26%)	1 (5%)	19 (34%)	**0.009**
Decliner (n - %)	20 (26%)	4 (19%)	16 (28%)	0.39

IPF: idiopathic pulmonary fibrosis, LMR: lymphocyte-to-monocyte ratio, GERD: gastroesophageal reflux disease, BMI: body mass index, FVC: forced vital capacity, DLCO: diffusing capacity of the lung for carbon monoxide. Values are express as no. (%) or median (range), as appropriate. Comparisons between groups are made using the Mann-Whitney U test for continuous variables, and the Chi-square test for categorical variables.

In univariate and multivariate Cox regression analysis, smoking history [HR: 9.1, 95%CI (1.04–79.03); p = 0.04] and lower FVC%pred. at diagnosis [HR: 0.93, 95%CI (0.93–0.99); p = 0.03] were risk factors for overall mortality, whereas an LMR <4.18 only trended towards significance [HR:6.9, 95%CI (0.92–51.6); p = 0.06]. In further analysis, LMR [odds ratio (OR) 0.57, 95% confidence interval (CI): 0.34–0.94; p = 0.03] and monocyte count [OR: 1.01, 95% CI: 1.00–1.01; p = 0.003] were found to be associated with a functional decline during the first year of therapy in univariate analysis. Multivariate analysis confirmed monocyte count as an independent factor related to functional progression despite antifibrotic therapy [OR: 1.004; 95%CI (1.00–1.01); p = 0.03]. The ROC curve for NLR was not statistically significant and was excluded from other analyses in the newly diagnosed IPF group (AUC: 0.57; 95%CI: 0.4356–0.7126; p = 0.33).

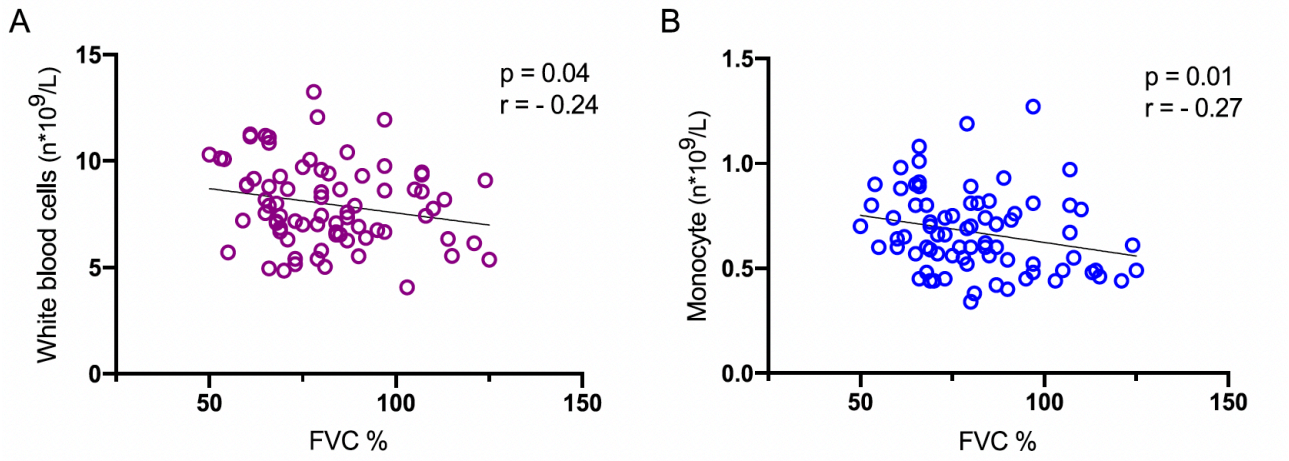

Figure 3. (A) Correlation between FVC (%)pred. and white blood cell count (n*109/L) in newly diagnosed IPF patients. (B) Correlation between FVC (%)pred. and monocyte count (n*109/L) in newly-diagnosed IPF patients. Spearman's rank correlation: r= - 0.24; p=0.04 and r= - 0.27; p=0.01; respectively. IPF: idiopathic pulmonary fibrosis.

Comparisons between IPF subgroup

LMR and NLR were similar in patients with newly diagnosed IPF and end-stage disease (Table 2, B). On the other hand, significant differences were observed in terms of neutrophil count ($p = 0.03$), monocyte count ($p = 0.0007$), LMR ($p < 0.0001$), and NLR ($p = 0.01$) between newly diagnosed IPF patients and IPF patients with lung cancer, while WBC and lymphocyte count did not differ between these two subgroups. (Table 2, C). Statistically significant differences were also observed in monocyte count, LMR, NLR, and neutrophil count between patients with end-stage IPF and those with lung cancer. In contrast, no between-group differences were found in terms of WBC, neutrophils, and lymphocytes. (Table 2, D). Finally, patients with IPF and lung cancer had significantly lower survival compared to both newly diagnosed IPF patients [HR: 4.4; 95%CI (1.35–14.4); $p < 0.0001$] and patients with end-stage disease [HR: 2.1; 95%CI (0.85–5.1) $p = 0.03$].

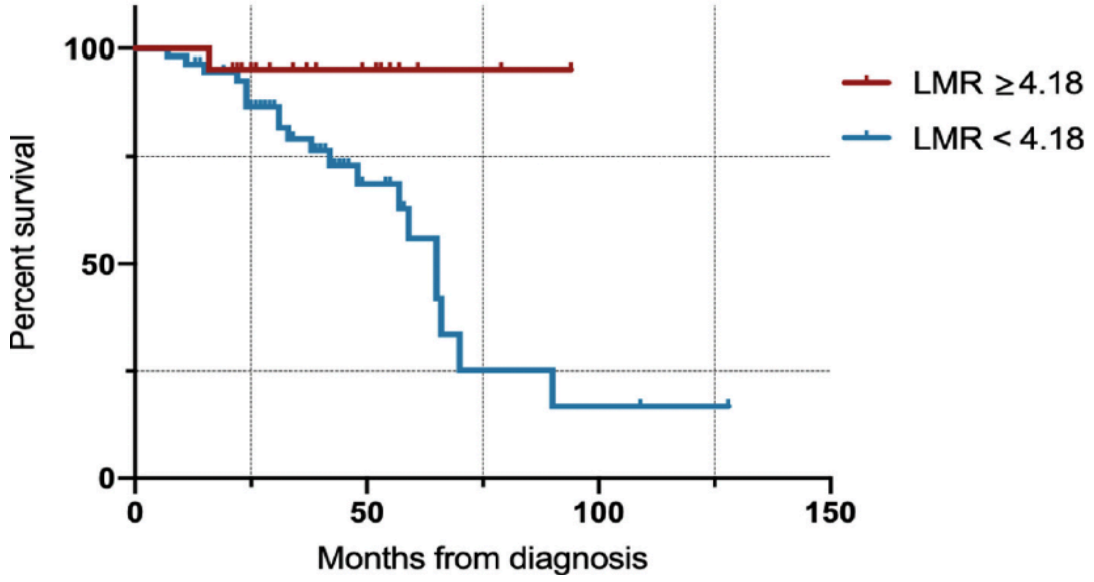

Figure 4. Kaplan-Meier curve for percent survival according to LMR levels in newly diagnosed IPF patients. The red line represents the survival in the newly-diagnosed IPF group with an LMR ≥4.18, and the blue line represents the survival in the newly-diagnosed IPF group with LMR <4.18. Kaplan-Meier analysis was used with a long-rank test [HR: 6.88; 95% CI (2.55–18.5) $p = 0.027$]. IPF: idiopathic pulmonary fibrosis, LMR: lymphocyte to monocyte ratio.

In conclusion, our study found that an LMR lower than 4.18 is associated with a significantly shorter survival in patients with newly diagnosed IPF. In addition, the LMR is substantially lower in patients with IPF and lung cancer compared with patients with IPF or end-stage lung disease. Furthermore, monocyte count is an independent predictor of disease progression during the first year of antifibrotic therapy. In contrast, white blood count and monocyte count, at baseline, negatively correlates with lung function. Monocyte count and LMR may represent an easy and inexpensive prognostic marker in patients with IPF.

Study 2) ***Monocyte count in ILD patients: a comparison with IPF population***
In collaboration with Dott.ssa Rosangela De Liberi (University of Palermo), Dott.ssa Elisabetta Balestro, Dott.Ssa Giulia Bacchin

This study aimed to investigate whether clinical and hematological features could predict progression in patients with ILD. As a link with the previously cited study (Study n°1), the second goal was to evaluate and compare the blood count at the time of the diagnosis between patients with idiopathic pulmonary fibrosis (IPF) and other ILDs that are not IPF.

Definition of disease progression
To define PF-ILD, two of the following three criteria need to be satisfied (in the last 12 months) with no alternative explanation [36]:

1. Worsening of respiratory symptoms
2. Physiologic evidence of disease progression assessed by worsening spirometry *(either of the following):*
- *Absolute decline in FVC > 5% predicted within one year of follow-up*
- *Absolute decline in DLCO (corrected for Hb) > 10% predicted within One year of follow-up*

3. Radiological evidence of disease progression (one or more of the following):
- *Increased extent or severity of traction bronchiectasis and bronchiolectasis*
- *New ground-glass opacity with traction bronchiectasis*
- *New fine reticulation*
- *New or increased honeycombing*
- *Increased lobar volume loss*

Patients previously prescribed antifibrotic therapy, transplanted/transplant list, or died due to the rapid evolution of pulmonary fibrosis were also considered progressive forms. IPF was selected as the control group representing the prototype of advanced fibrosis. Complete blood counts at diagnosis were collected for the ILD and IPF population.

Study population
The study initially involved 215 patients with interstitial lung disease, followed by the Division of Pulmonology at the University Hospital of Padua. Only 119 patients present available blood tests at the moment of diagnosis. One hundred forty-seven patients with IPF referred to the University Hospital of Padua and the University Hospital of Palermo were retrospectively enrolled. Data were collected from the beginning of 2017 up to May 2023. Demographic and clinical data were obtained at

the time of the diagnosis and during the follow-up, particularly one year before and at the last follow-up. Complete blood counts were collected at the time of the diagnosis. Regarding the ILD population, patients with cystic diseases (Langerhans cell histiocytosis (LCH), lymphangioleiomyomatosis (LAM)), CTD-ILD, and fibrotic sarcoidosis were excluded. In IPF patients, the concomitance of lung cancer was an exclusion criterion.

Statistical analysis

Descriptive statistics were applied to summarize the demographic and clinical features of patients: continuous variables were described as median value and range (min-max), whereas categorical variables were as absolute (n) and relative values (%). Mann-Whitney U test was used for quantitative variables, and Fisher's exact test was used for categorical variables. Correlation coefficients between data were calculated using the non-parametric Spearman's rank method. Overall survival was defined as the interval between diagnosis and death/lung transplant or between diagnosis and the patient's last follow-up. This parameter was estimated using the Kaplan-Meier method, reporting its median and the 95% confidence interval. All data are analyzed using SPSS software version 25.0 (New York, NY, US: IBM Corp. USA) and GraphPad Prism V8 (GraphPad Software, La Jolla, CA, USA). P-values < 0.05 were considered statistically significant.

Results

Clinical features of the study populations

Considering the overall population (IPF + ILD patients), male sex was predominant (67%), and the median age at the diagnosis was 68 years (30-87). More than half of the patients were former smokers (56 %) (Table 4). Moreover, IPF patients (n=147) were older at the time of diagnosis compared to ILD patients (n=119) [70 years (46-84) vs. 63 years (30-87); $p < 0.0001$]; they also differed in male prevalence, which is higher in the IPF patients (80% vs. 50%; $p < 0.001$). The two subgroups (ILD vs. IPF) showed no differences regarding BMI (27.1 kg/m^2 vs. 27.5 kg/m^2 p=0.79) and the number of current smokers (8.4% vs. 6% p=0.48). However, the number of pack years is significantly lower in the ILD population (0 vs. 17; p=0.0002).

Table 4: Demographics and clinical features of the overall patient with ILD and IPF.

	Overall (266)	**ILD (119)**	**IPF (147)**	**p-value**
Age at diagnosis – years	68 (30-87)	63 (30-87)	70 (46-84)	**<0.0001**
Sex – Male n° (%)	178 (67%)	60 (50%)	118 (80%)	**<0.0001**
BMI – (Kg/m^2)	27.4 (17.7-38.9)	27.1 (17.7-38.9)	27.5 (19.4-38.3)	0.79

Pack-Years	11.1 (0-160)	0 (0-160)	17 (0-100)	**0.0002**
Current smoker – n°(%)	19 (7%)	10 (8.4%)	9 (6%)	0.48
Former smoker – n°(%)	149 (56%)	53 (44%)	96 (65%)	**0.0008**
Comorbidities				
• **Cardiovascular – n° (%)**	178 (67%)	76 (64%)	102 (69%)	0.36
• **Metabolic – n° (%)**	109 (41%)	36 (30%)	73 (50%)	**0.002**
• **GERD – n° (%)**	99 (37%)	40 (34%)	59 (40%)	0.31
Pulmonary Function Tests				
• **FVC (L)**	2.6 (0.99-5.03)	2.61 (0.99-5.03)	2.63 (1.12-4.61)	0.38
• **FVC (%)**	79 (31-148)	80 (31-148)	78 (40-140)	0.16
• **DLCO**	55 (18-126)	59 (18-126)	53 (19-116)	0.07
Complete Blood Count				
• **WBC (x 10^9/L)**	7.92 (2.8-17.55)	7.30 (2.8-16.57)	8.24 (2.9-17.55)	0.28
• **Neutrophils (x 10^9/L)**	4.4 (0.78-14.9)	4.23 (0.94-14.55)	4.58 (0.78-14.9)	0.29
• **Neutrophils (%)**	58.26 (26.9-89.5)	60.3 (33-89.5)	57.9 (26.9-86.7)	0.16
• **Lymphocytes (x 10^9/L)**	2.14 (0.46-5.87)	1.8 (0.46-5.87)	2.25 (0.68-5.3)	**0.003**
• **Lymphocytes (%)**	28.82 (5.6-58.7)	28.35 (5.6-58.7)	29.5 (6.9-58.1)	0.10
• **Monocytes (x 10^9/L)**	0.64 (0.11-1,72)	0.62 (0.11-1.29)	0.67 (0.25-1.72)	0.19
• **Monocytes (%)**	8.3 (2.4-26.1)	8.3 (2.9-17.5)	8.29 (2.1-26.1)	0.74

BMI: Body Mass Index, GERD: Gastroesophageal reflux disease, FVC: Forced Vital Capacity, DLCO: Diffusion Lung CO, WBC: White Blood Cells. Values are expressed as numbers and (%) or median and range, as appropriate. To compare demographics between ILD and IPF, the chi-square test, Fisher's t-test for categorical variables, and Mann–Whitney t-test for continuous variables were used)

Regarding comorbidities, patients with IPF had more frequent metabolic comorbidities (50% vs. 30%; p=0.0008). No statistically significant difference was found regarding the values of FVC (L) (2.61 vs. 2.63 liters; p=0.38), FVC%pred (80% vs. 78%; p=0.16), and DLCO (59% vs. 53%; p=0.07) at diagnosis. Complete blood counts at the time of diagnosis revealed no statistically significant difference between ILD and IPF patients regarding WBC (7.30 vs. 8.24 p=0.28), neutrophils (n°) (4.23 vs. 4.58; p=0.29), neutrophils (%) (60.3 vs. 57.9 p=0.16), lymphocytes (%) (28.35 vs. 29.5;

p=0.10), monocytes (n°) (0.62-0.67 p=0.19), and monocytes (%) (8.3 vs. 8.29; p=0.7. However, the lymphocyte count was different between the two subgroups (1.8 vs. 2.25; p=0.003).

ILD population

Of the 119 patients diagnosed with ILDs, 43 were classified as progressors (progressive fibrosing ILD; PF-ILD) and 76 as non-progressors (Non-Progressive ILD; NP-ILD). The main diagnoses in the ILD group were: OP (23.5%); HP (18.5%), Unclassifiable (16.8%), Drug-related-ILD (10.1%); Smoking-related-ILD (8.4%) and NSIP (8.4%). Data regarding the diagnosis distribution in the two groups (NP-ILD and PF-ILD) were reported in Table 5.
Patients with PF-ILD are younger at the diagnosis in comparison with NP-ILD (59 vs. 65.5 years; p=0.008). Moreover, environmental exposures were more frequent in PF-ILD (69% vs. 48%; p=0.04). Comorbidities and symptoms were similar at the time of diagnosis, with only two exceptions: dyspnea on exertion that was more frequent in the case of PF-ILD (76% vs. 53%; p=0.02), and fever (2% vs. 16%; p=0.03), which on the contrary was more frequent in case of NP-ILD.
Focusing on HRCT, PF-ILD reported more frequent reticulations (89% vs. 62%; p=0.03), while NP-ILD reported more frequently the presence of consolidation (34% vs. 3% p=0.001). Regarding pulmonary function tests at the time of diagnosis, all the values are significantly lower in the PF-ILD compared to NP-ILD: FVC (L) (2.32 vs. 3.12 liters; p<0.0001; FVC%pred. (72% vs. 90%; < 0.0001); FEV1 (L) (2.13 vs. 2.57 liters; p=0.009); FEV1%pred. (79 vs. 96 p=0.0001); TLC (L) (3.56 vs. 4.53 liters; p= 0.0001); TLC%pred. (57.5% vs. 82%; p<0.0001); DLCO%pred. (49.5% vs. 65%; p=0.0001). To evaluate the possible progression of the disease, the worsening of symptoms, FVC, and HRCT of the last follow-up compared with that of the previous year were assessed. The comparison between PF-ILD and NP-ILD shows a statistically significant difference in worsening of symptoms (71% vs. 10% p<0.0001), HRCT (61% vs. 10% p<0.0001,) and FVC%pred (51% vs. 12% p<0.0001).

Table 5: Prevalence of different specific diagnoses in the ILD population.

	ILD (119)	**PF-ILD (43)**	**NP-ILD (76)**
OP – n° (%)	28 (23.5%)	4 (9.3%)	24 (31.6%)
HP – n° (%)	22 (18.5%)	13 (30.2%)	9 (11.8%)
Unclassifiable – n° (%)	20 (16.8%)	7 (16.3%)	13 (17.1%)
Drug-related – n° (%)	12 (10.1%)	2 (4.7%)	10 (13.1%)
Smoking-related – n° (%)	10 (8.4%)	5 (11.6%)	5 (6.6%)

NSIP – n° (%)	10 (8.4%)	5 (11.6%)	5 (6.6%)
PPFE – n° (%)	7 (5.9%)	4 (9.3%)	3 (3.9%)
Asbestosis and Silicosis – n° (%)	4 (3.4%)	1 (2.3%)	3 (3.9%)
IPAF – n° (%)	4 (3.4%)	1 (2.3%)	3 (3.9%)
Sarcoidosis (IV stage) – n° (%)	2 (1.7 %)	1 (2.3%)	1 (1.3%)

(PF-ILD: progressive-fibrosing ILD, NP-ILD: non-progressive ILD, OP: Organizing Pneumonia, HP: Hypersensitivity Pneumonitis, NSIP: Non-Specific Interstitial Pneumonia, PPFE: Pleuroparenchymal Fibroelastosis, IPAF: interstitial pneumonia with autoimmune features). Values are expressed as numbers and (%).

Blood tests in the study population

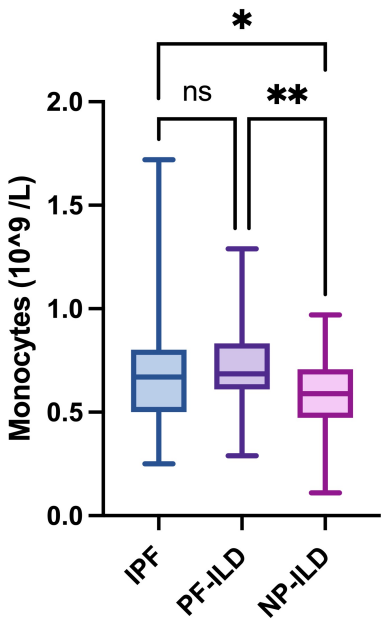

Complete blood counts of the diagnosis time were collected for ILD and IPF populations. Focusing on the ILD population (Table 6), no differences between PF-ILD and NP-ILD regarding the RBC, Hgb, WBC, neutrophils, lymphocytes, eosinophils, and basophils are reported. Still, the value of monocyte results is significantly higher in PF-ILD than in NP-ILD (0.68 vs 0.59 p=0.0007). Between IPF and NP-ILD, a statistically significant difference was found for both monocytes (0.67 vs. 0.59; p=0.008) and lymphocytes (2.25 vs. 1.78 x 109/L; p=0.0002), as shown in Table 7.

Figure 5: Levels of monocytes in IPF, PF-ILD, and NP-ILD. Horizontal bars represent median values; the bottom and top of each box plot are 25th and 75th (PF-ILD vs. NP-ILD p=0.0007; IPF vs. NP-ILD p=0.008).

On the contrary, no significant difference was found between IPF and PF-ILD (Table 8). Regarding the value of monocytes, the results of our study show a statistically significant difference between IPF and NP-ILD and between PF-ILD and NP-ILD. At the same time, there is no statistically significant difference between IPF and PF-ILD (Figure 5).

Table 6: Complete Blood Count of patients with NP-ILD and PF-ILD

	PF-ILD	NP-ILD	p
WBC (x 10^9/L)	7.91 (4.68-16.01)	7.06 (2.81-16.57)	0.08
Neutrophils (x 10^9/L)	4.54 (1.99-12.81)	4.06 (0.94-14.55)	0.10
Neutrophils (%)	61.2 (36.9-89.5)	59.4 (33.5-87.8)	0.37
Lymphocytes (x 10^9/L)	1.99 (0.60-4.8)	1.78 (0.46-5.87)	0.38
Lymphocytes (%)	28.15 (5.60-46.20)	28.45 (5.8-58.7)	0.44
Monocytes (x 10^9/L)	0.68 (0.29-1.29)	0.59 (0.11-0.97)	**0.0007**
Monocytes (%)	8.8 (3.10-13.70)	8.10 (2.90-17.5)	0.21

WBC: White Blood Cells Count. Values are expressed as median and range. To compare CBCs between IPF and NP-ILD Mann–Whitney t-test for continuous variables was used).

Table 7: Complete Blood Count of patients with IPF and NP-ILD

	IPF	NP-ILD	p
WBC (x10^9/L)	8.24 (2.9-17.55)	7.06 (2.81-16.57)	0.004
Neutrophils (%)	57.9 (26.9-86.7)	59.4 (33.5-87.8)	0.43
Neutrophils (x10^9/L)	4.58 (0.78-14.9)	4.06 (0.94-14.55)	0.06
Lymphocytes (%)	29.5 (6.9-58.1)	28.45 (5.8-58.7)	0.33
Lymphocytes (x10^9/L)	2.25 (0.68-5.3)	1.78 (0.46-5.87)	**0.0002**
Monocytes (%)	8.29 (2.1-26.1)	8.10 (2.90-17.5)	0.67
Monocytes (x10^9/L)	0.67 (0.25-1.72)	0.59 (0.11-0.97)	**0.008**

WBC: White Blood Cells Count. Values are expressed as median and range. To compare CBCs between IPF and NP-ILD Mann–Whitney t-test for continuous variables was used).

Table 8: Complete Blood Count of patients with IPF and PF-ILD. (WBC: White Blood Cells Count).

	IPF	PF-ILD	p
WBC (x10^9/L)	8.24 (2.9-17.55)	7.91 (4.68-16.01)	0.99
Neutrophils (%)	57.9 (26.9-86.7)	61.2 (36.9-89.5)	0.10
Neutrophils (x10^9/L)	4.58 (0.78-14.9)	4.54 (1.99-12.81)	0.51
Lymphocytes (%)	29.5 (6.9-58.1)	28.15 (5.60-46.20)	0.07
Lymphocytes (x10^9/L)	2.25 (0.68-5.3)	1.99 (0.60-4.8)	0.06
Monocytes (%)	8.29 (2.1-26.1)	8.8 (3.10-13.70)	0.21
Monocytes (x10^9/L)	0.67 (0.25-1.72)	0.68 (0.29-1.29)	0.22

WBC: White Blood Cells Count. Values are expressed as median and range. To compare CBCs between IPF and NP-ILD Mann–Whitney t-test for continuous variables was used).

Prognostic factors of radiological progression and disease progression

Concerning disease progression in the univariate analysis, age at the diagnosis (p=0.01), FVC (%) at the Pulmonary Function Tests at the diagnosis (p=0.0001), complete blood count at the time of the diagnosis with monocyte level of >0.6 x 109/L (p=0.003), finding of consolidations (p=0.005) and reticulations (p=0.005) at the HRCT and the presence of exposures (p=0.022) appear to be predictors. In the multivariate analysis FVC%pred. at the Pulmonary Function Tests at the diagnosis (p=0.002), complete blood count at the time of the diagnosis with monocyte level of >0.6 x 109/L (p=0.036), and the finding of reticulations at the HRCT (p=0.04) are independent factors of disease progression in the ILD population.

Survival

Furthermore, we analyze the probability of survival at 120 months of patients with a diagnosis of IPF, PF-ILD, and NP-ILD, and the results show a statistically significant difference (p<0.0001). Patients diagnosed with IPF have the lowest survival, followed by those with PF-ILDs, while NP-ILDs are the group with the best probability of survival.

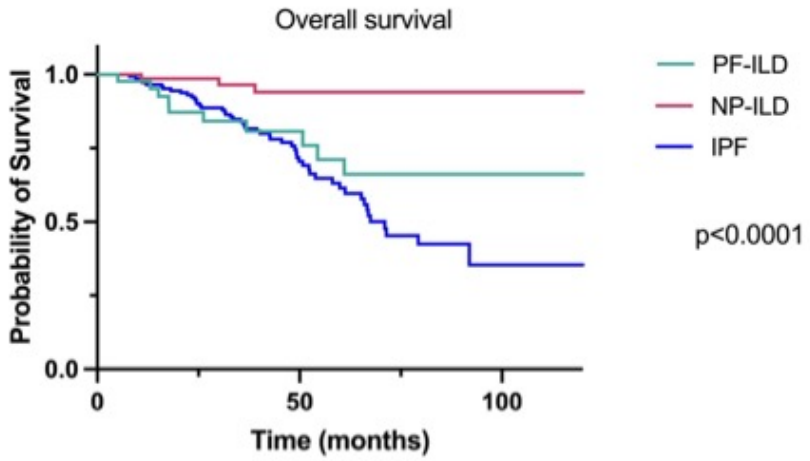

Figure 6: Overall Survival comparing patients with progressive interstitial lung disease (PF-ILD), non-progressive interstitial lung disease (NP-ILD), and idiopathic pulmonary fibrosis (IPF). Kaplan-Meier test and Long-rank test were used (p<0.0001).

In conclusion, we observed that the value of monocyte counts at the time of the diagnosis results significantly higher in patients with IPF compared with NP-ILD and patients with PF-ILD compared with NP-ILD. We also found that FVC%pred. at diagnosis, monocyte count > 0.6 x 109/L, and the finding of reticulations at the HRCT are independent factors of disease progression in the ILD population. Furthermore, we analyze the overall survival of patients diagnosed with IPF, PF-ILD, and NP-ILD at 10 years, and the results show a statistically significant difference in survival between the three groups.

Study 3) ***Histologic biomarkers for progressive fibrosing interstitial lung disease***

In collaboration with Prof. Fiorella Calabrese, Dr. Lauren D'sa, Dr. Francesca Boscaro, Dr. Elisabetta Balestro, and Dr. Anna Maria Chelu

The aim of this study was to understand if there are any histological factors that suggest the presence of a progressive ILD at an early stage. Currently, there is no specific histological biomarker that can reliably detect progressive lung disease in clinical practice. In this study, several histological features were evaluated for their high predictive value.

Study design

The population of this study was extrapolated from Study n°2 of my thesis. All patients were enrolled at the University Hospital of Padua. Only patients with an available transbronchial biopsy or surgical biopsy were definitively enrolled (48 patients). Progression was defined as PF-ILD criteria, as mentioned before in the Study n°2.

Histological Analysis

Histological analysis was performed by the pathological anatomy section of the University Hospital of Padua. Of the 215 patients initially enrolled in the study, 48 were selected based on the availability of slides and tissue blocks, which had a sufficient amount of residual tissue for further analysis to be performed. 37 patients had transbronchial biopsy; for 7 of them, only VATS was available, and for 4 of them, both transbronchial biopsy and VATS were available. Tissue specimens on which analysis was performed included formalin-fixed, paraffin-embedded transbronchial biopsies and specimens from video-assisted thoracic surgery. A representative slide of H&E and Masson's trichomes from each specimen was evaluated for adequacy and digitally scanned. The slides were analyzed by exploiting QuPath v.0.4.3 software. The evaluators of the slides were blinded, i.e., they were unaware of whether or not the patient had progressive ILD. Fibrosis was assessed with Image P in QuPath using a Masson scanned stained slide. The percentage of blue staining was calculated as a percentage of the total stained area using the Color Threshold function. In addition to histological analysis, a molecular analysis was also performed, which is still ongoing and is aimed at identifying which cytokines are most highly expressed in the context of lung tissue affected by interstitial lung disease. Molecular analysis aims to identify which genes for cytokine transcription are expressed in the analyzed tissue samples and BAL fluid.

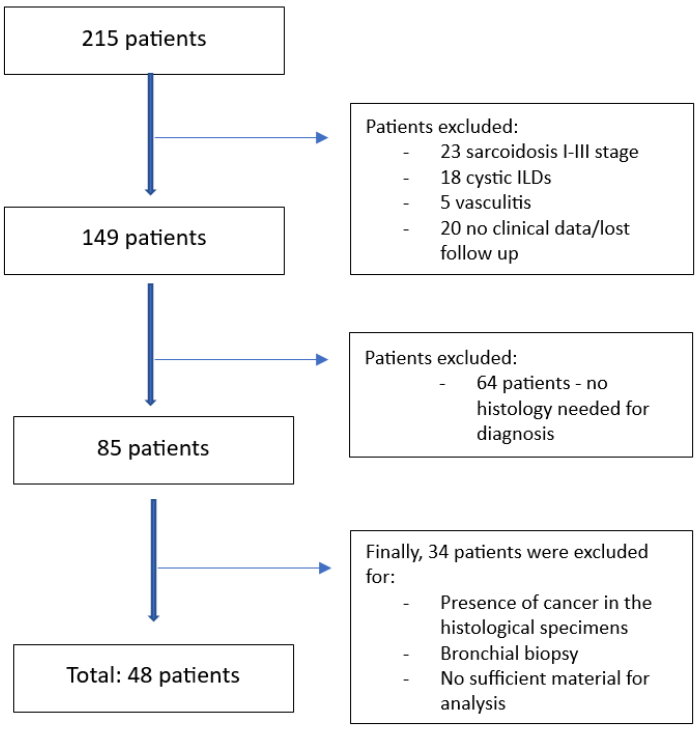

Figure 7: Selection of the study sample

RNA was extracted from each available sample collected. Cytokine gene expression was assessed using TaqMan™ Array Human Cytokine Network (Applied Biosystems) through conversion to cDNA, real-time PCR, and probes for 28 cytokine network-associated genes. The statistical analysis was the same as the study n°2.

Clinical characteristics of the study population

Considering the overall population, patients were predominantly male (64%), and the mean age at the moment of diagnosis was 62.1 years. The mean BMI (Body mass index) found was 28.6 kg/m2. Patients exposed to possible pneumotoxic agents were 60% of the total. Progressor patients were 15, while non-progressive patients were 33. Concerning the comorbidities affecting the study population, 34% of non-progressive patients had a second pulmonary comorbidity (different from the one that led them to be enrolled in the study) compared with 2% found in progressive patients (p=0.004). Other clinical and demographic characteristics are summarized in Table 9.

Table 9: Differences between progressor and non-progressor patients

	Overall (n.48)	ILD Progressive (n.15)	ILD Non-Progressive (n.33)	p
Age - years	62.1 (36.5-81.3)	63.2 (49.4-69.1)	61.6 (36.5-81.3)	0.83
Sex - male n° (%)	31 (64 %)	9 (60 %)	22 (66%)	0,80
BMI (kg/m^2)	28.6 (17.7-41.3)	29.4 (23.3-37.5)	28.6 (17.7-41.3)	0.26
Smoking:				
- Never	18 (38%)	3 (20%)	15 (45%)	0.12
- Active	3 (6%)	1 (6%)	2 (6%)	0.99
- Former	27 (56%)	11 (73%)	16 (48%)	0.13
- Pack/Years	10 (0-90)	17 (0-90)	2 (0-80)	0.15
- Other Exposition	29 (60%)	11 (73%)	18 (54%)	0.34
- Symptoms at diagnosis				
- Dyspnea at rest	29 (60%)	10 (66%)	19 (57%)	0.75
- Cough	29 (60%)	8 (53%)	21 (63%)	0.52
- Dyspnea on effort	4 (8%)	1 (6%)	3 (9%)	0.99
- Thoracic Pain	6 (12%)	2 (12%)	4 (12%)	0.99
- Asthenia	4 (8%)	1 (7%)	3 (9%)	0.99
Comorbidities:				
- CVD	35 (74%)	12 (80%)	23 (72%)	0.72
- Oncologic	9 (19%)	2 (13%)	7 (22%)	0.69
- Metabolic	15 (32%)	6 (40%)	9 (28%)	0.50
- Gastrointestinal	18 (38%)	7 (47%)	11 (34%)	0.52
- Pneumological	14 (30%)	3 (2%)	11 (34%)	**0.004**

BMI: body mass index, CVD: cardiovascular disease.

Respiratory function and radiological characteristics of the study population

Between PF-ILD and NP-ILD groups, statistically significant differences were found in FVC values. In the PF-ILD group, the average FVC at diagnosis was lower than the NP-ILD group (2.42 vs. 3.37 L; respectively. p=0.004). The same trend in TLC values was also found, with lower values in progressive patients than in non-progressive patients (3.83 vs. 4.65 L; p=0.03). Regarding the HRCT evaluation obtained at diagnosis, consolidations were more present in non-progressive patients than in progressive patients, although they did not reach statistical significance (20% progressive vs. 53% nonprogressive p=0.11). A reasonably significant gradient is also found for the distribution of bronchiectasis, bronchiectasis being more prevalent in progressive patients than in nonprogressive patients, although it does not reach statistical significance (33% progressive vs. 18% non-progressive p=0.28). Other characteristics analyzed are shown in Table 10.

Table 10: Differences between progressor and non-progressor patients regarding functional parameters and radiological evaluation

	Overall (n.48)	ILD Progressive (n.15)	ILD Non-Progressive (n.33)	p
Spirometry At Baseline:				
- *FVC (L)*	2,82 (1.52-5.03)	2.42 (1.52-3.76)	3.37 (2.02-5.03)	**0.004**
- *FVC (%)*	86 (46-129)	79 (48-108)	89 (46-129)	0.19
- *FEV1 (L)*	2.51 (1.53-4.46)	2.25 (1.83-4.46)	2.8 (1.53-3.89)	0.11
- *FEV1 (%)*	93 (46-130)	92 (58-119)	96 (46-130)	0.41
- *TLC (L)*	4.31 (2.54-8.12)	3.83 (2.54-7.75)	4.65 (3.19-8.12)	**0.03**
- *TLC (%)*	79.5 (46-109)	75 (47-105)	82 (46-109)	0.06
- *DLCO*	63.5 (30-105)	59 (33-105)	67 (30-95)	0.23
CT scan:				
- *Reticulation*	12 (26%)	3 (2%)	9 (3%)	0.73
- *Bronchiectasis*	11 (24%)	5 (33%)	6 (18%)	0.28
- *Consolidation*	19 (42%)	3 (20%)	16 (53%)	0.11
- *Groundglass*	17 (38%)	5 (33%)	12 (40%)	0.99

CT: computer tomography, FVC: forced vital capacity, TLC: total lung capacity, FEV1: forced expiratory volume in the first second, DLCO: diffusing lung capacity of CO.

Histological analysis

The results obtained from histological analysis did not yield statistically significant results but revealed significant gradients for some variables. Pigmented macrophages were shown to be slightly higher in progressors than in non-progressors (60% progressive vs. 45% non-progressive, p=0.53). Among the variables evaluated was the increase in alveolar macrophages, a moderate to severe increase; from this, it was found that macrophages appear to be increased in progressive patients compared to non-progressive patients (47% progressive vs. 24% non-progressive, p=0.17). Analysis of the lymphocyte distribution variable found that airway-centered distribution is more present in non-progressive patients than in progressive patients (6% progressive vs. 27% non-progressive, p=0.14). Assessment of the inflammation distribution pattern showed no differences between the two groups. Evaluation of the presence of OP pattern (organizing pneumonia)revealed, although not reaching statistical significance that OP pattern is more present in nonprogressive patients than in progressive patients (33% progressive vs. 64% nonprogressive, p=0.07). Going to assess the localization of fibrosis, subjects belonging to the progressive group showed to have a greater centrilobular distribution compared to the non-progressive group (40% progressive vs.15% non-progressive, p=0.17). The other distribution patterns (interstitial, alveolar, micro honeycombing) did not show significant differences between the two groups. Evaluating the pattern of fibrosis distribution, considered patchy or extensive, it was found that the patchy distribution is more frequently present in non-progressors than in progressors (47% progressive vs. 55% non-progressive p=0.13). Among the variables taken into analysis, the presence in the tissue sample of bronchial metaplasia,

anthracosis, and the presence of foamy and pigmented macrophages were evaluated. The results show that there are no substantial differences. Although the data does not reach statistical significance, bronchial metaplasia seems more incident in progressive patients (40% progressive vs. 24% non-progressive p=0.31). The presence of anthracosis occurs more in nonprogressive patients, but also, in this case, the statistical significance was not reached (53% progressive vs. 73% non-progressive p=0.21).

Prognostic Factors for Mortality

To detect predictors of mortality, logistic regression has been performed. In univariate analysis, micro honeycombing (p=0.057), spirometry worse (p=0.066), symptoms at the last follow-up worse (p=0.007), and increased alveolar macrophage (p=0.053), have been associated with the survival of patients. In multivariate analysis, it was found that micro honeycombing is an independent predictor of mortality (p=0.046). The study also evaluated the difference in ten-year survival between progressive and non-progressive patients, obtaining a statistically significant value as a result (p=0.02).

Table 11: cox regression analysis to predict mortality for the overall population.

	Univariate HR	p	Multivariate HR	p
Microhoneycombing	6.873 (0.943-50.096)	0.057	22.488 (1.060- 477.158)	**0.046**
Spirometry worsened	8.447 (0.868-82.171)	0.066	4.549 (0.096-215.051)	0.441
Symptoms at last follow-up worsened	20.213 (2.235-182.771)	**0.007**	11.722 (0.769-178.560)	0.076
Increased Alveolar Macrophages >34%	6.313 (0.975- 40.900)	0.053	25.098 (0.291- 2164.044	0.156

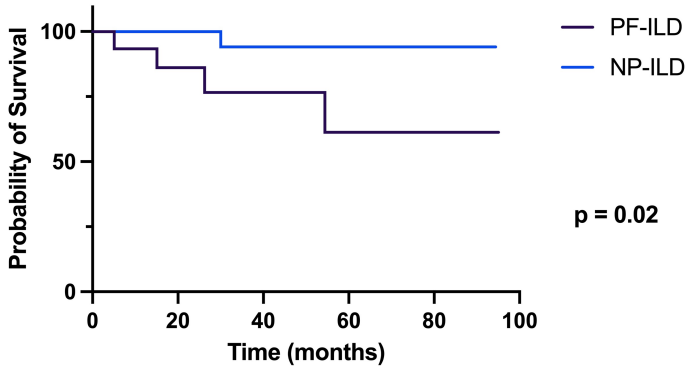

Figure 8: Difference in survival between progressives and non-progressors

In conclusion, significant findings emerged from our analysis. At univariate analysis, significant data were shown regarding the worsening of symptoms at the last follow-up p=0.007. The results of the analysis we performed showed that the presence of micro honeycombing in histological specimens at multivariate analysis is an independent mortality factor for patients p=0.046 and thus is a data point defining a group of patients at higher risk for disease progression

Study 4): ***Prevalence of loss of muscle mass in idiopathic pulmonary fibrosis (IPF)*** ***Bernardinello, N,*** *...et al. European Respiratory Society Congress, Barcellona, 2022.*

Sarcopenia is quite unexplored in patients with IPF and ILD and requires accurate muscle quantification. Using computed tomography (CT) and radiomics parameters, the aim of this study was to explore the role of low muscle mass (LOM) in IPF patients under antifibrotic therapy at the moment of diagnosis.

Materials and methods

In this study, 88 patients with IPF were retrospectively enrolled between March 2014 and December 2021. In order to quantify muscle density and in collaboration with our radiologists, we recorded the mean Hounsfield Unit (Hu) value of the right and left paravertebral muscle at the level of the 12° thoracic vertebra of the first CT scan of each patient enrolled [50]. We also defined loss of muscle mass as MeanHu < 30 (Figure 9). Moreover, using the CT images, we extracted radiomic features from the CT values; in particular, the Inverse Variance, Joint Entropy, GrayLevelNonUniformity, and HighGrayLevel were collected at the first baseline CT scan. Furthermore, we obtained the SMI (skeletal muscle index) parameter by dividing the calculated area (cm2) by height2 (m2) [51]. For all patients, functional parameters (FVC, FEV1, TLC, and DLCO), demographic characteristics, and comorbidities were retrospectively collected at baseline.

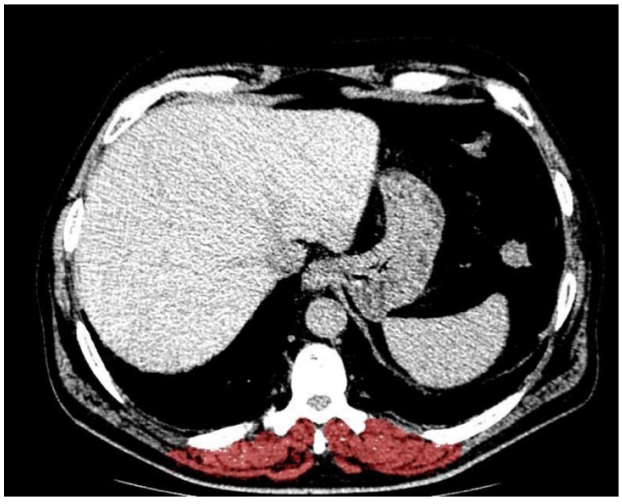

Figure 9: Axial Computed Tomography images, demonstrating the applied method of measurements of muscle densitometry.

The region of interest (that is highlighted in red) in Figure 9, was placed on the paravertebral muscle at the level of the 12th dorsal vertebra, and the mean Hounsfield unit value was collected. The mean HU is an important parameter to estimate muscle density. The Figure 9 proposes an example of a CT scan of our male patients collected at the moment of diagnosis.

Results

Patient characteristics and categorization are summarized in Table 12: we observed that the prevalence of loss of muscle mass at the time of diagnosis using the first CT performed was 46%. Considering only male patients, the prevalence was 42%. Patients with LOM were older compared with non-LOM patients (74 (59 – 87) vs. 67 (53 – 80) years; p<0.0001) and with less metabolic (39% vs. 63%; p=0.03) and GERD disease (27% vs. 55%; p=0.01). No differences were observed between patients with LOM at diagnosis and those without LOM with regard to smoking history, BMI, cardiological comorbidities, antifibrotic therapy, need for oxygen therapy, number of patients with functional decline over the years according to spirometry, and number of deaths at two years.

It was observed about respiratory function tests that patients with LOM at diagnosis had a lower FVC (L) than patients without LOM (2.5 vs 2.9; p=0.04), while no significant differences were observed about FVC %, TLC (L), and TLC %, and finally about DLco%. HighGrayLevel and Area (mm^2) were lower in patients with LOM in comparison with patients with normal muscle mass [12.7 (6.62 – 47.2) vs. 16.2 (14 – 20) and 3007 (772 – 5249) vs. 3462 (1651 – 6235); respectively]

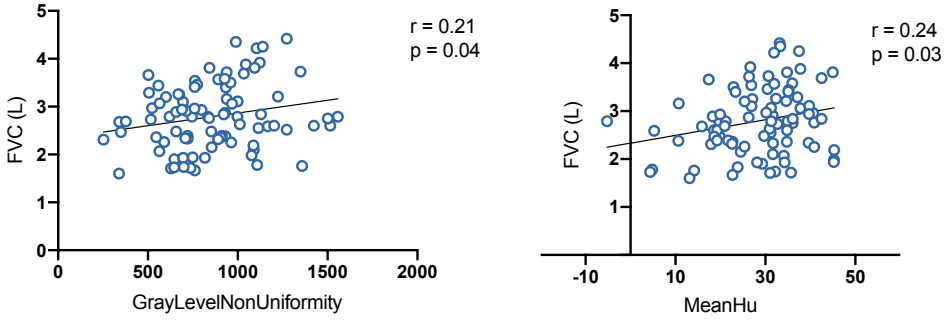

Figure 10: correlations between FVC (L) in the whole patient population and radiomic measurements (Mean Hu and GreyLevelUniformity). Spearman test was used for the correlation analysis.

In correlation analysis, performed with Spemann test, we found a positive correlation between FVC (L) and Mean HU (p= 0.04; r=0.21) and between FVC (L) and GreyLevelUniformity (p= 0.03; r=0.24). Using the Kaplan Meier survival analysis, we observed that the male patients with LOM had a lower survival rate at two years compared to male patients without LOM [HR 4.09 (95%CI 1.2 – 13.72); p=0.02]. (Figure 10). Data regarding survival in female patients was not shown because not statistically significant

Table 12: clinical, demographics, radiological, and functional characteristics of IPF patients (88) divided into loss of muscle mass (<30 HU) and not loss of muscle mass (>30 HU)

	Loss Muscle Mass (41)	**Not loss Muscle Mass (47)**	**p**
Age (years)	74 (59 – 87)	67 (53 – 80)	**<0.0001**
Sex – male n° (%)	31 (76%)	41 (87%)	0.18
Smoker			
• Current n° - (%)	3 (7%)	8 (17%)	0.21
• Ex n° - (%)	28 (68%)	30 (64%)	0.82
• Never n° - (%)	10 (24%)	9 (19%)	0.61
Pack years	15 (0 – 240)	20 (0 – 84)	0.97
BMI (Kg/m^2)	28 (22 – 37)	28 (20 – 32)	0.41
Hight (m)	1.7 (1.5 – 1.8)	1.7 (1.6 – 1.9)	0.55
Comorbidities			
• Cardiological n° - (%)	28 (68%)	26 (53%)	0.21
• Metabolic n° - (%)	16 (39%)	29 (62%)	**0.03**
• GERD n° - (%)	11 (27%)	25 (55%)	**0.01**
Therapy			
• Nintedanib n° - (%)	26 (63%)	27 (57%)	0.66
• Pirfenidone n° - (%)	15 (37%)	20 (42%)	
Spirometry at baseline			
• FVC (%)	81 (51 – 125)	80 (51 – 128)	0.69
• FVC (L)	2.6 (1.6 – 4)	2.9 (1.7 – 4.4)	**0.03**
• TLC (%)	71 (45 – 96)	72 (28 – 97)	0.86
• TLC (L)	4.4 (2.2 – 7)	4.7 (1.5 – 6.3)	0.18
• DLCO (%)	57 (20 – 106)	57 (26 – 87)	0.92
CT scan variables			
• Area (mm^2)	3007 (772 – 5249)	3462 (1651 – 6235)	**0.01**
• HU	21 (4.4 – 29.7)	35 (30 – 45)	**<0.0001**
• 10 percentile	-22 (-84 - -8)	-6 (-17 – 14)	**<0.0001**
• Inverse Variance	0.48 (0.36 – 0.51)	0.48 (0.38 – 0.51)	0.90
• Joint Entropy	4.10 (3.03 – 5.11)	3.94 (2.98 – 4.73)	0.09
• GrayLevelNonUniformity	798 (253 - 1515)	891 (506 - 1557)	0.14
• HighGrayLevel	12.7 (6.62 – 47.2)	16.2 (14 – 20)	**<0.0001**
Death at 2 years n° - %	8 (19%)	3 (6%)	0.10
Death at the end of FU	16 (39%)	15 (32%)	0.51
O_2 therapy on effort n° - (%)	23 (56%)	29 (62%)	0.66
O_2 therapy at rest n° - (%)	11 (27%)	12 (25%)	0.99
Time from diagnosis to O_2 effort	16 (0 – 75)	25 (0 – 54)	0.30

IPF: idiopathic pulmonary fibrosis, BMI: body mass index, FVC: forced vital capacity, TLC: total lung capacity; DLCO: diffusing capacity of carbon monoxide; SMI: skeletal muscle index; O2 therapy: oxygen therapy; GERD: gastroesophageal reflux; Hu: Hounsfield unit. Value are express as median (min-max) or %, as appropriate.

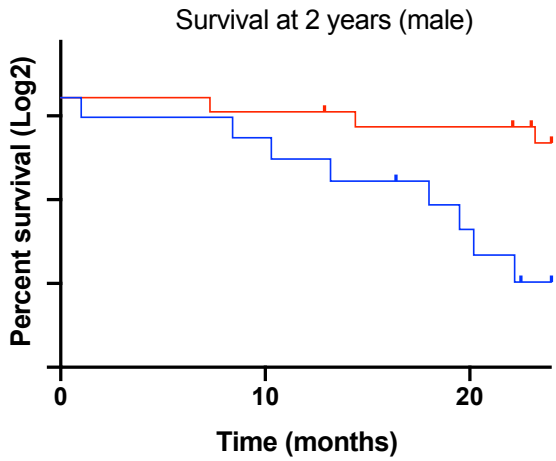

Figure 11: Kaplan-Meier curves at 2 years in IPF patients divided in male (n=72) and female (n=16) patients with and without loss of muscle mass (<30 HU and >30 HU, respectively). p=0.02

In Table 13 we reported the results by Cox regression analysis: low HighGreyLevelRunEmphasis at baseline [HR 0.53 (95%CI 0.31 – 0.88); p=0.01] and the use of oxygen therapy at rest [HR 10 (95%CI 2.2 – 49); p=0.003] were independent risk factors of death at 2 years in male patients. The optimal cut-off of HighGreyLevelRunEmphasis, in male patients, was 13.3 (sensibility 82% and specificity 64%; AUC 0.77; p=0.004)

Table 13: risk factors of death at two years in male patients with IPF (n=74).

	Multivariate	
	HR (95%CI)	p
Pack/years	1.0 (0.97 – 1.03)	0.94
FVC (L)	0.40 (0.03 – 5.65)	0.50
Mean Hu < 30 yes	0.44 (0.12 – 1.58)	0.21
HighGrayLevelRunEmphasis	0.53 (0.31 – 0.88)	**0.01**
O_2 at rest	10 (2.2 – 49)	**0.003**

In conclusion, loss of muscle mass is highly prevalent in IPF patients at the time of diagnosis. Moreover, male patients with muscle loss presented a reduction in survival rate at two years. At baseline, Low HighGreyLevelRunEmphasis and oxygen need at rest are independent predictors of mortality.

Study 5): ***Prevalence of diaphragm dysfunction in patients with interstitial lung disease (ILDs): the role of diaphragmatic ultrasound.***
Bernardinello N,*...et al. Respir Med. 2023 Sep;216:107293*

Our aims were to investigate the role of diaphragmatic function, as assessed by ultrasound, in ILD patients. Then, we investigated whether the TF is related to patients' lung function and, if a TF < 30% is a predictor of dyspnea.

Materials and methods

In this observational study, 41 adult patients with CTD-ILD and 41 with IPF were consecutively enrolled between March 2020 and October 2020 at the ILD-Unit of the University Hospital of Padova. High-Resolution Computed Tomography (HRCT) was evaluated by an expert thoracic radiologist. Fifteen sex- and age-matched healthy subjects served as controls and were recruited as volunteers in our hospital by word of mouth or leaflets. Exclusion criteria were the presence of emphysema/COPD, active infection, both past, and recent abdominal/thoracic surgery, oral prednisone equivalent or more than 25 mg/day, and neuromuscular disease. Pulmonary function tests, including FVC (forced vital capacity), FEV1 (forced expiratory volume in 1 s), TLC (total lung capacity), DLCO (diffusion lung carbon monoxide), maximal inspiratory pressure (MIP), and maximal expiratory pressure (MEP), were performed with CareFusion MasterScreen™ PFT, at the same time as DUS and according to the ATS/ERS guidelines. The presence of dyspnea was evaluated with the modified British Medical Research Council Questionnaire (mMRC). A score of 0–1 indicated mild dyspnea, a score of 2–3 indicated moderate dyspnea, and a score of 4–5 indicated severe dyspnea. Demographics and clinical and radiological data were also collected for all CTD-ILD and IPF patients.

Ultrasound measurement and analysis

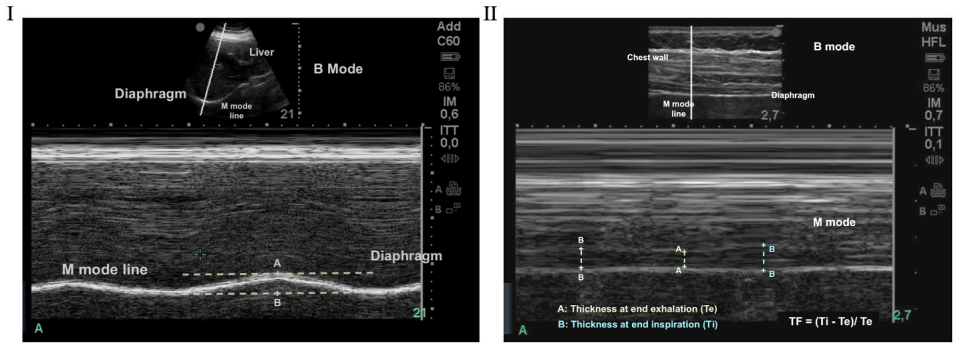

Fig. 12. Ultrasound measurement and analysis. Panel I measurement of diaphragm displacement; Panel II measurement of right diaphragm inspiratory thickness (Ti), and right expiratory thickness (Te).

A portable ultrasound unit (Sonosite M-Turbo©, Fujifilm, Amsterdam, Netherlands) was used to measure, during quiet breathing, right diaphragm displacement (DD),

right diaphragm inspiratory thickness (Ti), and right expiratory thickness (Te) at baseline and follow-up visits. The thickening fraction (TF) was calculated as previously described and expressed as a percentage: [(Ti – Te)/Te] x 100 [52], as reported in Figure 12. There is no standardized approach in the measurement of diaphragm thickening fraction in the literature. However, as a first study, we decided to evaluate only quiet breathing. As the resting diaphragm thickening fraction in healthy subjects is about 30–40%, we considered a TF<30% as a cut-off for diaphragmatic dysfunction in our analyses [53]. All ultrasound evaluations were conducted in a semi-recumbent position (40◦ head-up). For each parameter (Ti, Te, and DD), we used the mean of three consecutive measurements, and the values were reported in centimeters. A convex array (model C60xi – 2–5 MHz) was used to measure right diaphragm displacement (DD), and the convex probe was positioned dorso-cranially in the right anterior to mid-clavicular line. Diaphragm and respiratory excursions were then evaluated in M-mode. Measurements, in patients and controls, were performed after freezing the image of the diaphragmatic curve during the respiratory cycle and measuring the distance from the base of the curve to the apex. A linear probe (model HFL38x – 6–13 MHz) was used for the measurements of both right diaphragm inspiratory thickness (Ti) and right expiratory thickness (Te). The linear array was positioned in the right mid-axillary line, perpendicular to the diaphragm (approximately at the 8th - 10th intercostal spaces, as appropriate). Ti and Te were obtained with M-mode imaging, revealing the variation in diaphragm thickness over time. We reached acceptable measurements only in 61 patients, due to the loss of the hepatic acoustic window on this side. The agreement between the first 12 ultrasonographic measurements, collected by two different observers, was assessed through the intraclass correlation coefficient (ICC) using a two-way random effect model (good agreement = 0.75–0.90, excellent agreement >0.90). The remaining measurements were made by a single trained pneumologist who was blinded to the medical condition of the subject examined.

Statistical analysis

Categorical variables were described as absolute (n) and relative (%) values. Continuous variables were reported as median and range. The two groups were compared with the Mann-Whitney U test or Fisher's exact test as appropriate. A comparison between the three groups was made using the Kruskal-Wallis test. Then, we performed a multivariable logistic regression analysis considering, for the latter analysis, only parameters with a p-value ≥0.05 in the univariable analysis. Intraclass correlation coefficient (ICC) was used for agreement between the two DUS operators. Finally, Spearman's rank method was used for correlation analysis. All data were analyzed using SPSS Software version 25.0 (New York, NY, US: IBM Corp. USA). Graphs were created using GraphpadPrism 5 (Graphpad Software Inc., La Jolla California USA). We considered statistically significant a p-value <0.05.

Results

Clinical and demographic features of the study population

The demographics and clinical characteristics of the study population are shown in Table 14. CTD-ILD patients were less frequently male [8 (20%) vs. 32 (78%); p=<0.0001] and younger than patients with IPF [61 (28–78) vs. 74 (59–83) years; p=<0.0001]. Former smokers were less prevalent in the CTD-ILD group compared with the IPF group [12 (29%) vs. 25 (61%); p = 0.008]. Antifibrotic therapies (pirfenidone or nintedanib) were equally distributed between groups, while 23 (56%) CTD-ILD patients were on low-dose corticosteroids during ultrasound evaluation. Cardiovascular and metabolic diseases were less frequent in CTD-ILD patients than in IPF patients [10 (24%) vs. 30 (73%) p=<0.0001 and 2 (5%) vs. 9 (22%) p = 0.045] while the prevalence of gastroesophageal reflux disease (GERD) was similar in both groups.

Table 14: Demographics, clinical characteristics, respiratory function parameters, and diaphragm measurements during quiet breathing of the overall population and of patients with CTD-ILD, IPF, and healthy subjects.

	Overall population (n=82)	Healthy subjects (n=15)	P value	CTD-ILD (n=41)	IPF (n=41)	P value
Age (years)	70 (28 – 83)	54 (45 – 63)	**<0.0001**	61 (28 – 78)	74 (59 – 83)	**<0.0001**
Male - n (%)	40 (49%)	7 (47%)	0.999	8 (20%)	32 (78%)	**<0.0001**
Smoke history						
• **Current - n (%)**	3 (4%%)	1 (7%)	0.495	2 (5%)	1 (2%)	0.999
• **Former smokers - n (%)**	37 (45%)	1 (7%)	**0.004**	12 (29%)	25 (61%)	**0.008**
Pack/years	0 (0 – 80)	0 (0 – 5)	**0.006**	0 (0 – 30)	8 (0 – 80)	**0.001**
BMI (Kg/m^2)	27 (16.8 – 41)	25 (22.1 – 42.4)	0.321	26 (16.8 – 41)	28 (22.3 – 36.6)	0.109
Steroid therapy - n (%)	23 (28%)	-	-	23 (56%)	-	-
Antifibrotic therapy - n (%)	41 (50%)	-	-	-	41 (100%)	-
Nintedanib - n (%)	23 (28%)	-	-	-	23 (56%)	-
Pirfenidone - n (%)	18 (22%)	-	-	-	18 (44%)	-
Oxygen on effort - n (%)	13 (16%)	-	-	2 (5%)	11 (27%)	**0.013**
mMRC ≥ 2 - n (%)	36 (44%)	-	-	19 (46%)	17 (41%)	0.824
Months from diagnosis	35 (0 – 229)	-	-	43 (6 – 229)	30 (0 – 113)	**0.018**
Comorbidities			-			
Cardiovascular - n (%)	40 (49%)	-	-	10 (24%)	30 (73%)	**<0.0001**
GERD - n (%)	43 (52%)	-	-	24 (58%)	19 (46%)	0.377
Diabetes - n (%)	11 (13%)	-	-	2 (5%)	9 (22%)	**0.045**

Diaphragm measurements						
Ti dx (cm)	0.17 (0.08 – 0.34)	0.19 (0.12 – 0.24)	0.216	0.17 (0.08 – 0.27)	0.19 (0.11 – 0.34)	**0.036**
Te dx (cm)	0.12 (0.06 – 0.27)	0.14 (0.08 – 0.17)	0.591	0.12 (0.06 – 0.2)	0.14 (0.07 – 0.27)	0.087
TF (%)	40 (10 – 83)	44 (25 - 54)	0.303	36 (10 – 83)	42 (14 – 80)	0.447
TF < 30 %	24 (29%)	1 (7%)	0.105	15 (37%)	9 (22%)	0.219
DD dx (cm)	1.6 (0.6 – 2.8)	1.5 (1.1 – 2.4)	0.927	1.4 (0.6 – 2.8)	1.8 (0.9 – 2.6)	**0.021**
Respiratory function						
FVC (L)	2.5 (1.1 – 4.7)	-	-	2.4 (1.1 – 4.7)	2.6 (1.24 – 4.09)	0.386
FVC (%)	88 (43 – 152)	-	-	89 (43 – 152)	79 (47 – 139)	0.282
TLC (L)	3.8 (1.8 – 7.5)	-	-	3.6 (1.9 – 7.5)	3.9 (1.8 – 5.9)	0.575
TLC (%)	68 (38 – 112)	-	-	75 (42 – 112)	63 (38 – 100)	**0.014**
DLCO (%)	3.8 (1.8 – 7.5)	-	-	69 (27 – 115)	52 (23 – 88)	**0.0006**
MIP (cmH2O)	69 (14– 134)	-	-	57 (14 – 103)	77 (37 – 134)	**0.0009**
MEP (cmH2O)	80 (22 – 128)	-	-	77 (22 – 124)	89 (27 – 128)	0.075

CTD-ILD: connective tissue disease-associated interstitial lung disease, IPF: idiopathic pulmonary fibrosis, GERD: gastroesophageal reflux disease, BMI: body mass index, mMRC: Modified British Medical Research Council Questionnaire, TF: thickening fraction, Ti: inspiratory thickness, Te: expiratory thickness, DD: diaphragmatic displacement, FVC: forced vital capacity, DLCO: diffusion lung carbon monoxide, TLC: total lung capacity, FEV1: forced expiratory volume in 1 s, MEP: maximum expiratory pressure, MIP: maximum inspiratory pressure. Values are expressed as numbers and (%) or median and range, as appropriate. Chi-square test, Fisher's t-test (n < 5) for categorical variables, and Mann–Whitney t-test for continuous variables was used.

Diaphragm assessment, lung function, and radiologic evaluation

The incidence of diaphragmatic dysfunction was 37% in the CTD-ILD group, 22% in IPF, and 7% in the control group. Compared to the IPF group, CTD-ILD patients recorded the following ultrasound and functional respiratory parameters: i) lower DD and Ti [1.4 (0.6–2.8) vs. 1.8 (0.9–2.6) cm, p = 0.021 and 0.17 (0.08–0.27) vs. 0.19 (0.11–0.34) cm, p = 0.036; respectively] (Table 14); ii) greater functional parameters (TLC %pred and DLCO%) [75 (42–112) vs. 63 (38–100), p = 0.014 and 69 (27–115) vs. 52 (23–88), p = 0.0006; respectively] (Table 14); and iii) lower MIP [57 (14–103) vs. 77 (37–134) cmH2O; p = 0.0009] (Table 14). While comparing CTD-ILD with healthy subjects, Ti was lower [0.17 (0.08–0.27) vs. 0.19 (0.12–0.24) cm; p = 0.039] and diaphragmatic dysfunction was more frequent [15 (37%) vs. 1 (7%); p = 0.043]. No differences were observed between IPF and healthy subjects.

Considering the whole population, the multivariable model (Table 15) showed as a TF <30% was an independent predictor of moderate/severe dyspnea (mMRC ≥2) (OR 3.8, 95%CI [1.39–10.39]; p = 0.009 and OR 6.3, 95%CI [1.3–29]; p = 0.021; respectively), as well GERD (OR 8.4, 95% CI [1.8–39.3], p = 0.007).

Table 15: predictors of dyspnea (mMRC ≥ 2 at the follow-up visit) in the overall population

	Univariable Analysis		Multivariable Analysis	
	OR (95% IC)	**P value**	**OR (95% IC)**	**P value**
Age (years)	0.99 (0.95 – 1.02)	0.501	-	-
BMI (Kg/m^2)	**1.1 (1.02 – 1.3)**	**0.023**	1.1 (0.97 – 1.36)	0.095
DD (cm)	0.62 (0.26 – 1.5)	0.280	-	-
TF dx (%) < 30%	**3.8 (1.38 – 10.3)**	**0.009**	**6.3 (1.3 – 29)**	**0.021**
Sex Male	1.7 (0.69 – 4.02)	0.256	-	-
Diagnosis IPF	0.82 (0.34 – 1.96)	0.656	-	-
CTD-ILD	-	-	-	-
Smoke history Yes	0.89 (0.37 – 2.14)	0.803	-	-
Steroid use Yes	1.25 (0.47 – 3.28)	0.655	-	-
GERD Yes	**2.84 (1.14 – 7.05)**	**0.024**	**8.4 (1.8 – 39.3)**	**0.007**
Cardiovascular disease - yes	1.09 (0.46 – 2.6)	0.845	-	-
Disease duration (months)	0.99 (0.98 – 1.00)	0.632	-	-
FVC (%)	**0.96 (0.93 – 0.98)**	**0.001**	0.98 (0.95 – 1.01)	0.287
DLCO (%)	**0.93 (0.89 – 0.96)**	**0.0001**	0.96 (0.92 – 1.01)	0.139
Oxygen therapy (on effort) - yes	**22 (2.7 – 183.1)**	**0.004**	12.6 (0.86 – 185.4)	0.065

FVC: forced vital capacity, GERD: gastroesophageal reflux disease, TF: thickening fraction, BMI: body mass index, CTD-ILD: connective tissue disease-associated interstitial lung disease, DD, diaphragmatic displacement, DLCO: diffusion lung carbon monoxide, mMRC: Modified British Medical Research Council Questionnaire.

Correlation analysis between diaphragm evaluation and lung function

In the CTD-ILD group, we found a positive correlation between TF and FVC%pred. (r = 0.45, p = 0.003), TLC%pred. (r = 0.42, p = 0.006), FEV1 (L) (r = 0.39, p = 0.011) and DLCO% (r = 0.48, p = 0.001) (Fig. 2). Conversely, in the IPF group, no correlation was found between TF and all functional parameters assessed (data not shown), such as FVC%pred (r = 0.29, p = 0.058), and TLC%pred. (r = 0.25, p = 0.101), and DLCO% (r = -0.01, p = 0.915).

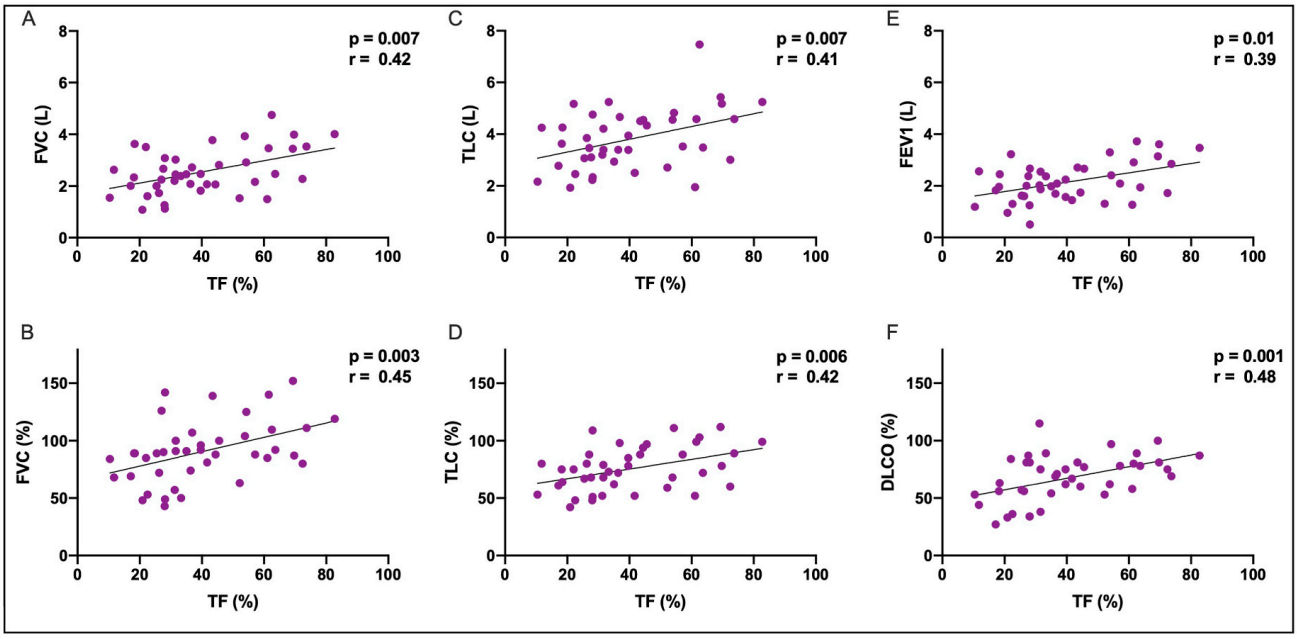

Fig. 13. Correlation between respiratory functional parameters and TF (%) during quiet breathing in patients with CTD-ILD. Legend: FVC: forced vital capacity, DLCO: diffusion lung carbon monoxide, TLC: total lung capacity, FEV1: forced expiratory volume in 1 s.

In conclusion, we found a prevalence of 29% of diaphragmatic dysfunction in outpatients with Interstitial Lung Disease. Moreover, a TF<30% was related to moderate/severe dyspnea and positively correlated with CTD-ILD patients' lung function. The ultrasound assessment of diaphragmatic function represents a non-invasive and reliable tool that could contribute, in combination with respiratory function tests, to the evaluation of ILD patients.

Study 6): ***Radiological scores in Idiopathic pulmonary fibrosis (IPF) patients according to MUC5B polymorphism***
Cocconcelli E, ***Bernardinello N,*** *....et al. IJMS, (2023).*

The aim of this study was to determine whether the MUC5B rs35705950 genotype affects the radiological patterns of IPF patients at diagnosis and its association with radiologic changes during the first year of treatment.

Study population and study design

In this longitudinal retrospective study, we consecutively collected and analyzed a cohort of well characterized patients with IPF referred to our center between April 2014 and June 2022. Seventy-eight patients were included (Table 16) due to the inclusion criteria of having two HRCT available, at diagnosis and after 1-year treatment. All patients were genotyped for MUC5B promoter's SNP rs35705950 [54] by PCR amplification and Sanger sequencing and finally categorized in two groups: the TT/TG genotype (n=54) and the GG genotype (n=24), respectively. Each patient provided a blood sample for DNA extraction and morphometric analysis before starting antifibrotic treatment. Patients were treated with pirfenidone or nintedanib, and the choice between these two drugs was made according to eligibility criteria and the risk of associated adverse events. Based on their annual rate of decline (≥ 5 or < 5% pred.) in absolute FVC% pred. during the first year of treatment, patients were defined as progressors or stable, respectively. Improvement of FVC (%pred. and mL) was expressed as negative value. The overall survival (OS) was calculated from the beginning of the treatment to death, transplant or loss to follow-up; survival data were censored at the end of the study (June 2022).

Table 16. Patient's demographics and clinical characteristics of the entire study population, and cathegorized in TT/TG genotype or GG gentotype.

	Entire Population (n =78)	**TT/TG genotype (n =54)**	**GG genotype (n =24)**	**p Value**
Male – n (%) **Female – n (%)**	64 (82) 14 (18)	44 (82) 10 (18)	20 (83) 4 (17)	0.84
Age at diagnosis – years	69 (44–82)	68 (44-82)	72 (50-82)	0.16
Body mass index (BMI) – kg/m²	27 (19-37)	26 (19-33)	27 (23-37)	0.83
Smoking history – pack years	10 (0–240)	10 (0-50)	30 (0 - 240)	**0.0006**
• **Current – n (%)**	7 (9)	5 (9)	2 (8)	0.36
• **Former – n (%)**	50 (64)	32 (59)	18 (75)	
• **Nonsmokers – n (%)**	21 (27)	17 (32)	4 (17)	

Radiological diagnosis – n (%) **Histological diagnosis – n (%)**	40 (51) 38 (49)	23 (43) 31 (57)	17 (71) 7 (29)	**0.02**
FVC at diagnosis – L	2.66 (1.53–4.61)	2.79 (1.67-4.36)	2.40 (1.53-4.61)	**0.03**
FVC at diagnosis – %pred.	77 (47–126)	79 (56–126)	72 (47–118)	0.08
TLC at diagnosis - %pred.	73 (40-96)	73 (45-96)	73 (40-93)	0.32
DL_{CO} at diagnosis – %pred.	56 (7–93)	56 (7-89)	56 (28-93)	0.60
Gastroesophageal reflux – n (%)	31 (40)	22 (41)	9 (38)	0.78
Cardiovascular diseases – n (%)	53 (68)	37 (69)	16 (67)	0.87
Metabolic syndrome – n (%)	33 (42)	22 (41)	11 (46)	0.67
Pirfenidone– n (%)	42 (54)	31 (57)	11 (46)	0.34
Nintedanib – n (%)	36 (46)	23 (43)	13 (54)	
FVC decline in the 1st year– mL	46 (-573–657)	59 (-573-657)	34 (-559-461)	0.70
FVC decline in the 1st year – %pred.	0 (-29-21)	1 (-29-21)	0 (-12-16)	0.80
Stable – n (%)	62 (79)	43 (80)	19 (79)	0.96
Progressors – n (%)	16 (21)	11 (20)	5 (21)	
Nausea and vomiting - n (%)	11 (14)	10 (19)	1 (4)	0.09
Diarrhea – n (%)	25 (18)	19 (20)	7 (29)	0.60
Weight loss - n (%)	14 (32)	10 (35)	5 (21)	0.81
Increase in AST, ALT – n (%)	2 (3)	2 (4)	0 (0)	0.33
Transplanted – n (%)	4 (5)	3 (6)	1 (4)	0.79
Deaths – n (%)	27 (35)	9 (17)	8 (33)	0.09

Values are expressed as numbers and (%) or median and ranges as appropriate. Negative values mean improvement of FVC. To compare demographic data and baseline clinical characteristics between TT / GT genotype and GG genotype, Chi square test and Fisher t test (n < 5) for categorical variables and Mann-Whitney U test for continuous variables were used. AST = aspartate aminotransferase; ALT = alanine aminostransferase. Values are expressed as numbers and (%) or median and ranges as appropriate. Negative values mean improvement of FVC. To compare demographic data and baseline clinical characteristics between TT / GT genotype and GG genotype, Chi square test and Fisher t test (n < 5) for categorical variables and Mann-Whitney U test for continuous variables were used.

Sample processing, DNA extraction and Sanger sequencing

Volumes of 5-10 mL of blood were collected from each patient, placed in EDTA tubes and stored at 4°C before plasma separation and centrifuged at 1,600 g for 10 min at 4°C within 8 h from collection. Plasma samples were transferred to 2 mL sterile tubes, which were shipped in a dry ice container. DNA was isolated from 300 uL of plasma using the QIAamp® DNA FFPE tissue kit (Quiagen, Netherlands) in accordance with the manufacturer's operational manual. DNA extracted from plasma was used as the template for the polymerase chain reaction (PCR). PCR was performed with this primer sequence 5'-3': forward GGTTCTGTGTGGTCTAGG, reverse: TGTTTGCTCAGCGTGTTTG The PCR reaction phase was performed as follows: (step 1) initial denaturation at 94°C for 5 minutes; (step 2) three step-cycle repeated for 40 cycles: denaturation at 94°C for 15 seconds, annealing at 56°C for 20 seconds and elongation at 72°C for 20 s; (step 3) final step maintaining the samples at 72°C for 5

min. The amplified DNA was evaluated by agarose gel electrophoresis and its size was estimated with GeneRuler 1 kb DNA Ladder (#SM0311 -ThermoFisher scientifics, Italy). The amplified DNA was purified with PureLink® PCR Purification Kit (#K310001 - ThermoFisher scientifics, Italy) and the concentration evaluated with NanoDrop 1000 Spectrophotometer V3.8 (ThermoFisher scientifics, Italy). The purified DNA was desiccated with the forward primer and sequenced using Sanger's technique with BigDyeTM Terminator v3.1 (ThermoFisher scientifics, Italy) on the instrument AB3730XL (ThermoFisher scientifics, Italy). Three possible results could be obtained: wild type (GG); heterozygosis (TG) or variant homozygous (TT).

Radiological scoring

The HRCTs available at treatment initiation (HRCT1) and at 12-month follow-up (HRCT2) were scored by two expert thoracic radiologists. The HRCTs were performed by a 64-slice Siemens Somatom Sensation (Siemens Healthcare, Erlangen, Germany) applying a slice thickness ≤ 1.5 mm. The two thoracic radiologists were blind to clinical and functional data. This represented a modification of the previously reported [55] scoring systems that allowed us to evaluate the interstitial "reticulations" more precisely. Specifically, the radiologic features considered in this study were ground glass opacities (GGO) (alveolar score, AS), reticulations (interstitial score, IS), and honeycombing (HC) (honeycombing score, HC). For each lung lobe, the two radiologists assessed the extent of AS, IS and HC using a scale from 0-100 and estimated the extent to the nearest 5%. After each individual lobe was scored, the result was expressed as the mean value of the five lobes in AS, IS, and HC. Finally, the IS and HC were pooled (IS+HC) to analyze the amount of fibrotic abnormalities. The level of interobserver agreement was obtained for each patient as a mean of 5 lobes and for each radiological abnormality and expressed as Cohen's k value. Disagreement between radiologists was resolved by consensus. The association between radiological change and FVC decline was calculated as the change in AS (ΔAS/month), IS (ΔIS/month), HC (ΔHC/month), pooled IS and HC (ΔIS+HC/month) and the change in FVC milliliters (ml) per month (ΔFVC ml/month) and FVC% pred. per month (ΔFVC% pred./month) between HRCT1 and HRCT2.

Statistical analysis

Categorical variables are described as absolute (n) and relative values (percentage, %), whereas continuous variables are described as median and range. To compare demographic data and baseline clinical characteristics between stable TT/TG and GG genotypes, the Chi-square test or Fisher's exact test for categorical variables and the Mann-Whitney U test for continuous variables were used as appropriate. Wilcoxon signed-rank test was performed to compare HRCT1 and HRCT2 for the grading scores of different variables in the entire population, in TT/TG patients and GG patients. Correlation coefficients between radiological and functional data were calculated using the nonparametric Spearman's rank method. The level of interobserver agreement between the two radiologists was evaluated by the kappa statistic measure. The overall

survival was calculated from treatment initiation to death or lung transplantation, with data censored in June 2022. The cumulative survival rate was calculated using the Kaplan-Meier method, and the difference in the survival time between the two groups (TT/GT and GG genotype) was assessed with a log-rank test. Radiological scores were evaluated to determine their relationship with survival in a univariate analysis of Cox proportional hazards regression testing. Variables with an association statistically significant with overall survival at univariate analysis were included in a multivariate Cox proportional hazard regression test to find the factors independently associated with mortality.All data were analyzed using SPSS Software version 25.0 (New York, NY, US: IBM Corp. USA) and figures were created with GraphPad Prism (version 8.3.1, GraphPad Software, La Jolla, CA, USA). P-values < 0.05 were considered statistically significant.

Results

Clinical and functional evaluation at baseline and during the 1-year follow-up.

Clinical and functional characteristics at baseline of the patients included in the study are shown in Table 16. Most patients were males (82%) and former smokers (64%) with a median age at diagnosis of 69 years (range 44–82). Based on the MUC5B rs35705950 genotyping, 54 patients were classified as having a TT/TG genotype and 24 patients had a GG genotype. At treatment initiation, the TT/GT and GG genotype groups were homogeneous for sex, age, body mass index (BMI), and main comorbidities (gastroesophageal reflux, cardiovascular diseases, and metabolic syndrome), while GG genotype patients have a heavier smoking history of 30 pack years (0 - 240) vs. 10 pack years (0 – 50; p = 0.0006). GG genotype patients have a significantly less preserved FVC (% pred. and L) at treatment initiation and a higher % of patients receiving a clinical - radiological diagnosis [17 (71%) vs. 23 (43%), p = 0.02], as compared to TT/TG genotype patients. Based on the annual FVC% pred. decline during treatment (≥ 5 or < 5% pred.), most patients were classified as stables [62 stable patients (79%) vs. 16 progressors (21%)], with equal proportion between the two groups (80% in TT/TG and 79% in GG genotype stable patients, and 20% progressors in TT/TG group and 21% in GG group, respectively). 27 (35%) patients died during the follow-up period, with equal proportion between the two genotyped groups. The allele frequency of the MUC5B rs35705950 T allele was 66/156 (42%), while the frequency of the wild-type G allele was 90/156 (58%). The MUC5B rs35705950 genotype frequencies met the Hardy–Weinberg equilibrium (Table 17).

Table 17. MUC5B rs35705950 genotype frequency.

		Observed	Expected	p Value
T allele: 66/156 (42%)	**TT genotype – n (%)**	12 (15)	16 (17)	
G allele: 90/156 (58%)	**TG genotype – n (%)**	42 (54)	43 (49)	0.82
	GG genotype – n (%)	24 (31)	30 (34)	

Chi square test for categorical variables was used.

Radiological scoring at baseline

Alveolar, honeycombing, interstitial and pooled honeycombing and interstitial score in the HRCT performed at diagnosis (HRCT1) were similar between the two genotype groups (Table 18). In particular, at baseline AS was 22% (0 - 62) in TT/TG and 16% (0 - 44) in GG (p=0.52), HC was 2% (0 - 41) in TT/TG and 3% (0 - 70) in GG (p=0.54), IS was 22% (0 - 52) in TT/TG and 25% (0 - 45) in GG (p = 0.91), HC+IS was 28% (9 - 73) % in TT/TG and 30% (8 - 89) in GG (p = 0.76) (Figure 13 Panel A-D). The inter-observer agreement between the two radiologists with regard to change in AS, IS, and HC was good (Cohen's kappa = 0.71 for IS, k=0.76 for AS, k=0.80 for HC), as previously described[9].

Table 18. Radiological scores at treatment initiation (HRCT1) of the entire study population, and cathegorized in TT/TG genotype or GG gentotype.

	Entire Population (n =78)	TT/TG genotype (n =54)	GG genotype (n = 24)	p Value
Alveolar score - %	20 (0-62)	22 (0-62)	16 (0-44)	0.53
Honeycombing score - %	2 (0-70)	2 (0-41)	3 (0-70)	0.54
Interstitial score - %	23 (0-52)	22 (0-52)	25 (0-45)	0.91
Pooled interstitial score and honeycombing - %	28 (8-89)	28 (9-73)	30 (8-89)	0.76

Values are expressed as median and ranges. To compare the radiological scores in HRCT1 between TT / GT and GG genotype groups, and Mann-Whitney U test for continuous variables was used.

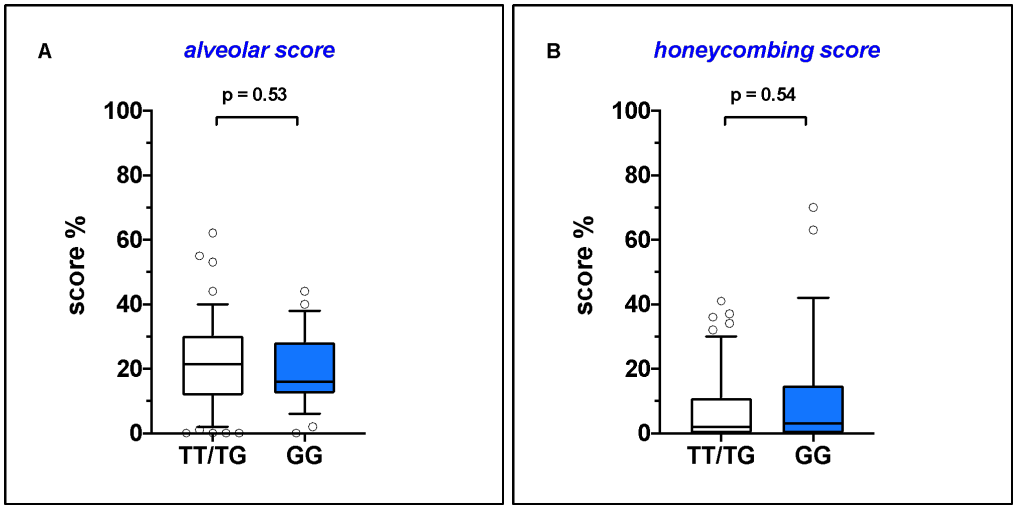

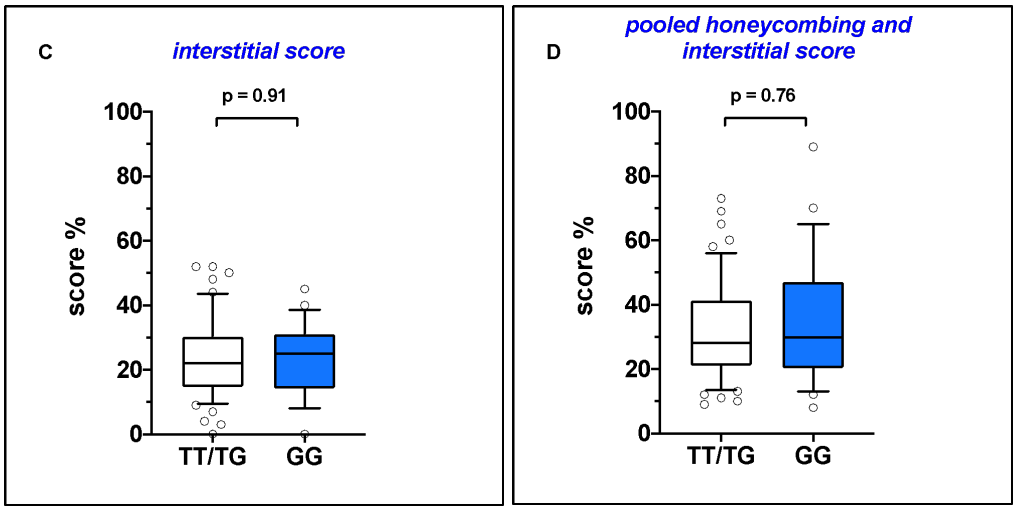

Figure 14. Radiological scores at treatment initiation (HRCT1) of the study population cathegorized in TT/TG genotype or GG gentotype. Values of alveolar score (Panel A), honeycombing score (panel B), interstitial score (panel C) and pooled honeycombing and interstitial score (Panel D) at treatment initiation (HRCT1) in TT/TG genotype patients (TT/TG) and GG genotype patients (GG). Horizontal bars represent median values; bottom and top of each box plot 25th and 75th, brackets 10th and 90th percentiles, while circles represent outliers. White boxes indicate TT/TG genotype patients and blue boxes GG genotype patients.

Radiological scoring during 1-st year follow up

In the entire study population, HC and HC+IS increased significantly between HRCT1 and HRCT2 from 2% (0 - 70) to 6% (0 – 70, $p < 0.0001$) and from 28% (8 - 89) to 33% (8 – 98, $p < 0.0001$), respectively (Figure 14). AS and IS remain similar between HRCT1 and HRCT2 from 20% (0 - 62) to 20% (0 – 64, $p = 0.16$) and from 22% (0 - 52) to 23% (0 - 59, $p = 0.12$), respectively (Figure 14). When the study population was stratified by MUC5B rs35705950 genotype, in TT/TG patients HC increased significantly between HRCT1 and HRCT2 from 2% (0 - 41) to 5% (0 – 63, $p = 0.001$) (Figure 15, Panel B), whereas AS and IS did not, from 22% (0 - 62) to 21% (0 – 64, $p = 0.81$) and from 22% (0 - 52) to 23% (0 – 59, $p = 0.47$) respectively (Figure 15, Panel A, C). Conversely, among GG patients both AS and HC increase significantly from 16% (0 - 44) to 18% (1 – 86, $p = 0.05$) and from 3% (0 - 70) to 7% (0-83, $p = 0.007$), whereas IS remain similar between HRCT1 and HRCT2: from 26% (0 – 45) to 26% (0 – 53, $p = 0.15$), respectively (Figure 15, Panel A-C). When HC and IS were pooled together, the HC+IN score increased significantly in TT/TG patients (from 28% (9 - 73) to 30% (9 - 93), $p = 0.001$), and in GG patients (from 28% (8 - 89) to 42% (8 – 89, $p = 0.002$), respectively (Figure 15, Panel D).

Table 19. Radiological scores at treatment initiation (HRCT1) and after one year of treatment (HRCT2) in the entire study population.

	$HRCT_1$	$HRCT_2$	p value		$HRCT_1$	$HRCT_2$	p value
AS	20 (0-62)	20 (0-64)	0.16	**IS**	22 (0-52)	23 (0-59)	0.12

HC	2 (0-70)	6 (0-83)	**< 0.0001**	**HC+IS**	28 (8-89)	33 (8-98)	**< 0.0001**

AS = alveolar score; IS = interstitial score; HC = honeycombing; HC+IS = pooled interstitial score and honeycombing. Values are expressed as median and range. P values refer to comparisons between HRCT1 and HRCT2, and Wilcoxon signed rank test for pared non parametric data was used.

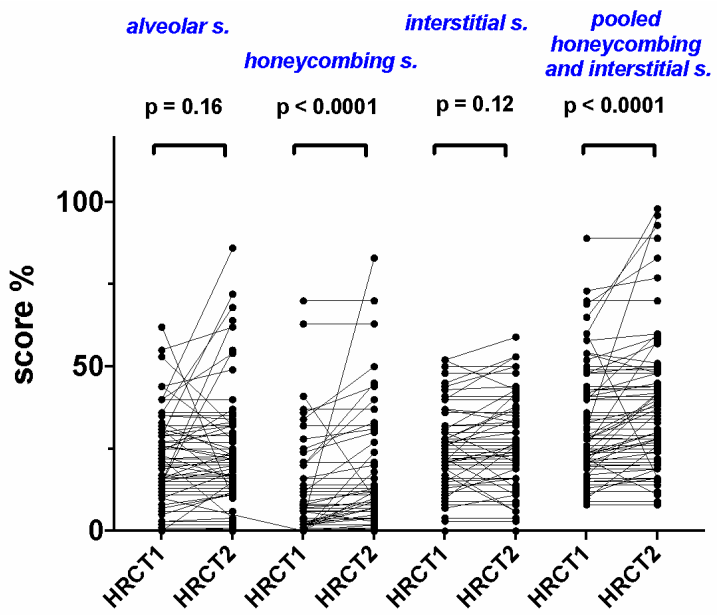

Figure 15. Radiological scores at treatment initiation (HRCT1) and after one year of treatment (HRCT2) in the entire study population. Change in alveolar score, interstitial score, honeycombing and pooled interstitial score and honeycombing at treatment initiation (HRCT1) and after one year of treatment (HRCT2) in the entire study population.

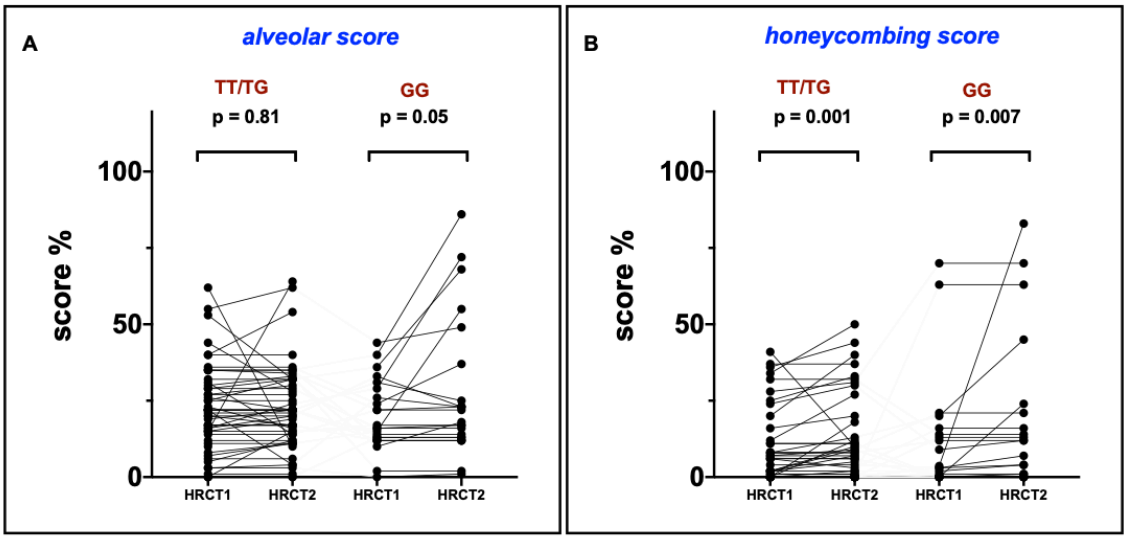

	HRCT1	HRCT2		HRCT1	HRCT2
TT/TG	22 (0-62)	21 (0-64)	GG	16 (0-44)	18 (1-86)*

	HRCT1	HRCT2		HRCT1	HRCT2
TT/TG	2 (0-41)	5 (0-50)*	GG	3 (0-70)	7 (0-83)*

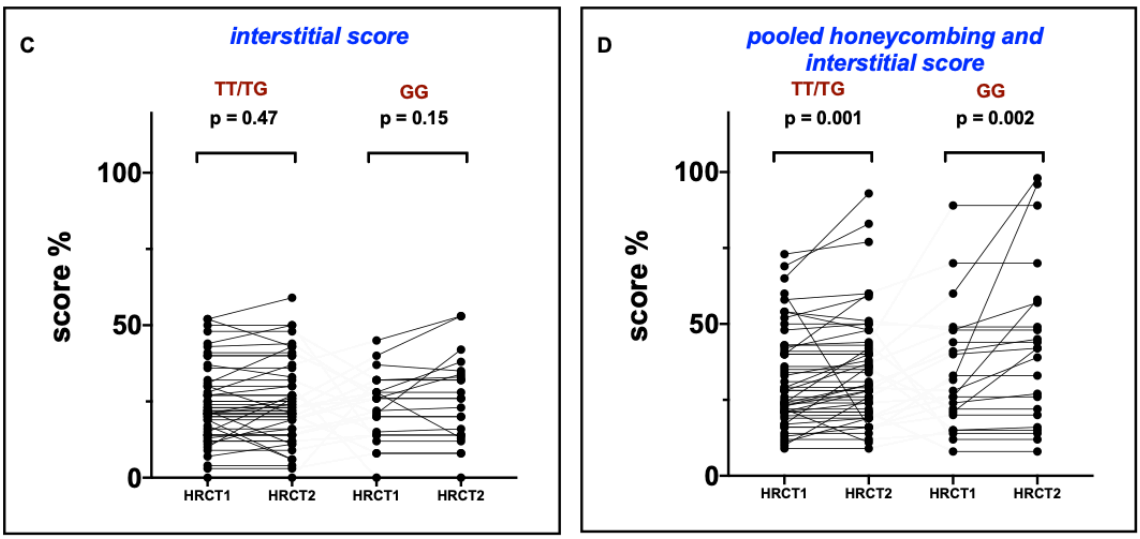

	HRCT$_1$	HRCT$_2$		HRCT$_1$	HRCT$_2$
TT/TG	22 (0-52)	23 (0-59)	GG	26 (0-45)	26 (0-53)

	HRCT$_1$	HRCT$_2$		HRCT$_1$	HRCT$_2$
TT/TG	28 (9-73)	30 (9-93)*	GG	28 (8-89)	42 (8-98)*

Figure 16. Change in alveolar score (Panel A), honeycombing (Panel B), interstitial score (Panel C) and pooled interstitial score and honeycombing (Panel D) at treatment initiation (HRCT1) and after one year of treatment (HRCT2) in TT/TG and GG genotype patients. P values and * refer to comparisons between HRCT1 and HRCT2 and Wilcoxon signed rank test for pared non parametric data was used.

Survival analysis and multivariate analysis

We had the chance to analyze a longer observational period as compared with our previous study and we were able to confirm that the overall survival of TT/TG genotype patients was higher than overall survival of GG genotype patients. Indeed, the proper median survival was 69 months for TT/TG genotype patients and 41 months for GG genotype patients (HR 0.52, 95% CI 0.28 – 0.98; p= 0.04) (Figure 16). To detect if radiological scores may be considered factors predictive of survival in the entire IPF population, we used Cox proportional hazards regression analysis. Univariate analysis of radiological factors associated with survival revealed that IS, HC+IS on HRCT1, AS, IS, HC+IS on HRCT2, the absolute increase in honeycombing and in HC had a significant positive association with survival in the entire IPF population (Table 20). Multivariate analysis performed, including variables having statistical significance in univariate analysis, revealed that only HC+IS on HRCT2 (HR: 1.02; 95%CI: 1.00 – 1.03; p = 0.01) are independent predictors of mortality in IPF patients (Table 20).

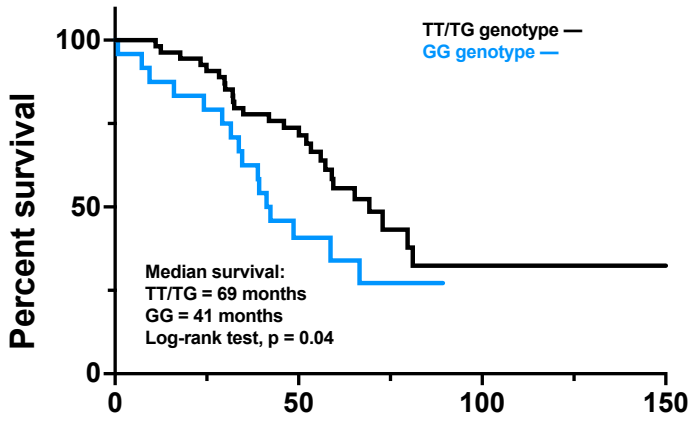

Figure 17. Survival of the study population categorized in TT/TG genotype or GG genotype.
Survival analysis of TT/TG and GG genotype patients. The black line represents the survival in the TT/TG group and the blue line represents the survival in the GG group. Kaplan Meier analysis was used with a log-rank test (HR 0.52, 95% CI 0.26 – 0.96; p= 0.04).

Table 20. Predictive factors of overall mortality in the entire population of IPF patients treated with antifibrotics.

	Univariate analysis		Multivariate analysis	
	HR (95% IC)	**p**	**HR (95% IC)**	**p**
Alveolar score in HRCT1 (%)	1.01 (0.99 – 1.03)	0.11	-	-
Honeycombing in HRCT1 (%)	1.00 (0.98 – 1.02)	0.52	-	-
Interstitial score in HRCT1 (%)	1.03 (1.00 – 1.05)	**0.01**	1.08 (0.99 – 1.17)	0.07
Interstitial s. and honeycombing in HRCT1 (%)	1.01 (1.00 – 1.03)	**0.02**	0.97 (0.93 – 1.01)	0.15
Alveolar score in HRCT2 (%)	1.02 (1.00 – 1.04)	**0.008**	1.01 (0.99 – 1.04)	0.15
Honeycombing in HRCT2 (%)	1.01 (0.99 – 1.03)	0.16	-	-
Interstitial score in HRCT2 (%)	1.03 (1.00 – 1.05)	**0.009**	0.94 (0.88 – 1.01)	0.14
Interstitial s. and honeycombing in HRCT2 (%)	1.02 (1.00 – 1.03)	**0.003**	1.02 (1.00 – 1.03)	**0.01**
Change in Alveolar score (%)	1.00 (0.99 – 1.05)	0.98	-	-
Change in Interstitial score (%)	1.02 (0.94 – 1.10)	0.44	-	-
Change in Honeycombing (%)	1.03 (1.01 – 1.06)	**0.03**	1.05 (0.97 – 1.13)	0.18
Change in Interstitial s. and honeycombing (%)	1.02 (0.99 – 1.05)	0.058	-	-

Values are expressed as HR (95%CI). Univariate and multivariate Cox proportional hazard regression tests were used to determine the relationship of radiological scores with survival.

In conclusion, the current study showed that patients who carriers the mutant rs35705950 T allele presented better survival than the wild-type group, regardless of the extension of HRCT changes at baseline which was similar in the two groups. We also observed that the alveolar score was significantly increased after treatment in the GG genotype patients but not in the TT/TG group. This evidence confirmed the protective role of MUC5B polymorphism on the prognosis of patients with IPF.

Study 7): ***Evaluation of the potential inhibition of Galectine-3 by Hyaluronic Acid.*** *In collaboration with Dr. A. Casara, Dr. M. Conti, Prof. E. Bazzan, Prof. M. G. Cosio, and Prof. M. Saetta.*

The scope of this project was to test if Hyaluronic Acid (in the concentration of 3.0 mg/ml) could inhibit the production of galectin-3 (Gal-3), collagen-one (Col-1), and TGF beta (TGFb) in a vitro model of pulmonary fibrosis. Moreover, we try to investigate the effects of Gal-3 at the cellular level.

Materials and methods

For the first part, THP1 (human monocytic leukemia cells-Merk, Darmstadt, Germany) cells were used. For the second part, human-immortalized fibroblast cell cultures (IMR-90-HLF) were used. Before fibroblast culture, flasks were pre-treated with collagen to ameliorate cellular adherence.

All cell culture experiments were performed with a technical duplicate or triplicate for all variants measured and a biological triplicate (at least 3 cell culture set-ups), thus ensuring adequate experimental reproducibility.

All variables were analyzed with the following ELISA RUO kits: KIT for GAL-3: Sino Biological Inc. SEK10289; KIT for TGFb: RayBio® - ELH-TGFb1; KIT for COL-I: Nordic BioSite AB - EKX-F9VPFN-96; KIT for COL-III: Nordic BioSite AB - EKX-QWPJF7-96. All ELISA experiments were conducted following the kit instructions. All ELISA RUO-reported results had a coefficient of variation within 10% among different samples for the same variable as recommended for research measurement.

Part one: THP1 experiments

As the first part of the project, we try to induce the transition from THP1 cells to mature macrophages. The transition was obtained after a pro-inflammatory stimulation and was induced following a specific protocol (PMA + LPS + INFg), as reported by Baxter et al. [56] In Figure 17, we reported THP1 (panel A) and mature macrophages (B).

A) B)

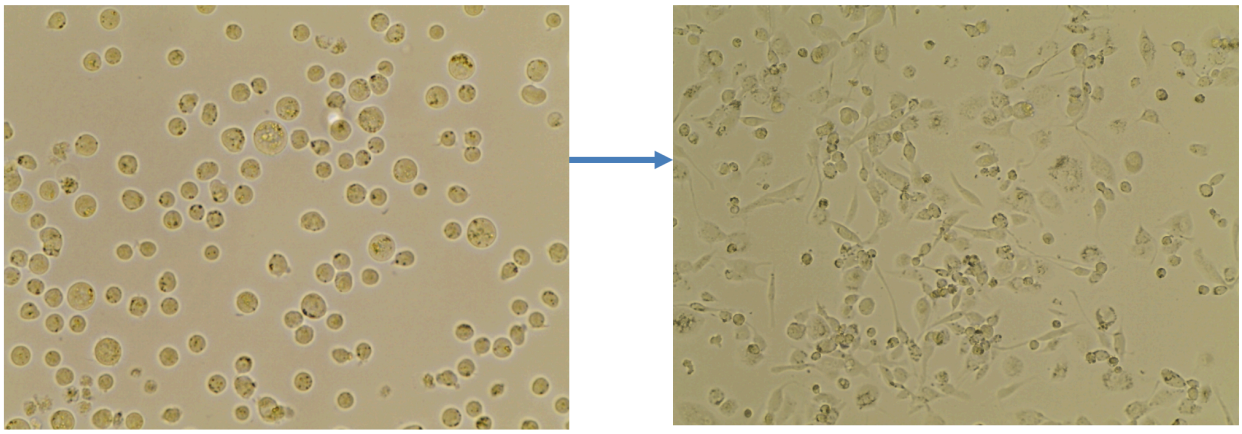

Figure 17: in panel A, floated macrophages as shown. In panel B, mature macrophages were shown after PMA, LPS, and INFg exposure. In this second picture, macrophages are adherent to the surface and change cellular shape according to their function.

After this transformation, macrophages produced larger quantities of Gal-3 in free form (pgr/ml). Supernatant values of Gal-3, in comparison with basal level, were significantly higher ($p<0.0001$). Moreover, after the exposure of hyaluronic acid at 3.0 mg/ml, the level of Gal-3 reduced significantly ($p<0.0001$). These data are reported in Figure 18).

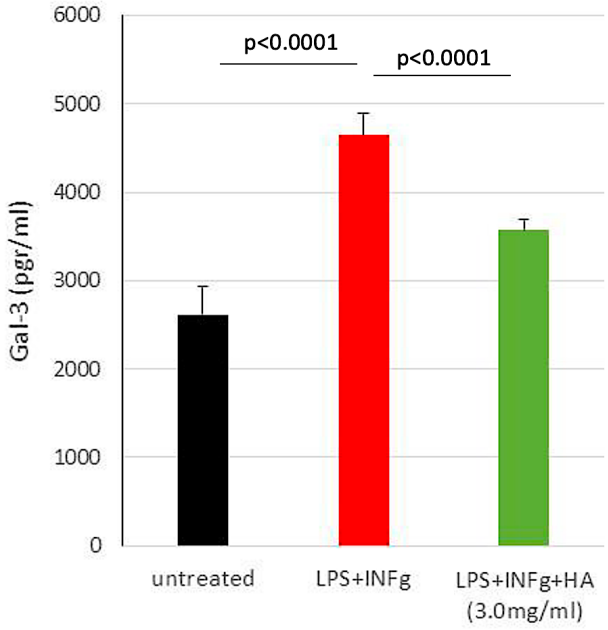

Figure 18): Levels of Gal-3 at basal condition (black bar). Levels of Gal-3 after PMA+LPS+INFg exposure (red bar). Level of Gal-3 after Hyaluronic acid exposure (green bar).

Part two: fibroblast experiments

In the second part, we aimed to test if fibroblasts can produce TGFb, Collagene one, and Galectin-3. In Figure 19, we show that after the exposure of macrophage supernatant at 40%, the product of TGFb was significantly increased by fibroblasts (p=0.008). 40% was selected because it was the best concentration that allowed the survival and activity of the macrophages. After hyaluronic acid exposure (3.0 mg/ml), the level of TGFb decreased significantly (p=0.008).

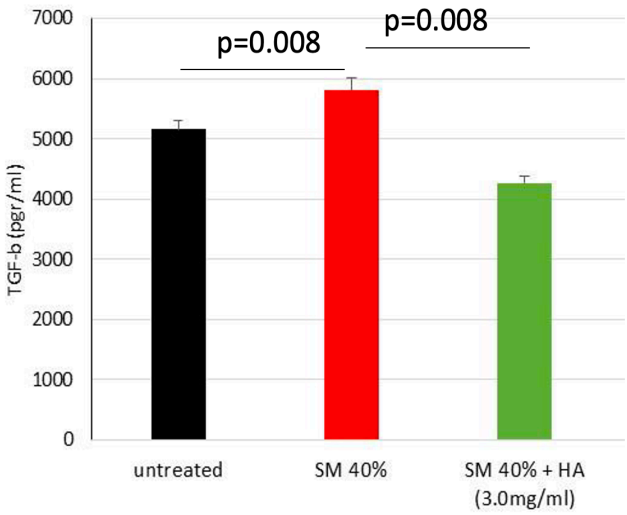

Figure 19): Levels of TGFb at basal condition (black bar). Levels of TGFb after the exposure of macrophages supernatant at 40% (red bar). Level of TGFb after Hyaluronic acid exposure at 3.0 mg/ml concentration (green bar).

Moreover, we aimed to test if fibroblasts can produce Collagene one (COL1) after TGFb stimulation. In Figure 20, we show that after TGFb stimuli, the product of Collagen-one was significantly increased by fibroblasts (p=0.0001). After hyaluronic acid exposure (3.0 mg/ml), the level of COL-1 decreased significantly (p=0.008).

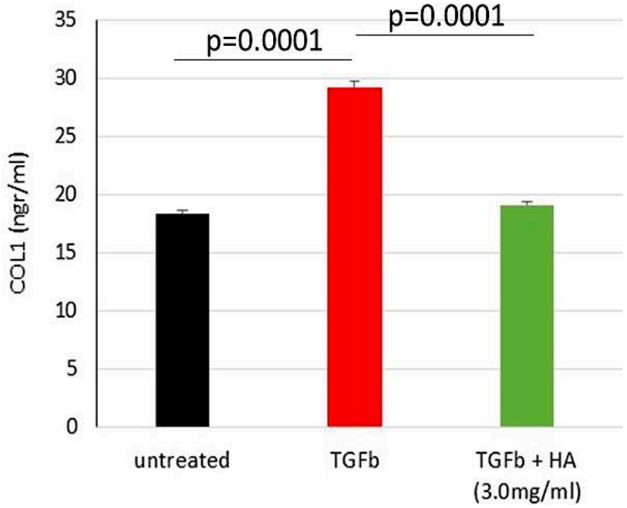

Figure 20): Levels of COL1 at basal condition (black bar). Levels of COL1 after TGFb exposure (red bar). Level of COL1 after Hyaluronic acid exposure at 3.0 mg/ml concentration (green bar).

Finally, we tested if fibroblasts can auto-produce Galectin-3 after TGFb stimuli given at two different time points (48 hours and 72 hour). In Figure 21, we show that after TGFb stimuli, the product of Galectin-3 was significantly increased by fibroblasts after 48 hours (p=0.001). After hyaluronic acid exposure (3.0 mg/ml), the level of Gal-3 decreased significantly (p=0.001). After 72 hours, the production of Gal-3 increased again (p=0.001), whereas, after hyaluronic acid exposure, levels of TGFb decreased significantly (p=0.001).

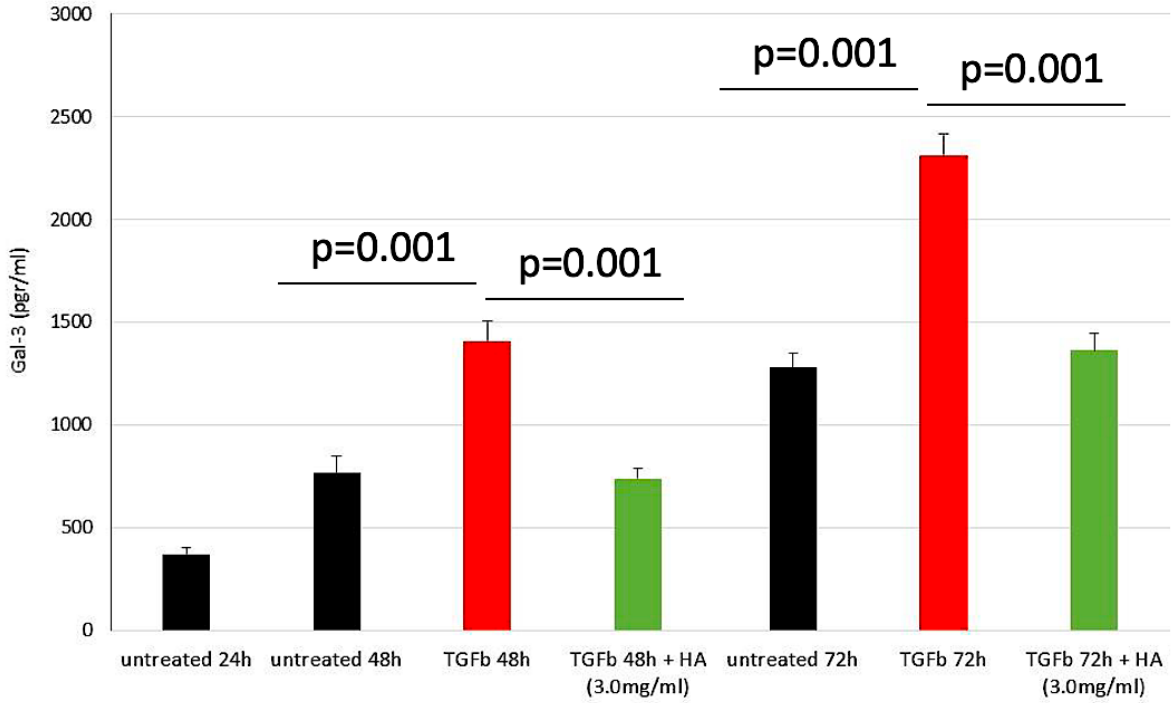

Figure 21: Levels of COL1 at basal condition (black bar). Levels of COL1 after TGFb exposure (red bar). Level of COL1 after Hyaluronic acid exposure at 3.0 mg/ml concentration (green bar).

In conclusion, for the first time, we have demonstrated that Hyaluronic Acid (HA) might have a role in preventing and treating fibrotic lung diseases, reducing the production of Gal-3, Col-1, and TGFb by stimulated fibroblasts.

Study 8): ***COVID-19 pneumonia: when do eosinophils matter?***
Bernardinello N*,…et al. European Respiratory Society Congress, Milan 2023*

The aim of this study was to evaluate the significance of hematological values in patients hospitalized for COVID-19 pneumonia in our hospital. The first goal was to investigate a possible association between these serum values and the intensity of care that patients need during hospitalization. The second goal was to explore the relationship between eosinophils and COVID-19sequela after discharge.

Study design and population
In this study, 327 well-characterized patients with SARS-CoV-2, referred to the University Hospital of Padua (Division of Infectious and Tropical Diseases, Respiratory Diseases Unit, and Intensive Care Unit), were retrospectively enrolled. Data were collected during the first and second pandemic waves, from February 2020 to September 2021. Clinical, radiological, and demographic data were obtained at the hospital admission and at the first follow-up visit, which is conducted after 3 months from hospital discharge.

Level of medical care definition
High-intensity medical care was defined as the need for a high-flow nasal cannula (HFNC) or invasive/non-invasive ventilation (IVM/NIV) [56]; conversely, low-intensity medical care is considered when patients need only low-flow oxygen supplementation (via nasal cannula or face mask). Based on this definition, the study population was categorized into two groups: low intensity care group (n=214) and high intensity care group (n=113). A second blood test in order to calculate the biomarkers mentioned above was obtained at the time of discharge. Hospital treatment (hydroxychloroquine, azithromycin, ceftriaxone, other antibiotics, lopinavir/ritonavir, remdesivir, tocilizumab, steroids, heparin, convalescent plasma) during hospitalization is finally reported. Differences in eosinophils between discharge and on admission were calculated and presented as Δ eosinophils (Δ eosinophils = eosinophils at discharge minus eosinophils on admission). Based on the radiological resolution of the lung changes, at the first follow-up visit (3 months) patients are divided into recovery group (n=168) and not-recovery group (n=159). Moreover, for a subgroup of patients (n=113) two expert thoracic radiologists blinded to clinical data scored the images independently with a composite semi-quantitative scale. With this method, ground glass opacities, consolidations, and reticulation are analyzed. For each lung lobe, the extent of ground glass (GGO), consolidations (CONS) and reticulation/Interstitial Score (IS) are assessed using a scale from 0 to 100. Only 54 patients presented a CT scan at the time of admission and were evaluated with the same semiquantitative score.

Statistical analysis

Descriptive statistics were used to summarise the characteristics of patients. Categorical variables are described as absolute (n) and relative values (%), whereas continuous variables as median and range (min-max). Fisher's exact test was used for categorical variables. Instead, the Whitney U test is used for quantitative variables. Wilcoxon signed-rank test was used to compare eosinophils values between admission and discharge. To assess the risk of not-REC at the first follow-up visit, univariate and multivariate regression analyses are performed. Continuous variables are dichotomized based on the median value for univariate and multivariate regression. Correlation coefficients between data are calculated using the non-parametric Spearman's rank method. All data are analysed using SPSS software version 25.0 (New York, NY, US: IBM Corp. USA) and GraphPad Prism V8 (GraphPad Software, La Jolla, CA, USA). P-values < 0.05 were considered statistically significant.

Results

Clinical characteristics of the study population

Considering the whole population, patients were more frequently male (64%) and no smokers (61%), with a median BMI of 27 (16 – 57). Moreover, the median age at SARS-CoV-2 diagnosis was 62 years (22 – 88). Other demographic characteristics of 327 patients are summarized in Table 21. We also divided patients based on the intensity of medical care: 214 patients required low-intensity medical care (LIMC), and 113 subjects needed high-intensity medical care (HIMC).

Table 21: Demographics and clinical characteristics of the overall population and patients divided into low-intensity of medical care group (n = 214) and high-intensity medical care group (n = 113).

	Overall (n=327)	**LIMC (n=214)**	**HIMC (n=113)**	**p**
Age - (years)	62 (22 – 88)	60 (22 – 87)	65 (25 – 88)	**0.01**
Sex – male, n° (%)	210 (64%)	137 (64%)	73 (65%)	0.92
BMI (kg/m^2)	27 (16 – 57)	26 (16 – 57)	27 (19 – 48)	0.19
Pack-years	0 (0 – 90)	0 (0 – 66)	0 (0 – 90)	0.27
Smoking History - n°	126 (39%)	75 (35%)	51 (45%)	0.09
Comorbidities				
• **Cardiological – n°**	162 (50%)	92 (43%)	70 (62%)	**0.001**
• **Pneumological – n°**	51 (16%)	37 (21%)	14 (12%)	0.24
• **Immunological - n°**	45 (14%)	29 (16%)	16 (16%)	0.88
• **Metabolic – n°**	151 (46%)	85 (40%)	66 (58%)	**0.001**
• **Oncological – n°**	54 (17%)	31 (14%)	23 (20%)	0.17
Symptoms – at admission				
• **Fever – n°**	303 (93%)	194 (91%)	109 (96%)	0.06
• **Asthenia – n°**	117 (36%)	81 (38%)	36 (32%)	0.28
• **Dyspnoea – n°**	156 (48%)	84 (39%)	72 (64%)	**0.0003**
• **Cough – n°**	184 (56%)	120 (56%)	64 (57%)	0.92

• **GI symptoms – n°**	71 (22%)	44 (21%)	27 (24%)	0.39
P/F	283 (40 – 542)	309 (121 – 542)	224 (40 – 461)	**<0.0001**
FiO2 – at admission	21 (21 – 100)	21 (21 – 88)	29 (21 – 100)	**<0.0001**
Hospitalization - days	11 (2 – 67)	8 (2 – 49)	18 (3 – 67)	**<0.0001**
CT scan – at admission				
- **Alveolar score**	7 (0 – 62)	5 (0 – 38)	18 (0 – 62)	**0.01**
- **Consolidation score**	1 (0 – 26)	0.8 (0 – 10)	4 (0 – 26)	**0.001**
- **Interstitial score**	1.6 (0 – 29)	0.8 (0 – 29)	10 (0 – 23)	**0.001**
Not-Rec patients - n°	159 (49%)	87 (41%)	72 (64%)	**0.0007**
Δ eosinophils	0.05 (-0.15 – 0.72)	0.04 (-0.15 – 0.3)	0.1 (-0.03 – 0.72)	**<0.0001**

BMI: body mass index, GI: gastrointestinal, CT scan: computer tomography, Not-Rec: not recovery. Values are expressed as numbers and (%) or median and range, as appropriate. To compare demographics between HIMC and LIMC, the chi-square test and Fisher's t-test for categorical variables, and Mann–Whitney t-test for continuous variables were used)

These two groups didn't differ in sex (64% vs. 65%; p=0.92), smoking history (35% vs. 45%; p=0.09), and number of pack-years (0 vs. 0; p=0.27); however, patients in the HIMC group were older in comparison to LIMC patients (65 vs 60 years; p=0.01). Regarding comorbidities, patients with HIMC present more frequently cardiological concomitant conditions (62% vs. 43%; p=0.001) and metabolic disease (58% vs. 40%; p=0.001). Moreover, they have reported more frequent respiratory symptoms at admission, such as dyspnea (64% vs. 39%; p=0.0003), but lower anosmia/ ageusia (19% vs. 33%; p=0.009). HIMC group patients had a significantly greater deterioration of respiratory gas exchange, with a higher FiO2 request, (29 vs 21; p<0.0001) and a worse PaO2 on room air (61 vs 71 mmHg; p<0.0001) at hospital admission. Considering radiological evaluation during hospitalization, subjects with LIMC present a lower rate of the alveolar score (5 vs. 18; p=0.01), consolidation score (0.8 vs. 4; p=0.001), and interstitial score (0.8 vs. 10; p=0.001) in comparison to subjects of the HIMC group.

Blood tests in the study population

Inflammatory indexes and blood cell count were considered at admission. Therefore, patients of the HIMC group had higher white blood cell count (6.9 vs. 5.46; p<0.0001), neutrophils (5.68 vs. 3.97; p<0.0001), NLR (7.28 vs. 4.05; p<0.0001), CRP (98 vs 43; p<0.0001) and ferritin (806 vs. 529; p<0.0001). Conversely, patients of the LIMC group show a higher lymphocyte count (0.98 vs. 0.73; p<0.0001), eosinophil count (0 vs. 0; p<0.0001), and monocyte count (0.46 vs. 0.38; p=0.02); whereas no differences were observed for D-dimer (164 vs 187; p=0.07) and LMR (2.23 vs 1.97; p=0.14). A second blood test was collected at discharge from the hospital ward, and no differences were detected for WBC count (7.3 vs 7.46; p=0.48), neutrophils (4.6 vs 4.43; p=0.18) and monocytes (0.66 vs 0.66; p=0.78). Differently from the first blood sample, both lymphocytes (1.84 vs. 1.62; p=0.04) and eosinophils

(0.1 vs. 0.05; p<0.0001) are higher in the HIMC group. In comparison to HIMC, ferritin (612 vs 822; p=0.04) and D-dimer (166 vs 213; p=0.006) are lower in the LIMC group, but the latter present a higher CRP level (6.7 vs 4.8; p=0.003). We further analyzed eosinophils' trend from admission to discharge: the low eosinophil count at admission reached normal values in both groups, however in the HIMC group, eosinophils reached significantly higher levels as compared with LIMC patients (0.1 vs 0.04; p<0.0001). Figure 22 reports eosinophils' change from admission to discharge in the two groups (HIMC and LIMC).

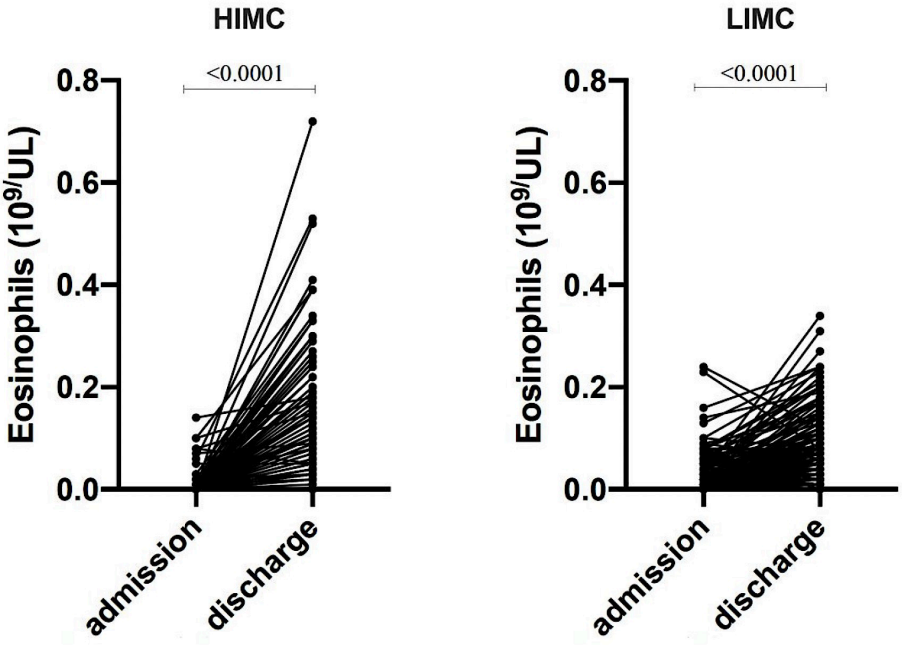

Figure 22: Eosinophil trends from admission to hospital discharge in HIMC and LIMC groups. Wilcoxon signed-rank test was used to compare eosinophil values between admission and discharge in HIMC patients (p<0.0001) and LIMC patients (p<0.0001).

First follow-up

Patients were evaluated at the post-COVID clinic after 3 months from discharge. In the overall population, the median FVC liters was 3.37 (1.46 – 7.96), and the median FEV1 in liters was 2.83 (0.84 – 6.11). In the whole population, the median FVC was 92% predicted (45 – 136), and the median FEV1 was 95% predicted (31 – 137). Despite lung function being normal in both groups, we found a lower FEV1 (%predicted) (92% vs. 96%; p=0.05) and FVC (%predicted) (87% vs. 93%; p=0.001) in the HIMC group. In the HIMC group compared with LIMC, we observed a higher percentage of patients with persistent lung damage at the first follow-up visit (not-REC group) (64% vs 41%; p=0.0007) and with higher radiological involvement in the first CT scan after discharge (alveolar score: 3.2 vs 0.6; p=0.005; interstitial score: 0 vs 0; p=0.01). During the follow-up visit, both groups of patients showed the same symptoms, except for muscular dizziness, which is more prevalent in HIMC patients

(21% vs. 12%; p=0.02). During the follow-up visit, both groups of patients showed the same symptoms, except for muscular dizziness, which is more prevalent in HIMC patients (21% vs. 12%; p=0.02).

Table 22: clinical and functional characteristics at first follow-up (3 months) of the overall population (327) and patients divided into LIMC (214) and HIMC (113).

	Overall (327)	LIMC (214)	HIMC (113)	p-value
First follow-up visit after discharge				
• *FEV1 (L)*	2.83 (0.84 – 6.11)	2.8 (0.84 – 6.11)	2.86 (1.09 – 4.25)	0.26
• *FEV1 (%pred)*	95 (31 – 137)	96 (31 – 137)	92 (53 – 130)	**0.05**
• *FVC (L)*	3.37 (1.46 – 7.96)	3.48 (1.46 – 7.96)	3.23 (1.57 – 5.09)	0.06
• *FVC (%pred)*	92 (45 – 136)	93 (45 – 136)	87 (58 – 119)	**0.001**
• *LUS score*	1 (0 – 15)	1 (0 – 9)	2 (0 – 15)	**<0.0001**
Not-Rec CT scan (yes)	159 (49%)	87 (41%)	72 (64%)	**0.0007**
CT scan at first follow-up				
• *Alveolar score*	1.4 (0 – 68)	0.6 (0 – 26)	3.2 (0 – 68)	**0.005**
• *Consolidation score*	0 (0 – 10)	0 (0 – 7)	0 (0 – 10)	0.80
• *Interstitial score*	0 (0 – 18)	0 (0 – 16)	0 (0 – 18)	**0.01**
Symptoms at first follow-up visit				
• *Asthenia*	144 (44%)	94 (44%)	50 (44%)	0.96
• *Dyspnea*	100 (31%)	62 (29%)	38 (34%)	0.38
• *Cough*	29 (9%)	18 (8%)	11 (10%)	0.69
• *Anosmia/Ageusia*	22 (7%)	17 (8%)	5 (4%)	0.23
• *Muscular Dizziness*	51 (16%)	26 (12%)	25 (21%)	**0.02**
• *GI Symptoms*	4 (1%)	2 (1%)	2 (2%)	0.51

FVC: forced vital capacity, FEV1: flow expiratory volume in the first second, GI: gastrointestinal. Values are expressed as numbers and (%) or median and range, as appropriate. To compare demographics between HIMC and LIMC, the chi-square test and Fisher's t-test (n < 5) for categorical variables and Mann–Whitney t-test for continuous variables were used.

Prognostic factors for radiological sequelae at follow-up

To detect predictors for not-REC at the first CT scan, logistic regression was performed. In the univariate analysis, age ≥ 62 years (p=0.002), a high degree of medical care (p=0.0001), NL ratio at admission ≥ 4.64 (p=0.02), neutrophils at admission ≥ 4.25 x109/L (p=0.002), CRP at admission ≥ 59.5 (mg/dl) (p=0.007), ferritin at admission ≥ 589 (ng/ml) (p=0.04), Δ eosinophils ≥ 0.05 (p=0.002) and oncological diseases (p=0.04) are associated with persistent radiological abnormalities at follow-up. In multivariate analysis, age ≥ 62 years (p=0.03) and Δ eosinophils ≥ 0.05 (p=0.03) are two independent predictor factors of radiological lung sequelae in the whole patient population.

Table 23: predictive factors of radiological sequelae at follow-up in patients hospitalized for SARS-COV-2-related pneumonia.

	Univariate		Multivariate	
	HR(0.95CI)	P	HR(0.95CI)	P
Age ≥ 62 Years	2.04 (1.3 – 3.2)	**0.002**	1.75 (1.05 – 2.94)	**0.03**
Sex – Male	1.37 (0.87 – 2.16)	0.17	-	-
BMI ≥ 27 (Kg/m^2)	0.95 (0.59 – 1.50)	0.82	-	-
Pack - Years ≥ 0	1.04 (0.66 – 1.65)	0.85	-	-
Severity - HIMC	2.56 (1.60 – 4.10)	**0.0001**	1.53 (0.86 – 2.72)	0.15
Pre-Admission Hematological Values				
• *LM Ratio ≥ 2.16*	1.23 (0.79 – 1.91)	0.35	-	-
• *NL Ratio ≥ 4.64*	1.66 (1.07 – 2.58)	**0.02**	0.87 (0.47 – 1.62)	0.66
• *Neutrophils ≥ 4.25 ($x10^9/L$)*	2.03 (1.31-3.16)	**0.002**	1.40 (0.78 – 2.53)	0.26
• *Lymphocytes ≥ 0.92 ($x10^9/L$)*	0.89 (0.58-1.39)	0.62	-	-
• *Monocytes ≥ 0.43 ($x10^9/L$)*	0.87 (0.57-1.35)	0.55	-	-
• *Eosinophils ≥ 0 ($x10^9/L$)*	0.78 (0.49 - 1.23)	0.28	-	-
• *CRP ≥ 59.5 (mg/dl)*	1.85 (1.18 – 2.89)	**0.007**	1.04 (0.57 – 1.88)	0.89
• *D-Dimer ≥ 169 (mcg/ml)*	1.21 (0.77 – 1.90)	0.42	-	-
• *Ferritin ≥ 589 (ng/ml)*	1.66 (1.03 – 2.66)	**0.04**	1.50 (0.84 – 2.49)	0.18
Pre-Discharger Haematological Values				
• *LM Ratio ≥ 2.63*	1.2 (0.78 – 1.86)	0.40	-	-
• *NL Ratio ≥ 2.45*	0.92 (0.59 – 1.42)	0.70	-	-
• *Neutrophils ≥ 4.58 ($x10^9/L$)*	1.36 (0.88 – 2.10)	0.17	-	-
• *Lymphocytes ≥ 1.17 ($x10^9/L$)*	1.39 (0.90 – 2.16)	0.13	-	-
• *Monocytes ≥ 0.66 ($x10^9/L$)*	1.54 (0.99 – 2.39)	0.051	-	-
• *Δ Eosinophils ≥ 0.05*	2.03(1.30 – 3.17)	**0.002**	1.75 (1.05 – 2.9)	**0.03**
• *CRP ≥ 6.00 (mg/dl)*	0.92 (0.58 – 1.46)	0.72	-	-
• *D-Dimer ≥ 191 (mcg/ml)*	1.27 (0.73 – 2.2)	0.39	-	-
• *Ferritin ≥ 723 (ng/ml)*	2.25 (0.68 – 7.41)	0.18	-	-
Cardiological – yes	1.29 (0.84 – 1.99)	0.25	-	-
Oncological – yes	2.44 (1.32 – 4.51)	**0.04**	1.8 (0.9 – 3.7)	0.09
Pneumological – yes	1.12 (0.61 – 2.03)	0.71	-	-
Metabolic – yes	1.03 (0.67 – 1.59)	0.89	-	-
Autoimmunity – yes	1.53 (0.81 – 2.89)	0.19	-	-

BMI: body mass index, GI: gastrointestinal, WBC: white blood cells, LM: lymphocytes-tomonocytes ratio NL: neutrophils-to-lymphocytes ratio, CPR: C-Reactive Protein; HIMC: high-intensity medical care. Values are expressed as numbers and (%) or median and range, as appropriate)

In conclusion, we found that NLR at admission and higher Δ eosinophils positively correlate with radiological score (interstitial and alveolar) at the first CT scan after discharge (3 months). Moreover, older age and Δ eosinophils ≥ 0.05 are two independent factors of radiological sequelae in post-COVID CT scans. Based on our findings, Δ eosinophils and NLR at baseline could be potential predictors of radiological sequelae in CT scans, even though further studies are needed to investigate the role of blood values in post-COVID-19 sequelae.

Study 9): ***Characteristics and Prognostic Factors of Pulmonary Fibrosis after COVID-19 pneumonia***
Cocconcelli E, ***Bernardinello N****, ...et al. Front. Med. 8:823600.*

This study aims to characterize, among patients hospitalized for COVID-19 pneumonia, those presenting persisting pulmonary sequelae during follow-up, and to define which clinical and radiological features are predictive of persistent radiological abnormalities.

Study Population and Study Design
We prospectively collected patients evaluated at the University Hospital of Padova post-COVID clinic between June and December 2020. The patients assessed at the post-COVID clinic were initially admitted to the Division of Infectious and Tropical Diseases of the University Hospital of Padova between February and September 2020 for SARS-CoV-2 infection confirmed by the real-time polymerase chain reaction (RT-PCR) at nasopharyngeal swab. Among all patients evaluated, we precisely followed up every 3 months with those presenting a COVID-19-related severe disease according to the WHO criteria (n = 220) [58]. Demographics and clinical data at hospital admission [symptoms, gas exchange values (paO2/FiO2)] and during hospitalization [days of hospital stay, maximal FiO2 (FiO2 max) needed, level of care, treatment] were collected. Comorbidities were categorized as cardiovascular diseases (CVDs), respiratory diseases, metabolic diseases (including diabetes mellitus, obesity, and dyslipidemia), autoimmune diseases, and oncologic diseases (including lung, prostate, pancreatic, breast, and colon cancer). Based on the patient's clinical conditions during hospitalization, we distinguished those requiring a low- (LIMC) and high-intensity medical care (HIMC), as previously described.

Radiological Evaluation
At follow-up, HRCT was available for the entire study population (HRCT1), whereas, at hospital admission, it was available in only a subgroup of patients (HRCT0) (n = 79, 36%). The HRCTs were performed by a 64-slice Siemens Somatom Sensation (Siemens Healthcare, Erlangen, Germany), applying a slice thickness of 0.5 mm. According to the presence or absence of radiological abnormalities on HCRT1, the study population was categorized as recovered patients (REC, n = 175) or not recovered patients (NOT-REC, n = 45). Two expert thoracic radiologists (CG and AG), who were blinded to clinical data and timing of HRCTs, scored the images independently using a composite semiquantitative scale. This represented a modification of the previously reported scoring systems standardized by our group. Specifically, ground glass opacities (GGO) (alveolar score, AS), consolidations (CONS), and reticulations (interstitial score, IS) were analyzed. For each lung lobe, the two radiologists assessed the extent of AS, CONS, and IS using a scale from 0 to

100 and estimated the extent to the nearest 2%. The result was expressed as the mean value of the five lobes in AS, CONS, and IS. The level of interobserver agreement was obtained for each patient as a mean of 5 lobes and for each radiological abnormality (AS, CONS, and IS) and expressed as Cohen's k value. Disagreement between radiologists was resolved by consensus.

Statistical Analysis

Categorical variables were described as absolute (n) and relative values (%), whereas continuous variables were described as median and range. To compare demographic and clinical data between REC and NOT-REC patients, the chi-square test and Fisher's exact test ($n < 5$) for categorical variables and Mann–Whitney U tests for continuous variables were used, as appropriate. To compare radiological scores at HRCT1 in NOT-REC patients, the Mann–Whitney U test for continuous variables was used, whereas the Wilcoxon signed-rank test was used to compare radiological scores between HRCT0 and HRCT1. A univariate logistic regression analysis, followed by a regression model adjusted for gender, pack-years, paO2/FiO2 at admission, degree of medical care (high or low), and FiO2 max, was performed to detect the predictive factors of radiologic sequelae (NOT-REC at follow-up. All data were analyzed using SPSS Software version 25.0 (US: IBMCorp., New York, NY, USA). p-Values < 0.05 were considered statistically significant. The graphs were obtained using the statistical package GraphPad Prism 7.0 (GraphPad Software, Inc., La Jolla, CA, USA).

Results

Clinical Evaluation at Hospital Admission and During Hospitalization Two hundred and 20 patients with COVID-19 pneumonia evaluated at the post-COVID clinic were included in the study (Table 24). A total of 115 patients (52%) were men, with a median age of 59 years (range 19–84) and body mass index (BMI) 26 (18–39). The most prevalent comorbidities were CVDs ($n = 98$, 45%), followed by chronic respiratory diseases (18%). Based on the presence of radiological sequelae on HRCT performed at follow-up (HRCT1), 175 (80%) patients were categorized as REC and 45 (20%) as NOT-REC. Baseline demographic and clinical data of REC and NOT-REC patients are summarized in Table 24. No differences in sex, smoking history, or BMI were observed between the two groups, with a prevalence of men in NOTREC compared to REC (64 vs. 49%, respectively). NOT-REC patients were significantly older compared to REC [66 (35–85) vs. 56 (19–87) years; $p < 0.0001$]. CVDs were substantially more frequent in NOT-REC compared to REC [26 (58%) vs. 72 (41%); $p = 0.04$], whereas autoimmune, metabolic, and oncologic diseases did not differ between the two groups. Symptoms before hospital admission were also similar, except for a higher proportion of patients presenting with dyspnea in NOT-REC compared to the REC group [33 (73%) vs. 64 (37%); $p < 0.0001$] (Supplementary Table 24). At hospital admission, NOT-REC had a worse gas exchange with a lower PiO2/FiO2 ratio than REC [233 (40–424) vs. 318 (33543); $p = 0.04$]. In addition,

compared to REC, during hospitalization, NOT-REC required more frequently high-intensity medical care (HIMC) (20, 44 vs. 37, 21%; p =0.002), higher FiO2 max [45 (21–100) vs. 27 (21–100); p < 0.0001], and longer in-hospital stay [16 (0–75) vs. 8 (1–52) days; p < 0.0001]. The majority of patients were admitted during the first SARS-CoV-2 wave when no standardized protocols existed for the treatment of hospitalized patients. NOT-REC patients were more frequently treated with hydroxychloroquine (n = 37, 82 vs. 111, 63%; p = 0.01), antibiotics other than ceftriaxone and azithromycin (n = 25, 56 vs. 44, 25%; p < 0.0001), remdesevir (n = 7, 16 vs. 10, 6%, p = 0.02), tocilizumab (n = 8, 18 vs. 12, 7%; p = 0.02), and steroids (n = 27, 60 vs. 74, 42%; p = 0.03) compared to REC. Conversely, the two groups did not differ about the use of ceftriaxone, azithromycin, lopinovir/ritonavir, and hyperimmune plasma. At discharge, a similar proportion of patients in both groups were prescribed steroids.

Table 24. Baseline demographics and clinical features of the overall population evaluated at post-COVID Clinic, and of the two subgroups categorized according to the presence of radiological recovery during the follow up period.

	Overall population (n =220)	**REC (n = 175; 80%)**	**NOT - REC (n = 45; 20%)**	***p* Value**
Male – *n (%)*	115 (52)	86 (49)	29 (64)	0.06
Age at admission – *years*	59 (19 - 87)	56 (19 - 87)	66 (35 - 85)	**< 0.0001**
Smoking history – *pack years*	0 (0 - 67)	0 (0 - 67)	0 (0 - 60)	0.07
· **Current – *n (%)***	15 (7)	10 (6)	5 (11)	0.20
· **Former – *n (%)***	70 (32)	54 (31)	16 (36)	0.54
· **Non smokers – *n (%)***	135 (61)	111 (63)	24 (53)	0.21
BMI - (kg/m^2)	26 (18 - 39)	27 (18 - 39)	26 (21 - 35)	0.35
Cardiovascular diseases - n (%)	98 (45)	72 (41)	26 (58)	**0.04**
Respiratory diseases - n (%)	39 (18)	30 (17)	9 (20)	0.65
Autoimmune diseases - n (%)	36 (16)	25 (14)	11 (24)	0.10
Metabolic diseases - n (%)	102 (4)	78 (45)	24 (53)	0.29
Oncologic diseases - n (%)	25 (11)	17 (8)	8 (18)	0.12
PaO_2 / FiO_2 at admission	314 (33 - 543)	318 (33 - 543)	233 (40 - 424)	**0.04**

FiO_2max during hospitalization - %	28 (21 - 100)	27 (21 - 100)	45 (21 - 100)	**< 0.0001**
Hospitalization - days	9 (0 - 75)	8 (1 - 52)	16 (0 - 75)	**< 0.0001**
Low degree of care – n (%)	163 (74)	138 (79)	25 (56)	**0.002**
High degree of care – n (%)	57 (26)	37 (21)	20 (44)	

Values are expressed as numbers and (%) or median and range, as appropriate. To compare demographic between recovery (REC) and not recovery (NOT-REC), Chi square test and Fisher t test (n < 5) for categorical variables and Mann-Whitney t test for continuous variables were used.

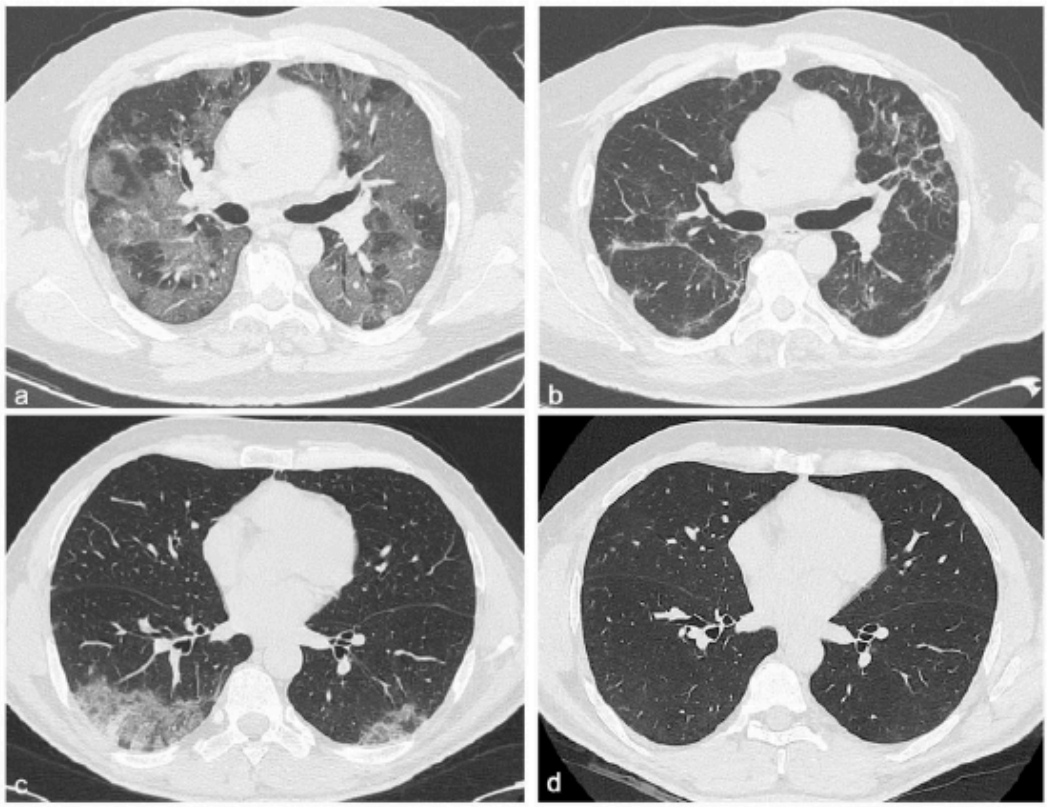

Figure 23. Chest CT features of two patients with COVID-19 pneumonia at different time points: hospitalization and 6 months after discharge. CT images of a 58-year-old male patient with COVID-19, not recovery patient (a,b). The first CT performed at admission shows bilateral areas of ground-glass opacities in a peripheral distribution (a) and after 6 months from discharge, CT shows persistent of interlobular septal thickening with peripheral distribution (b). Chest CT images of a 51-year-old male patient with COVID-19, recovery patient (c,d). The first CT shows, at admission, a small consolidation at the right lower lobe accompanied by ground glass opacities in both lower lobes (c) and after 6 months from discharge, no residual abnormalities were observed (d).

Clinical, Functional, and Radiologic Evaluation at Follow-Up

Patients were evaluated at post-COVID clinic at regular 3-month intervals after discharge. At first evaluation, NOT-REC patients presented more frequently modified Medical Research Council (mMRC) scores of 1 and 2 compared to REC [15 (33%)

vs. 22 (13%), p = 0.0009 and 7 (16%) vs. 3 (2%), p < 0.0001, respectively]. In the overall population, pulmonary function tests (PFTs) revealed a median forced vital capacity (FVC) of 3.40 liters (L) (range 1.40–7.96), 96%pred. and a median total lung capacity (TLC) of 5.36 L (3.63–8.09), 89% pred. within the normal range. Likewise, NOT-REC patients showed preserved lung volumes within the normal range). A number of 32 patients out of 220 (14.5%) had an abnormal diffusing capacity of the lung for carbon monoxide (DLCO) at the 6-month follow-up, which occurred in those with persistent interstitial lung abnormalities (NOT-REC patients). At follow-up CT (HRCT1), NOT-REC patients presented higher ALV [2.8 (0.0–40.0)] compared to CONS [0.0 (0.0–2.0); p < 0.0001] and IS [0.6 (0.0–24.0); p < 0.0001] (Supplementary Figure 25). Overall, the interobserver agreement between the two radiologists with regard to change in AS, CONS, and IS was good (Cohen's kappa = 0.79 for AS, k = 0.88 for CONS, and k = 0.81 for IS).

Longitudinal Evaluation of Radiologic Manifestation: From Hospitalization to Follow-Up

At hospital admission, HRCT (HRCT0) was available for 79/220 (36%) patients. ALV [5.0 (0.0–62.0)] was significantly more prevalent compared to CONS [0.8 (0.0–26.0); p < 0.0001] and IS [0.8 (0.0–29.0); p < 0.0001]. When this patient subgroup was stratified in NOT-REC and REC, NOT-REC patients (n = 20) had at hospital admission higher ALV [14.0 (0.0–62.0) vs. 4.4(0.0–44.0); p = 0.0005] (Figure 23A), CONS [1.9 (0.0–26.0 vs. 0.4 (0.0–18.0); p=0.0064] (Figure 23B), and IS [11.5 (0.0–29.0) vs. 0.0 (0.0–22.0); p < 0.0001] (Figure 23C) compared to REC patients (n= 59) (Table 25). Finally, when comparing HRCT0 with HRCT1, we observed that in NOT-REC patients, ALV [from 14 (0.0–62.0) to 2.6 (0.0–40.0); p < 0.0001], CONS [from 1.9 (0.0–26.0) to 0.0 (0.0–2.2); p = 0.0001], and IS [1.5 (0.0–29.0) to 1.4 (0.0–24.0)] decreased significantly (Figure 25).

Table 25. HRCT scores during hospitalization ($HRCT_0$) of the overall population evaluated at post-COVID Clinic, and of the two subgroups categorized according to the presence of radiological recovery during the follow up period.

	Overall population (n =220)	**REC (n = 175; 80%)**	**NOT - REC (n = 45; 20%)**	***p* Value**
Alveolar score - %	5.0 (0.0 – 62)	4.4 (0.0 – 44.0)	14.0 (0.0 – 62.0)	**0.0005**
Consolidations - %	0.8 (0.0 – 26.0)	0.4 (0.0 – 18.0)	1.9 (0.0 – 26.0)	**0.006**
Interstitial score - %	0.8 (0.0 – 29.0)	0.0 (0.0 – 22.0)	11.5 (0.0 – 29.0)	**< 0.0001**

Values are expressed as median and range, as appropriate. To compare HRCT scores at hospitalization ($HRCT_0$) between recovery (REC) and not recovery (NOT-REC), Mann-Whitney t test for continuous variables was used.

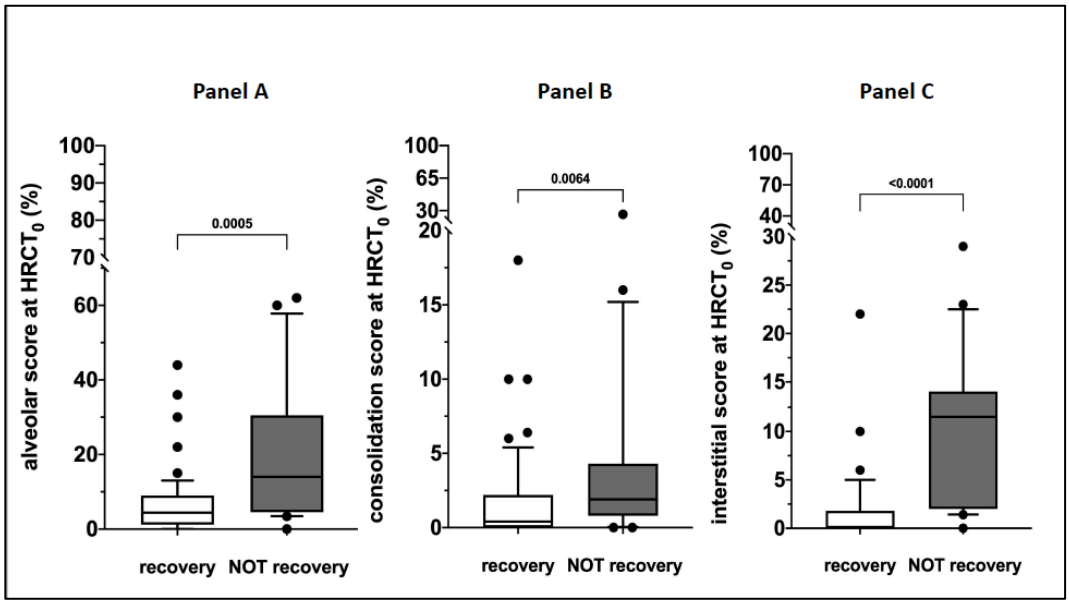

Figure 23. HRCT scores during hospitalization (HRCT0) of the two subgroups categorized according to the presence of radiological recovery [recovery (REC) or NOT-recovery (NOT-REC)] at follow up period. Horizontal bars represent median values; bottom and top of each box plot 25th and 75th; brackets show 10th and 90th percentiles; and circles represent outliers. White boxes indicate values for recovery group and grey boxes not recovery group. Panel A: ALV [14.0 (0.0 – 62.0) vs. 4.4 (0.0 – 44.0); p = 0.0005]; Panel B: CONS [1.9 (0.0 – 26.0 vs. 0.4 (0.0 – 18.0); p = 0.0064]; Panel C: INT [11.5 (0.0– 29.0) vs. 0.0 (0.0 – 22.0); p < 0.0001].

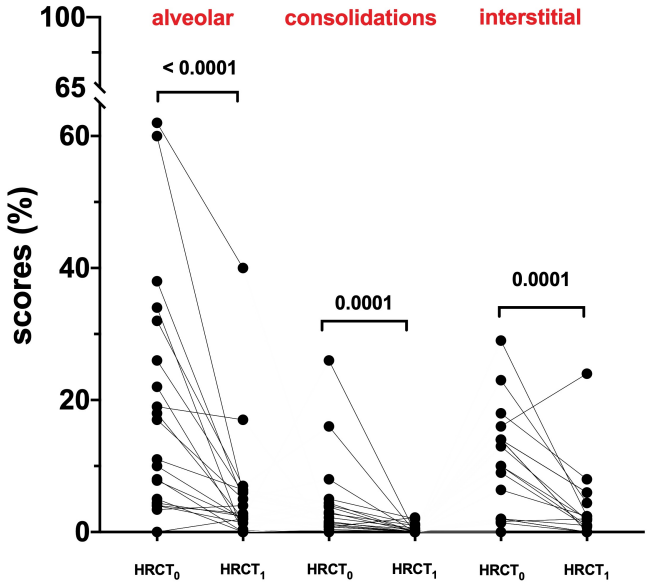

Figure 25. HRCT scores of the not recovery population (NOT-REC) from HRCT0 to HRCT1: ALV [from 14 (0.0 – 62.0) to 2.6 (0.0 – 40.0); p < 0.0001], CONS [from 1.9 (0.0 – 26.0) to 0.0 (0.0 – 2.2); p = 0.0001] and INT [1.5 (0.0 – 29.0) to 1.4 (0.0 – 24.0)].

Prognostic Factors for Radiological Sequelae at Follow-Up

Univariate analysis showed that older age, a prolonged hospital stay, a lower PiO2/FiO2 at hospital admission, cardiovascular comorbidities, a higher degree of medical care, a higher FiO2 max, and higher ALV, CONS, and INT scores at HRCT0,

not use of hydroxychloroquine, antibiotics other than azithromycin and ceftriaxone, tocilizumab, remdesevir, and systemic steroids are associated with persistent radiological abnormalities at follow-up. Multivariate analysis revealed that CONS [OR: 20.6 (95%CI: 1. −301.2); p = 0.02] and IS score [23.0 (1.4–377.2); p = 0.02] are independent predictors of radiological sequelae at follow-up. Finally, on multivariate analysis adjusted for gender, packyears, PiO2/FiO2 ratio at admission, degree of care (high or low), and FiO2 max, both CONS and IS at HRCT0 are independent predictors of radiological sequelae at follow-up with an OR of 14.87 (95% CI: 1.25–175.8; p = 0.03) and 28.9 (95% CI: 2.17– 386.6; p = 0.01), respectively (Table 26).

Table 26. Multivariate analysis for factors independently associated with radiological sequelae at follow-up in patients hospitalized for SARS-COV-2-related pneumonia.

Multivariate analysis*	OR (95% IC)	p
Alveolar score HRCT0 - %		
• **< 7**	Ref.	-
• **≥ 7**	1.80 (0.39 – 8.20)	0.44
Consolidations HRCT0 - %		
• **< 0.8**	Ref.	-
• **≥ 0.8**	14.87 (1.25 – 175.8)	**0.03**
Interstitial score HRCT0 - %		
• **< 1.4**	Ref.	-
• **≥ 1.4**	28.9 (2.17 – 386.6)	**0.01**

Values are expressed as OR (95%CI). Univariate and multivariate-adjusted odds ratio for radiological NOT recovery according to radiological patterns during hospitalization ($HRCT_0$). *Adjusted for gender, pack years, PiO_2/FiO_2 ratio at admission, degree of care (high or low), FiO_2 max.

In conclusion, in our study, about 20% of patients with COVID-19 pneumonia had radiological sequelae at follow-up. Patients who did not fully recover showed a more severe impairment at hospital admission and during hospitalization. Moreover, the presence of reticulation and consolidation on the initial chest CT is predictive of persistent radiological interstitial changes at follow-up.

Study 10): ***Predictor of pulmonary sequelae after COVID-19 pneumonia: a 12-month follow-up study***
Bernardinello N*, ...et al. Front. Med. 2023 Feb; 10:1084002*

The main aim of this project was to identify and characterize, among patients hospitalized for SARS-CoV-2 infection, those exhibiting persistent pulmonary sequelae at 12 months of follow-up, and then to investigate which clinical characteristics could predispose to these radiological findings.

Study population and design

In this single-center observational cohort study, 421 patients were consecutively evaluated at the post-COVID-19 clinic of our hospital after discharge. Eligible patients were previously admitted to the Division of Infectious and Tropical Diseases of the University Hospital of Padova from the end of February 2020 until the end of April 2021. Inclusion criteria were: (i) age > 18 years at the moment of hospital admission and (ii) diagnosis of SARS-CoV-2 infection by positive real-time polymerase chain reaction (RT-PCR) on the nasopharyngeal swab or on bronchoalveolar lavage (BAL). Exclusion criteria were: (i) pregnancy or breastfeeding status, (ii) having only one or more chest-X-ray (CXR) as a unique radiological investigation, (iii) missing on follow-up visit, or (iv) absence of computed tomography (CT) scan imaging at 12 months. For studying purposes, we completed the recruiting process in April 2021, which allowed the collection of all the data until April 2022, for a global period of 1-year follow-up. During hospitalization, positivity to SARS-CoV-2 was confirmed by a nasal or oropharyngeal swab RT-PCR (12). High-resolution CT (HRCT) was used to evaluate the persistence and characteristics of radiological changes during follow-up visits. Based on the CT changes at 12 months, the whole population was then categorized into two groups: the NOT-RECOVERED group (NOT-REC) when CT still showed lung abnormalities and the RECOVERED group (REC) when CT demonstrated normal lung parenchyma along the follow-up. Symptoms, maximal FiO2 (FiO2 max.), gas exchange values (PaO2/FiO2), days of hospital stay, and treatment during hospitalization were collected. Comorbidities were categorized as cardiovascular diseases (CVDs), respiratory diseases, metabolic diseases (including diabetes mellitus, obesity, and dyslipidemia), autoimmune diseases, and oncologic diseases (including lung, prostate, pancreatic, breast, and colon cancer). Based on the level of care, we distinguished those requiring low-intensity medical care (LIMC) and high-IMC (HIMC), as previously described. Pulmonary function tests were collected during follow-up visits, indeed the study was planned for two follow-up visits at 6 and 12 months from hospital discharge. Results from 6 months follow-up, as well as inclusion and exclusion criteria and study procedures, are summarized in the manuscript by Cocconcelli et al.

Figure 26: Enrollment flow-chart of patients discharged from hospital and included in the study cohort.

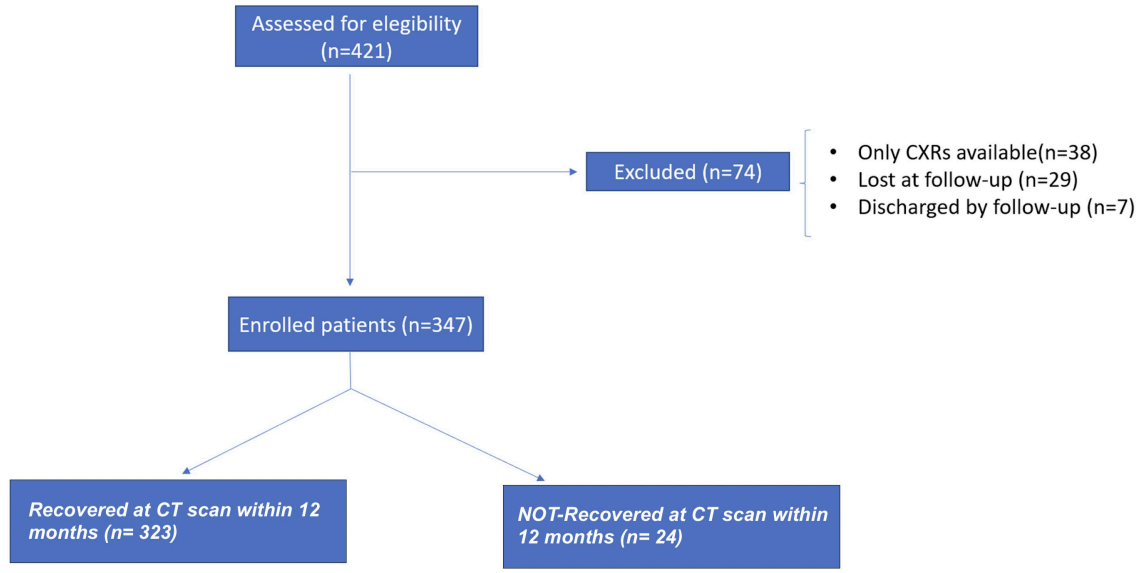

CXR= chest-X-ray, CT= Computed Tomography.

Radiological evaluation

All the CTs were performed by a 64-slice Siemens Somatom Sensation (Siemens Healthcare, Erlangen, Germany), with a slice 0.05. Radiological evaluation (REC vs. NOT-REC) was made by two expert radiologists (CG, GF), who were blinded to clinical data and with experience in the evaluation and quantitation of interstitial lung diseases (ILDs) features. After independent evaluation, disagreement between radiologists was resolved by consensus. All the CT images were scored through a composite semi-quantitative scale, as previously described. In particular, the extent of ground glass opacities (GGO), interstitial thickening (IT), and consolidations (CO) was assessed for each lobe using a scale from 0 to 100 and the result was expressed as the mean value of the five lobes for each radiologic feature. The presence or absence of bronchiectasis and curvilinear or linear band opacities for each of the five lung lobes were also evaluated. The level of interobserver agreement was obtained for each patient and expressed as Cohen's k value. For dichotomic parameters (bronchiectasis and band opacities), the patient was considered affected by these abnormalities whenever at least one single lobe was involved.

Statistical analysis

Continuous variables were described as median and interquartile range (IQR; 25–75), while categorical variables were shown as absolute (n) and relative values (%). We used the chi-square and Fisher's exact tests for categorical variables, while the Mann–Whitney U tests were used for continuous variables. Univariable and multivariable logistic regression analyses were performed to detect the factors associated with radiological consequences (NOT-REC) at 12 months. SPSS Software version 25.0

(IBM Corp., New York, NY, USA) was used for all data analysis. We considered a statistically significant p-value < 0.05.

Results

Baseline characteristics of the entire study population

A total of 421 patients started the follow-up evaluation at our post-COVID-19 clinic and were initially considered the study population. At the end of the study at 12 months, 347 patients met inclusion and exclusion criteria and were enrolled (Figure 26). Analysis of the cohort that completed the 12 months showed that patients were predominantly men (62%) with a median age of 63 years old (53–72 years) and a body mass index (BMI) of 27 (24–30 kg/m2), as reported in Table 27. Current smokers were 5%, while non-smokers and former smokers were 63% and 33%, respectively. Patients were predominantly affected by CVDs (50%) and metabolic diseases (45%). Almost the entire population manifested fever during hospitalization (n = 331; 99%), while cough and dyspnea were present in almost half of the patients (54 and 47%; respectively). Regarding treatment during hospitalization, the most administered therapies were heparins (81%) and corticosteroids (69%). After discharge, corticosteroids were prescribed in 56% of patients.

Table 27: baseline characteristics of the study cohort followed in the post-COVID clinic (n=347) according to CT scan recovery at 12 months.

	Available data	Overall population (n=347)	REC (n=323)	NOT-REC (n=24)	p
Demographic data					
Male – n (%)	347	217 (62)	200 (62)	17 (71)	0.51
Age at admission - years	347	63 (53 – 72)	63 (53 – 71)	67 (62 – 76)	**0.02**
BMI – kg/m^2	247	27 (24 – 30)	27 (25 – 30)	26 (24 – 30)	0.23
Smoking history					
Pack years	334	0 (0 – 5)	0 (0 – 5)	3.1 (0 – 21)	0.06
Current – n (%)	344	16 (5)	12 (4)	4 (17)	**0.02**
Non-smoker – n (%)	344	216 (63)	205 (64)	11 (46)	0.08
Former – n (%)	344	114 (33)	105 (33)	9 (37)	0.66
Comorbidities					
Cardiovascular diseases – n (%)	347	174 (50)	161 (50)	13 (54)	0.83
Respiratory diseases – n (%)	347	50 (14)	44 (14)	6 (25)	0.13
Autoimmune diseases – n (%)	347	52 (15)	45 (14)	7 (29)	0.07
Metabolic diseases – n (%)	347	158 (45)	147 (45)	11 (46)	0.99
Oncologic diseases – n (%)	347	57 (16)	52 (16)	6 (21)	0.57

Hospitalization characteristics					
FiO_2 max during hospitalization	337	36 (27 – 70)	36 (24 – 66)	75 (32 – 100)	**0.01**
Hospitalization - days	347	10 (6 – 17)	10 (6 – 16)	17 (10 – 41)	**0.001**
High degree of care – n (%)	347	69 (20)	57 (18)	12 (50)	**0.0006**
PaO_2/FiO_2 at admission	205	295 (218 – 342)	295 (223 – 343)	201 (101 – 314)	**0.01**
Symptoms during hospitalization					
Fever – n (%)	335	331 (99)	289 (92)	22 (100)	0.39
Asthenia – n (%)	335	119 (35)	112 (36)	7 (32)	0.70
Dyspnea – n (%)	335	158 (47)	140 (45)	18 (75)	**0.0008**
Anosmia/Ageusia – n (%)	335	104 (31)	96 (31)	8 (33)	0.58
Muscular alterations – n (%)	335	61 (18)	55 (18)	6 (25)	0.25
Headache – n (%)	335	36 (11)	35 (11)	1 (4.2)	0.33
Gastrointestinal – n (%)	335	74 (22)	69 (22)	5 (21)	0.94
Cough – n (%)	335	182 (54)	168 (54)	14 (58)	0.36

Values are expressed as numbers and (%) or median and interquartile range (IQR), as appropriate. To compare demographics between recovered (REC) and not-recovered (NOT-REC), the chi-square test and Fisher's t-test (n < 5) for categorical variables and Mann–Whitney t-test for continuous variables were used.

Baseline characteristics and lung function according to radiological sequelae CT findings at 12 months

At the end of the 1-year follow-up, 24 out of 347 patients (6.9%) presented radiological sequelae at 12 months (NOT-REC). Clinical and demographic characteristics of patients divided into REC (n = 323) and NOT-REC groups (n = 24) are summarized in Table 27. NOT-REC were significantly older [67 (62–76) years vs. 63 (53–71) years; p = 0.02] and more frequently current smokers [4 (17%) vs. 12 (4%); p = 0.02]. Regarding hospital stay and disease severity, the NOT-REC group displayed significantly worsen parameters compared with the REC group: the median of the maximum FiO2 reached during the hospitalization was higher [75% (32–100) vs. 36% (24–66); p = 0.01], the median duration of hospitalization was longer [17 (10–41) days vs. 10 (6–16) days; p = 0.001], and the median of the PaO2/FiO2 ratio at admission was lower [201 (101–314) vs. 295. (223–343); p = 0.01]. Among all treatments, in the NOT-REC group, other antibiotics (62% vs. 31%; p = 0.003) and corticosteroids (87% vs. 67%; p = 0.04) were more frequently used during the hospital stay, compared with the REC group. For all the other drugs, including the administration of corticosteroids after discharge, we did not find any between-group difference (p = 0.20). Regarding radiological sequelae, in NOT-REC patients (n = 24), the most frequent alteration was IT, which was observed in 21 patients (88%) and with a median extension of 4%. GGO was found in 19 patients (79%) with a median extension of 3.5%, while CO were present in only 2 patients (8%) with an extension of <1%. The linear and curvilinear band opacities were

reported in 16 patients (66%) and bronchiectasis in 7 patients (29%), as reported in Table 28. Analyzing pulmonary function tests in the whole population, we observed normal lung volume at first follow-up [Forced Vital Capacity (FVC% pred.): 92% (81–104) and Forced Expiratory Volume in the first second (FEV1% pred.): 95% (84 –137)]. Moreover, patients from the NOT-REC group showed similar parameters to patients from the REC group, as reported in table 29.

Table 28: Chest HRCT scan characteristics of the NOT-REC group (n=24) at 12-month

Ground-glass opacities	
Ground-glass opacities, n (%)	19 (79%)
Extent of Ground-glass opacities	3.5%
Interstitial thickening	
Interstitial thickening, n (%)	21 (88%)
Extent of Interstitial thickening	4%
Consolidations	
Consolidations, n (%)	2 (8%)
Extent of Consolidations	<1%
Bronchiectasis	
Bronchiectasis, n (%)	7 (29%)
Curvilinear and liner band opacities	
Curvilinear and liner band opacities, n (%)	16 (66%)

Table 29: pulmonary function tests of patients at first follow-up visit according to CT scan recovery at 12 months (n=347)

	Overall population (n=347)	**REC (n=323)**	**NOT-REC (n=24)**	***p***
FVCabs – litres	3.3 (2.8 – 4.0)	3.3 (2.8 – 4.0)	3.2 (2.4 – 4.6)	0.38
FVCpred - %	92 (81 – 104)	92 (81 – 104)	97 (70– 103)	0.79
FEV1abs -litres	2.8 (2.3 – 3.3)	2.8 (2.3 – 3.3)	2.6 (2.0 – 3.5)	0.37
FEV1pred - %	95 (84 – 137)	95 (84 – 137)	99 (55 – 121)	0.74

FVC: forced vital capacity, FEV1: flow expiratory volume at first second, BMI: body mass index, PFT: pulmonary function test. Values are expressed as median and IQR (interquartile range). To compare the pulmonary function test at first follow-up between recovered (REC) and not recovered (NOT-REC), the Mann-Whitney test for continuous variables was used.

Predictors of post-COVID-19 pulmonary sequelae

At the univariable analysis, age 63 years [2.8 OR; 95% CI (1.09–7.33); p = 0.03] and being a current smoker [5.2 OR; 95% CI (1.53–17.53); p = 0.008] were identified

as risk factors for having persistent radiological sequelae at 12 months follow-up after COVID-19 pneumonia. Among hospital stay characteristics, an hospitalization time 10 days [OR 2.9; 95% CI (1.14–7.61), p = 0.03], the high degree of care [4.7 OR; 95% CI (1.99–10.92); p = 0.0001]; FiO2 max. 36% [2.6 OR; 95% CI (1.01–6.78); p = 0.047] and other antibiotics [3.6 OR; 95% CI (1.54–8.61); p = 0.003], resulted as dependent risk factors for having post-COVID-19 pulmonary changes (Table 30). On the multivariable analysis, adjusted for the previous risk factor, we found that smoking history, particularly being a current smoker, was an independent predictor for lung sequelae after 12 months from COVID-19 pneumonia and hospitalization [5.6 OR; 95% CI (1.41–22.12), p = 0.01].

Table 30: risk factors associated with the persistence of pulmonary sequela in the overall population (n=347).

	Univariable Analysis		**Multivariable Analysis**	
	OR (95%CI)	**p**	**OR (95%CI)**	**p**
Demographics				
Age ≥ 63 years	**2.8 (1.09 – 7.33)**	**0.03**	2.6 (0.96 – 7.18)	0.06
BMI ≥ 27 kg/m^2	0.4 (0.15 – 1.07)	0.07		
Smoking History				
Current smoker- yes	**5.2 (1.53 – 17.53)**	**0.008**	**5.6 (1.41 – 22.12)**	**0.01**
No-smoker - yes	2.0 (0.86 – 4.58)	0.11		
Comorbidities				
Cardiovascular disease - yes	1.2 (0.52 – 2.73)	0.68		
Respiratory disease - yes	2.1 (0.79 – 5.61)	0.13		
Autoimmune disease - yes	2.5 (0.99 – 6.48)	0.051		
Metabolic disease - yes	1.0 (0.44 – 2.33)	0.98		
Oncologic disease - yes	1.4 (0.49 – 3.84)	0.55		
Hospitalization characteristics				
Hospitalization time ≥ 10 days	**2.9 (1.14 – 7.61)**	**0.03**	1.0 (0.25 – 3.29)	0.89
High degree of care - yes	**4.7 (1.99 – 10.92)**	**0.0001**	2.6 (0.83 – 8.35)	0.10
FiO_2 max ≥ 36%	**2.6 (1.01 – 6.78)**	**0.047**	1.1 (0.31 – 3.86)	0.89
$PaO_2/FiO_2 ≥ 295$	0.4 (0.14 – 1.25)	0.12		
Treatment during hospitalization				
Hydroxychloroquine/chloroquine - yes	1.4 (0.61 – 3.24)	0.42		
Azithromycin - yes	0.7 (0.33 – 1.75)	0.52		
Ceftriaxone - yes	1.1 (0.44 – 2.38)	0.95		
Other antibiotics - yes	**3.6 (1.54 – 8.61)**	**0.003**	2.4 (0.84 – 3.28)	0.10
Lopinavir/ritonavir - yes	1.9 (0.74 – 4.73)	0.18		
Remdesivir - yes	1.4 (0.58 – 3.24)	0.47		
Other antiviral - yes	2.7 (0.31 -24.6)	0.36		
Tocilizumab - yes	2.9 (0.78 – 10.9)	0.11		
Corticosteroids - yes	3.4 (0.98 – 11.6)	0.052		

Heparins - yes	0.88 (0.32 – 2.46)	0.81		
Corticosteroids during follow-up - yes	1.8 (0.74 – 4.59)	0.19		

In conclusion, aftter 12 months from hospitalization for COVID-19 pneumonia, fibrotic-like changes on CT are observed in a small percentage of the study population. These radiological sequelae are minimal and do not affect lung function. Finally, being a current smoker, at the time of infection, is an independent predictor of persistent lung changes after 1 year. Further studies are needed to validate these findings.

DISCUSSION

In the studies performed during my Ph.D., I tried to analyze the role of hematological, radiological, and molecular characteristics in the development and progression of ILDs and the possible relationships with survival.

In the last few years, more studies have investigated the role of blood count in patients with interstitial lung diseases (ILDs). For example, Kreuter and colleagues performed a retrospective pooled analysis including IPF patients enrolled in four phase III randomized, placebo-controlled trials (n = 2.067). They showed that patients with a monocyte count of 0.60 to $<0.95 \times 109/L$ or $\geq 0.95 \times 10^9/L$ had hospitalization over one year [59].
My first study showed that high monocyte count at diagnosis is an independent predictor of functional decline after the first year of antifibrotic therapy and negatively correlates with lung function at diagnosis. Moreover, a lymphocyte-to-monocyte ratio (LMR) lower than 4.18 was significantly associated with shorter survival in patients with newly diagnosed IPF.
A high monocyte count is also an independent risk factor for acute exacerbation in patients with fibrosing ILDs [60]. In addition, Scott and co-workers found that a high monocyte count is associated with shorter survival in patients with IPF, systemic sclerosis-associated ILD, and myelofibrosis. Patients maintain the exact monocyte count and, consequently, the same risk profile over time [61]. We confirmed that blood cell count and ratios in newly diagnosed IPF patients at diagnosis display similar values after one year of antifibrotic therapy, ensuring that patients maintain the same risk profile despite treatment. About the LMR and NLR, there are no universally agreed upon cut-off values available in IPF, although their role is well established in patients with lung cancer and other types of neoplasm [62–64]. Several studies have shown that the inflammatory response associated with cancer impacts blood cell count by increasing the number of neutrophils and/or decreasing the number of lymphocytes. In a recent meta-analysis, Wen Li et al. analyzed data from eight clinical trials involving 3,954 lung cancer patients [65]. They concluded that a high LMR is associated with better PFS and OS. The authors speculated that, as macrophage infiltration into the tumor microenvironment is associated with poor survival, a high LMR may reflect low monocyte concentration and consequently reduced tumor growth.

Monocytes might be key players in the pathogenesis of IPF by contributing to alveolar inflammation and releasing many profibrotic cytokines [66]. In the second study, I also investigated the role of monocytes in a broad ILD group and compared them with the IPF population. The value of monocytes was significantly higher in PF-ILD compared to NP-ILD (0.68 vs. 0.59 x 109/L p=0.0007). Furthermore, between IPF

and NP-ILD, a statistically significant difference was found for monocytes (0.67 vs. 0.59 x 109/L; p=0.008) and lymphocytes (2.25 vs. 1.78 x 109/L; p=0.0002). Instead, no significant difference was found regarding monocytes between IPF and PF-ILD (p=0.22). As mentioned, the literature confirms that in IPF, the founding of elevated monocyte count (> 0,60 x 109/L) is associated with increased risks of progression, hospitalization, and mortality over one year.

Concerning disease survival, another aim was to compare survival between IPF patients, PF-ILD, and NP-ILD. Is IPF the worst disease ever? Our data show a statistically significant difference (p<0.0001) to answer this question. Indeed, patients diagnosed with IPF have the lowest survival, followed by those with PF-ILDs, while NP-ILDs are the group with the best probability of survival. Despite the recent advantages in disease management and drug treatment, the prognosis of IPF remains poor.
Moreover, my study shows that in the multivariate analysis, FVC (%) at the diagnosis (p=0.002), complete blood count at the time of the diagnosis with monocyte level of >0.6 x 109/L (p=0.036), and the presence of reticulations at the first HRCT (p=0.04) were independent factors of disease progression in the ILD population. This could be an essential point since the literature reports that the monocyte count is an independent predictor of IPF progression during the first year of antifibrotic treatment [66]. Our results confirm that patients with IPF have the worst survival compared to the whole population. However, focusing on patients diagnosed with PF-ILD, the probability of survival at ten years is not suitable for suitability even though IPF is the prototype of progressive disease; patients diagnosed with PF-ILD have comparable outcomes with patients with IPF: progressive decline in lung function, worsening symptoms, end-stage fibrosis, and early mortality [67].

From our cohort of 48 patients with histological specimens available, histological findings emerged that the presence of micro honeycombing could be an independent factor of mortality for all causes (p=0.046). The presence of honeycombing is characteristic of idiopathic pulmonary fibrosis, the disease that serves as a prototype for all fibrosing interstitial diseases of the lung. As mentioned before, IPF is a disease that, by its nature, is progressive with an inauspicious prognosis. With the information available to us to date, we know that progressive fibrosing ILD has a similar course to IPF [68].

Beyond blood biomarkers, another argument of high interest is the role of sarcopenia in IPF and patients with ILDs [69]. Firstly, I try to study the primary respiratory muscle (diaphragm) with ultrasound (US); secondly, I try to deeply investigate spinal muscle in a well-characterized cohort of patients with IPF.
My study showed that the prevalence of diaphragmatic dysfunction was nearly 30% in ILD patients. Moreover, TF<30% was more prevalent in CTD-ILD than healthy subjects and correlated to patients' respiratory functional parameters, while not in IPF

patients. A TF value < 30% was related to moderate/severe dyspnea considering the overall ILD population (mMRC>2). Conversely, diaphragmatic displacement during quiet breathing was similar between IPF and controls.
This agrees with a previous study, which found similar results during quiet breathing in a smaller group of patients with IPF [70]. When the authors investigated diaphragmatic displacement during deep breathing, they observed decreased values in IPF patients compared with healthy controls. Unlike previous studies, we assessed the first-time diaphragm function in CTD-ILD, IPF patients and healthy subjects. Interestingly, we showed that CTD-ILD patients had lower DD and Ti than the IPF group; lower Ti and more diaphragmatic dysfunction (TF <30%), as opposed to controls. In the CTD-ILD group, a lower diaphragmatic displacement and thickening fraction probably reflect a "global" muscle dysfunction and deconditioning [71], less prevalent in IPF patients. Being a systemic condition, connective tissue disease could reduce muscle strength (diaphragm and expiratory muscles), limiting the overall respiratory function; on the contrary, IPF is a chronic disease limited to the lung, and muscle strength seems more preserved. Despite a higher diaphragm dysfunction, CTD-ILD patients had a better-preserved lung function in both lung volumes and diffusing capacity. CTD-ILD patients were younger, but previous studies suggested that age did not affect diaphragmatic function.

However, the diaphragm is not the only muscle that could be involved by ILD. In another retrospective analysis, we found a high prevalence of loss of muscle mass (LOM) at the time of the diagnosis in IPF patients (46%). Loss of muscle mass can cause a severe decline in quality of life and an increase in mortality. In line with the literature [72], we found that male IPF patients with loss of muscle mass presented a reduction in survival rate at two years (p=0.02), confirming that IPF patients with sarcopenia had a poor prognosis. The combination of physical exercise, pulmonary rehabilitation, nutritional supplements, and drug therapy may potentially counteract LOM in IPF patients, just at the time of diagnosis. In the end, with these two studies, I tried to underline the necessity to screen for muscle strength in patients with ILD. By establishing early evaluation methods and comprehensive treatment strategies, we can effectively delay the progression of LOM and diaphragmatic dysfunction in IPF and ILD patients and improve their quality.

Since the study of biomarkers is becoming of great interest in the field, we investigated, for the first time, the association between MUC5B rs35705950 genotype and radiological features, as assessed by HRCT, in a well-characterized IPF cohort, both at baseline and after antifibrotic treatment. Despite similar radiological scores between the two groups (TT/TG and GG group) at treatment initiation, we observed that, after treatment, the alveolar score was significantly increased in GG patients but not in the TT/TG group. In contrast, the HC score was significantly increased in both groups. Of interest, carriers of the GG genotype showed a heavier smoking history and a lower respiratory function at treatment initiation than TT/TG carriers. When

evaluating our study population as a whole, we observed that, at treatment start, on univariate analysis, IS and HC were significantly associated with mortality.
In contrast, AS, IS, and HC + IS were significantly associated with mortality after treatment. This latter, HC + IS, remained the independent predictor of mortality in multivariate analysis. In addition, carriers of the mutant rs35705950 T allele displayed better survival than non-carriers, regardless of the extension of HRCT changes at baseline, which was similar in the two groups.
Previous studies had demonstrated that a common variant (rs35705950) in the promoter region of the mucin 5b (MUC5B) gene was significantly associated with susceptibility to familial and sporadic IPF, suggesting a potential role for the distal airways and mucus overproduction in the pathogenesis of pulmonary fibrosis [73-74]. Specifically, it was reported that MUC5B rs35705950 T-carrier status was associated with increased expression of MUC5B glycoprotein in both distal airways and honeycomb cysts in IPF lungs [75-76] Interestingly, IPF patients carrying the minor T allele, either in homozygous or heterozygous form, appeared to have a better outcome, compared to IPF patients who did not carry the T allele, although the mechanisms underlying this association remain to be elucidated [77-78]. In line with previous reports, we confirmed the association between the rs35705950 T allele and more prolonged survival in patients with IPF. Importantly, we confirmed this finding over a more extended observation period (median time 52 months), compared to previous studies, and in patients on antifibrotic treatment.

During the last period of my Ph.D. course, I also moved into a basic science project for one year. I joined the lab of my service for one year, and I could learn new skills about cellular culture, flow cytometry, and extracellular vesicles. More specifically, during this period, I try to evaluate the potential inhibition of galectin-3 by hyaluronic acid. As mentioned before, Galectine-3 (Gal-3) is an essential member of the Galectin family; it is a carbohydrate-binding protein involved in many physiological functions, such as inflammation, immune responses, and cell migration, but also linked to diseases such as fibrosis, cancer, and heart and eye diseases [79-81]. On the other hand, hyaluronic acid has been implicated in treating many diseases, such as joint diseases, ocular diseases, and skin diseases [82-83]. We used a cellular vitro model composed of THP-1 monocytes and human-immortalized fibroblasts to test this hypothesis. As the first step, THP1 was posed in culture media and was differentiated into macrophages by PMA and then with LPS+INF-γ with and without the addition of HA to the media concentrations (3.0 mg/ml). The supernatant was analyzed by ELISA test for the quantification of Gal-3. IMR-90-HLF fibroblast cells were also used and stimulated as follows. The THP-1 macrophage Gal-3 production, after stimulation with PMA+LPS+INF-γ, increased significantly with statistical significance ($p<0.0001$). After the exposure to HA), the THP-1 macrophage Gal-3 production decreased significantly (HA 3.0 mg/ml: $p=<0.001$). With this experiment, we showed that macrophages can produce free Gal-3. We then stimulate fibroblast (IMR-90-HLF) with 40% macrophage supernatant. TGFb was significantly high after

stimulation (p=0.008), and HA showed decreased TGFb production (p=0.008). Fibroblasts were stimulated with commercial TGFb, and the level of COL-1 was evaluated. Again, HA reduced the production COL-1 with statistical evidence (p=0.001). Finally, after GAL-3 stimulation, HA has been demonstrated to minimize TGFb production in IMR-90-HLF fibroblast after 48 hours (p=0.01) and 72 hours (p=0.01).
In conclusion, for the first time, we have demonstrated that Hyaluronic Acid (HA) might have a role in preventing and treating fibrotic lung diseases, reducing the production of Gal-3, TGFb, and COL-I by stimulated fibroblasts. These preliminary results are novel and highlight the critical potential of Hyaluronic acid in preventing and treating fibrotic diseases. Moreover, we found that both monocyte and fibroblasts can produce high levels of galectin-3. In this complex mechanism, fibroblasts can auto-produce and auto stimulate themself to produce Gal-3, causing a "vicious circle."

In the meantime, with the pandemic burden, my research on Coronavirus disease 2019 (COVID-19) wanted to investigate potential clinical and hematological predictors of pulmonary sequela.
In link with the previous ILD project, I want to focus my research in hematological predictors, so I started to evaluate serological values' role in COVID-19 pneumonia. In this retrospective study, we obtained 327 patients, 214 classified as LIMC and 113 as HIMC. In the LIMC group, patients were younger and had lower cardiological and metabolic disorders than HIMC. Moreover, the LIMC group presented higher PaO2 and P/F. The two groups are similar regarding symptoms at admission, such as fever, asthenia, and cough; on the other hand, HIMC patients had a higher rate of dyspnea. Concerning blood values at admission, WBC count, neutrophils NLR, and CRP were more elevated in HIMC compared to LIMC. Contrariwise, the LIMC group had higher eosinophils and monocytes at admission.
Notably, many authors evaluated the role of NLR and eosinophils as prognostic biomarkers in patients with COVID-19. Yu-Qing Cai et al. reported that high levels of NLR, LDH, D-dimer, and CT scores were significantly correlated with COVID-19 severity [84]. Furthermore, in a study conducted by Jimeno S. et al., the authors report, in their multivariate logistic regression analysis, age, CRP at admission, and peak NLR were significantly associated with a higher risk of death [85]. In addition, in non-survivors, Yan et al. reported a lower number of lymphocytes and increased neutrophils with a consequent elevation of NLR. It is well established that neutrophils are mainly involved in the innate immune response, and lymphocytes are part of adaptative immunity. Hence, an alteration of the NLR is the reflection or an imbalance in the inflammatory response that occurs in COVID-19 patients and other infectious diseases. Authors argued that high NLR at admission could strongly predict in-hospital mortality in patients with COVID-19 infection [86].
In our analysis, NLR at admission was higher in patients with HIMC. As concerns blood tests at discharge, a recovery of neutrophil count and eosinophil count have

been found in both groups. However, we noticed an unexpected eosinophils rising in the HIMC group compared to the LIMC group. For that reason, we calculated the Δ eosinophils with the same method used by Chen et al. (Δ eosinophils= eosinophils at discharge minus eosinophils on admission) [87] to find out if this index may be used as a predictor for not-recovery a the first follow-up visit (3 months). In HIMC patients, the median Δ eosinophils from admission to discharge was 0.1 (-0.03 – 0.72), whereas patients with LIMC had 0.04 (-0.15 – 0.3) ($p<0.0001$). Fraiss`e et al. reported in their study an unexpected eosinophilia in critically ill patients; that finding was a late-onset event in the course of ICU stay, and this could positively impact survival. However, this is difficult to interpret, because patients developing eosinophilia were exposed to a survival bias. Our results support this hypothesis. Fraiss`e et al. also speculated that SARS-CoV-2 was directly or indirectly responsible for eosinophilia, as a consequence of infection or recovery [88]. However, we evaluate only alive patients and not dead patients. Surprisingly, our findings also suggest an increased risk of pulmonary sequelae in terms of fibrotic residuals in patients with a higher increase of eosinophil count compared to a normal eosinophil rise, regardless of the level of medical care. In our univariate and multivariate analysis, more elevated eosinophils rise during hospitalization and older age are two independent risk factors of pulmonary sequelae at the first follow-up CT scan [1.75 (1.05 – 2.94); p=0.03 and 1.75 (1.05 – 2.9); p=0.03]. This is in line with Yang Zhen Lu et al. since they reported higher levels of eosinophil count in COVID-19 patients with evidence of fibrotic change. Moreover, high total scores on peak CT, eosinophil count, ESR, and advancing age were related to fibrotic change in CT at the early recovery stage in patients with COVID-19 [89].
Furthermore, Toraldo and coworkers reported the same in their study conducted in 75 patients with COVID-19. Eosinophil count, IL-6, and GPT showed a significant association with radiological sequelae at month 3 [90]. Several other studies suggest eosinophils' role in releasing pro-fibrotic cytokines. In particular, IL-5 can promote fibrosis in the lung by recruiting eosinophils that produce TGF-β1, PDGF, and IL-13 [91]. It is also known that persistent low eosinophil count might be an ominous sign of severe disease and a higher risk of death. Maybe our HIMC patients have increased the eosinophils count, which is positive because they survive. On the other hand, an extra-rising can induce an over-protective repair, consisting of more radiological sequelae.

Because radiological lung sequela after COVID-19 pneumonia was greatly feared at the beginning of the pandemic [92], we tried to investigate and quantify lung damage after hospital discharge in collaboration with our radiologist.

This second study involved 220 patients, and we demonstrated that only a significant minority of patients hospitalized for COVID-19 pneumonia have persistent radiological abnormalities at follow-up. Patients who did not recover are mainly older men, with a more severe gas exchange impairment at hospital admission and a more

severe clinical course during hospitalization. Interestingly, the presence of reticulation and consolidation at admission predicted persistent interstitial changes at follow-up. To date, different studies have reported on the follow-up of patients hospitalized for COVID-19 pneumonia [94-95]. Other approaches based on disease severity have been proposed to standardize patients' follow-up. Specifically, the British Thoracic Society guidelines for managing post-COVID-19 syndrome distinguished patients with severe pneumonia requiring intensive care from patients with mild-to-moderate pneumonia treated in a medical ward or at home [96]. However, it is becoming increasingly clear that radiological changes following COVID-19 pneumonia do not resolve completely in a significant minority of patients. From the Wuhan cohort, Han and colleagues investigated 114 patients with severe pneumonia according to the WHO criteria [97] and observed fibrotic changes in one-third at the 6-month follow-up. Of note, multivariate analysis found that a higher baseline/initial CT lung involvement score (>18 in a score of 25) was independently associated with fibrotic-like changes in the lung. Huang and colleagues conducted a cohort study that included 353 patients who were enrolled between January and May 2020 who underwent HRCT at follow-up after discharge. They found more than 50% of the patients had residual lung abnormalities. In our hospital, the first patients with COVID-19 pneumonia were admitted in February 2020 and were evaluated in the post-COVID clinic in June 2020. We enrolled prospective patients diagnosed with COVID-19 pneumonia according to the WHO criteria. We found that as many as 20% of our patient population had radiological pulmonary sequelae at follow-up. This percentage is lower than that observed in previous studies [98]. Still, our patients' population has been followed up for a more extended period, thus allowing nonfibrotic pulmonary abnormalities to clear. Patients who did not recover (NOT-REC) were older, mostly men, and had worse disease impairment at admission and during hospitalization than patients without radiological sequelae at follow-up. Furthermore, we have shown that, in NOT-REC patients, the HRCT performed at hospital admission is more likely to display ground-glass opacities, consolidations, and reticulation. These data suggest that the risk of pulmonary sequelae may be related to the severity of the acute illness and the intensity of care needed. However, mechanical ventilation, ventilator-induced lung injury, and high-flow oxygen therapy might also have contributed to the development of fibrotic-like changes. However, it remains uncertain whether the fibrotic-like changes we observed represent irreversible pulmonary fibrosis and further monitoring is warranted to answer this question.

In the third study, we tried to extend the duration of the follow-up, and we wanted to investigate the percentage of pulmonary sequela after 12 months of follow-up. Three hundred forty-seven patients were evaluated, and only 24 (6.9%) subjects presented radiological changes on CT scans after a 1-year follow-up (NOT-REC group). In line with a previous study [99], these patients were older than those who REC (67 years vs. 63 years; $p = 0.02$); adults older than 63 years showed nearly three times the risk

of developing abnormalities on CT scan at 12 months, as shown by univariable analysis. Furthermore, NOT-REC patients had a worse clinical course, compared to patients who REC, during the hospital stay. The median maximum FiO2 required was two-fold higher, and the PaO2/FiO2 ratio was lower in NOT-REC patients. Even if a strong correlation resulted between the severity of the acute illness and the persistence of lung changes, none of the indicators received further confirmation as independent predictors in multivariable analysis. This is in line with previous studies. Indeed, it has been reported that patients who presented a more severe acute COVID-19 pneumonia, as indicated by ventilatory support, gas exchange index, and duration of hospital stay, are the same who present radiologic involvement during follow-up visits (at 4, 6, or 12 months) [100-101]. Similar results were displayed by Faverio et al. [102], who observed a cohort of 287 patients at 12-month follow-up from hospitalization. The authors showed that fibrotic sequelae at HRCT scans were found in a strict minority of patients (3, 1% of the study cohort). In comparison, the so-called "mild non-fibrotic radiological abnormalities" were observed in the majority of cases (66% of the entire cohort) with interstitial lung involvement, particularly GGO and reticular abnormalities, as subpleural curvilinear lines, as the main radiologic pattern. Besides, as in our cohort, the anatomical extension of these abnormalities was limited, with a mean lobar involvement that ranges between 13 and 17% of each single lobe. Overall, in our study, the lung involvement at 12 months was minimal since the median involvement reached 4% for IT and 3.5% for GGO (with the maximum lung involvement of 21 and 22% in one patient, regarding IT and GGO, respectively). Indeed, it remains to be elucidated if the infection strictly causes fibrotic lesions or if the contribution of mechanical ventilation to lung injury should be considered. Interestingly enough, both the univariable and multivariable analyses confirmed that being an active smoker, at the time of infection, represents an independent predictor for long-term pulmonary sequelae with a five times greater risk regardless of the severity of COVID-19 pneumonia. As very recently summarized by Benowitz et al. [103], smokers have a greater risk of developing severe disease following SARS-CoV-2 infection than nonsmokers, and the main mechanisms underlying this association might include up-regulation of angiotensin-converting enzyme-2 receptors, immune suppression, oxidative stress, inflammation, and vascular injury. As the pandemic has evolved, important research questions have emerged, particularly regarding the so-called post-COVID-19 or long COVID-19 and how tobacco product use might affect these long-term sequelae. Within this topic, our finding seems to point out, for the first time, the potential association between cigarette exposure and the persistence of fibrotic-like lung changes following SARS-CoV-2 infection. Interestingly, as previously shown in patients with Idiopathic Pulmonary Fibrosis, cigarette smoking exposure has been shown to impair adaptive humoral and cellular responses and exaggerate proinflammatory and innate immune responses, limiting the physiological tissue damage/repair responses after viral infection [104-105]. Moreover, recently, using a murine model in which animals were exposed to cigarette smoking and subsequently infected with the H1N1 influenza

virus, the authors have found an exaggerated fibroblastic response with the proliferation of lung fibroblasts providing new insights into the role of smoking in the dysregulation of healing and fibroblastic processes after a respiratory viral infection [106]. Thus, we can speculate that active smokers, infected with SARS-CoV-2, could have an increased likelihood of developing a lung fibroblastic response and unsuccessful lung repair. When considering hospital treatment strategy, we found that the category of antibiotics resulted in a risk factor for the persistence of lung damage long term even though at univariate analysis, and we can speculate that the NOT-REC group included severe patients, which needed a wider approach to managing acute COVID-19 pneumonia. For the same reason, during hospitalization, the NOT-REC group received, more frequently than the REC-group, corticosteroids, which may characterize the management of critically ill patients during the acute phase. On the other hand, the use of corticosteroids after hospitalization, in our cohort, is not a confounder since the percentage of administration in the two groups was similar. Furthermore, lung function tests were normal, in particular lung volume. Steinbeis demonstrated that, at 12 months, the degree of pulmonary function impairment still correlates with severity during the acute phase, but it improves over time [107]. However, in our study, the total lung capacity (TLC) and diffusion of lung carbon monoxide (DLCO) were not routinely assessed. DLCO permits the early detection of interstitial lung involvement but is not considered a reliable parameter for monitoring patients with pulmonary fibrosis. Indeed DLCO scores were not used as the primary endpoint in clinical studies of new medications for idiopathic pulmonary fibrosis (IPF) [108- 109]

In conclusion, during my Ph.D. years, I, along with my peers, have been able to investigate important predictors and novel biomarkers that contribute to ILD pathogenesis and progression. The study of peripheral monocytes in IPF, and monocytes in ILDs, has triggered our research on basic science models, to find new possible target therapies and molecules. Moreover, we learned how to combine innovative technologies such as diaphragm ultrasound, muscle mass density, and radiomic measures in these complex diseases. Our results will provide the basis for future research to better understand the pathogenesis of interstitial lung diseases. In COVID-19, we started to investigate the links between eosinophils and other blood tests to pulmonary sequela, and we tried to estimate the prevalence of lung scarring after a long period follow-up.

BIBLIOGRAPHY

1) Kaul B, Cottin V, Collard HR, Valenzuela C. Variability in Global Prevalence of Interstitial Lung Disease. Front Med. 2021;8:751181.
2) Olson A, Hartmann N, Patnaik P, Wallace L, Schlenker-Herceg R, Nasser M, et al. Estimation of the Prevalence of Progressive Fibrosing Interstitial Lung Diseases: Systematic Literature Review and Data from a Physician Survey. Adv Ther. 2021;38(2):854–67.
3) Approach to the adult with interstitial lung disease: Clinical evaluation - UpToDate [Internet]. [citato 18 marzo 2023]. Disponibile su: https://www.uptodate.com/contents/approach-to-the-adult-with-interstitial-lung-disease-clinical-evaluation/print?search=ILD%20classification&source=search_result&selectedTitle=1~150&usage_type=default&display_rank=1
4) George PM, Spagnolo P, Kreuter M, Altinisik G, Bonifazi M, Martinez FJ, et al. Progressive fibrosing interstitial lung disease: clinical uncertainties, consensus recommendations, and research priorities. Lancet Respir Med. 1 settembre 2020;8(9):925–34.
5) Cottin V, Hirani NA, Hotchkin DL, Nambiar AM, Ogura T, Otaola M, et al. Presentation, diagnosis and clinical course of the spectrum of progressive-fibrosing interstitial lung diseases. Eur Respir Rev [Internet]. 31 dicembre 2018 [citato 16 marzo 2023];27(150). Disponibile su: https://err.ersjournals.com/content/27/150/180076
6) Valenzuela C, Cottin V. Epidemiology and real-life experience in progressive pulmonary fibrosis. Curr Opin Pulm Med. 1 settembre 2022;28(5):407–13.
7) Kishaba T. Current perspective of progressive-fibrosing interstitial lung disease. Respir Investig. 1 luglio 2022;60(4):503–9.
8) Griese M. Etiologic Classification of Diffuse Parenchymal (Interstitial) Lung Diseases. J Clin Med. 21 marzo 2022;11(6):1747.
9) Galvin JR, Frazier AA, Franks TJ. Collaborative radiologic and histopathologic assessment of fibrotic lung disease. Radiology. giugno 2010;255(3):692–706.
10) Camus P, Fanton A, Bonniaud P, Camus C, Foucher P. Interstitial Lung Dis-ease Induced by Drugs and Radiation. Respiration. 2004;71(4):301–26.
11) Hanania AN, Mainwaring W, Ghebre YT, Hanania NA, Ludwig M. Radiation-Induced Lung Injury. Chest. luglio 2019;156(1):150–62.
12) American Thoracic Society; European Respiratory Society. American Thoracic Society/European Respiratory Society International Multidisciplinary Consensus Classification of the Idiopathic Interstitial Pneumonias. This joint

statement of the American Thoracic Society (ATS) and the European Respiratory Society (ERS) was adopted by the ATS board of directors in June 2001 and by the ERS Executive Committee in June 2001. Am J Respir Crit Care Med. 2002 Jan 15;165(2):277-304.

13) Travis WD, Costabel U, Hansell DM, King TE Jr, Lynch DA, Nicholson AG, Ryerson CJ, Ryu JH, Selman M, Wells AU, Behr J, Bouros D, Brown KK, Colby TV, Collard HR, Cordeiro CR, Cottin V, Crestani B, Drent M, Dudden RF, Egan J, Flaherty K, Hogaboam C, Inoue Y, Johkoh T, Kim DS, Kitaichi M, Loyd J, Martinez FJ, Myers J, Protzko S, Raghu G, Richeldi L, Sverzellati N, Swigris J, Valeyre D; ATS/ERS Committee on Idiopathic Interstitial Pneumonias. An official American Thoracic Society/European Respiratory Society statement: Update the international multidisciplinary classification of the idiopathic interstitial pneumonias. Am J Respir Crit Care Med. 2013 Sep 15;188(6):733-48.

14) Churg A. Hypersensitivity pneumonitis: new concepts and classifications. Mod Pathol. 2022 Jan;35(Suppl 1):15-27. doi: 10.1038/s41379-021-00866-y

15) Costabel U, Miyazaki Y, Pardo A, Koschel D, Bonella F, Spagnolo P, et al. Hypersensitivity pneumonitis. Nat Rev Dis Primer. 6 agosto 2020;6(1):65.

16) Cottin V, Castillo D, Poletti V, Kreuter M, Corte TJ, Spagnolo P. Should Patients With Interstitial Lung Disease Be Seen by Experts? Chest. 1 settem-bre 2018;154(3):713–4.

17) De Sadeleer LJ, Meert C, Yserbyt J, Slabbynck H, Verschakelen JA, Verbeken EK, et al. Diagnostic Ability of a Dynamic Multidisciplinary Discussion in Interstitial Lung Diseases: A Retrospective Observational Study of 938 Cases. Chest. 1 giugno 2018;153(6):1416–23.

18) Cosgrove GP, Bianchi P, Danese S, Lederer DJ. Barriers to timely diagnosis of interstitial lung disease in the real world: the INTENSITY survey. BMC Pulm Med. 17 gennaio 2018;18(1):9.

19) Jameson J Larry, Kasper DL, Longo DL, Fauci A, Hauser S, Localzo J. Harrison Principles of Internal Medicine. 20ª ed.

20) Zibrak JD, Price D. Interstitial lung disease: raising the index of suspicion in primary care. NPJ Prim Care Respir Med. 2014 Sep 11;24:14054.

21) Meyer KC. Diagnosis and management of interstitial lung disease. Transl Respir Med. 2014 Feb 13;2:4.

22) Sunjaya A, Poulos L, Reddel H, Jenkins C. Qualitative validation of the modified Medical Research Council (mMRC) dyspnoea scale as a patient-reported measure of breathlessness severity. Respir Med [Internet]. 1 no-vembre 2022 [citato 31 marzo 2023];203. Disponibile su: https://www.resmedjournal.com/article/S0954-6111(22)00249-9/fulltext

23) Krüger K, Holzinger F, Trauth J, Koch M, Heintze C, Gehrke-Beck S. Chronic Cough. Dtsch Ärztebl Int. febbraio 2022;119(5):59–65.

24) Madison JM, Irwin RS. Chronic cough in adults with interstitial lung disease. Curr Opin Pulm Med. settembre 2005;11(5):412–6.

25) Kahlmann V, Moor CC, Wijsenbeek MS. Managing Fatigue in Patients With Interstitial Lung Disease. Chest. 2020 Nov;158(5):2026-2033.
26) Spagnolo P, Ryerson CJ, Putman R, Oldham J, Salisbury M, Sverzellati N, et al. Early diagnosis of fibrotic interstitial lung disease: challenges and opportunities. Lancet Respir Med. settembre 2021;9(9):1065–76.
27) Maher TM, Bendstrup E, Dron L, Langley J, Smith G, Khalid JM, et al. Global incidence and prevalence of idiopathic pulmonary fibrosis. Respir Res. 7 luglio 2021;22(1):197.
28) Kropski JA. Familial Interstitial Lung Disease. Semin Respir Crit Care Med. 2020 Apr;41(2):229-237.
29) Caminati A, Harari S. Smoking-related interstitial pneumonias and pulmonary Langerhans cell histiocytosis. Proc Am Thorac Soc. giugno 2006;3(4):299–306.
30) Steele MP, Speer MC, Loyd JE, Brown KK, Herron A, Slifer SH, et al. Clinical and pathologic features of familial interstitial pneumonia. Am J Respir Crit Care Med. 1 novembre 2005;172(9):1146–52.
31) MANFREDI A, CASSONE G, VACCHI C, PANCALDI F, Della CASA G, CERRI S, et al. Usefulness of digital velcro crackles detection in identification of interstitial lung disease in patients with connective tissue diseases. Arch Rheumatol. 25 giugno 2020;36(1):19–25.
32) Deconinck B, Verschakelen J, Coolen J, Verbeken E, Verleden G, Wuyts W. Diagnostic Workup for Diffuse Parenchymal Lung Disease: Schematic Flowchart, Literature Review, and Pitfalls. Lung. 1 febbraio 2013;191(1):19–25.
33) Shumar JN, Chandel A, King CS. Antifibrotic Therapies and Progressive Fi-brosing Interstitial Lung Disease (PF-ILD): Building on INBUILD. J Clin Med. gennaio 2021;10(11):2285.
34) Hambly N, Farooqi MM, Dvorkin-Gheva A, Donohoe K, Garlick K, Scallan C, et al. Prevalence and characteristics of progressive fibrosing interstitial lung disease in a prospective registry. Eur Respir J. ottobre 2022;60(4):2102571.
35) Selman M, Pardo A. When things go wrong: exploring possible mechanisms driving the progressive fibrosis phenotype in interstitial lung diseases. Eur Respir J [Internet]. 1 settembre 2021 [citato 1 aprile 2023];58(3). Disponi-bile su: https://erj.ersjournals.com/content/58/3/2004507Myers KA, Farquhar DR. The rational clinical examination. Does this patient have clubbing? JAMA. 18 luglio 2001;286(3):341–7.
36) Raghu G, Remy-Jardin M, Richeldi L, Thomson CC, Inoue Y, Johkoh T, et al. Idiopathic Pulmonary Fibrosis (an Update) and Progressive Pulmonary Fibrosis in Adults: An Official ATS/ERS/JRS/ALAT Clinical Practice Guideline. Am J Respir Crit Care Med. 205(9):e18–47. Herrick AL, Wigley FM. Raynaud's phenomenon. Best Pract Res Clin Rheu-matol. febbraio 2020;34(1):101474.
37) Komatsu M, Yamamoto H, Kitaguchi Y, Kawakami S, Matsushita M, Uehara T, et al. Clinical characteristics of non-idiopathic pulmonary fibrosis,

progressive fibrosing interstitial lung diseases: A single-center retrospective study. Medicine (Baltimore). 2 aprile 2021;100(13):e25322.
38) Wells AU, Hirani N. Interstitial lung disease guideline. Thorax. 1 settembre 2008;63(Suppl 5):v1–58.
39) Flaherty KR, Wells AU, Cottin V, Devaraj A, Walsh SLF, Inoue Y, Richeldi L, Kolb M, Tetzlaff K, Stowasser S, Coeck C, Clerisme-Beaty E, Rosenstock B, Quaresma M, Haeufel T, Goeldner RG, Schlenker-Herceg R, Brown KK; INBUILD Trial Investigators. Nintedanib in Progressive Fibrosing Interstitial Lung Diseases. N Engl J Med. 2019 Oct 31;381(18):1718-1727.
40) Shao G, Hawle P, Akbari K, Horner A, Hintenberger R, Kaiser B, et al. Clinical, imaging, and blood biomarkers to assess 1-year progression risk in fibrotic interstitial lung diseases—Development and validation of the honeycombing, traction bronchiectasis, and monocyte (HTM)-score. Front Med [Internet]. 2022 [citato 15 marzo 2023];9. Disponibile su: https://www.frontiersin.org/articles/10.3389/fmed.2022.1043720
41) Chikhoune L, Brousseau T, Morell-Dubois S, Farhat MM, Maillard H, Ledoult E, et al. Association between Routine Laboratory Parameters and the Severity and Progression of Systemic Sclerosis. J Clin Med. 30 agosto 2022;11(17):5087.
42) Raghu G, Collard HR, Egan JJ, et al. An Official ATS/ERS/JRS/ALAT Statement: Idiopathic pulmonary fibrosis: Evidence-based guidelines for diagnosis and management. Am J Respir Crit Care Med 2011;183(6):788–824.
43) Lynch DA, Sverzellati N, Travis WD, et al. Diagnostic criteria for idiopathic pulmonary fibrosis: a Fleischner Society White Paper. Lancet Respir Med. 2018 Feb;6(2):138-153.
44) Raghu G, Chen SY, Hou Q, Yeh WS, Collard HR. Incidence and prevalence of idiopathic pulmonary fibrosis in US adults 18-64 years old. Eur Respir J. 2016 Jul;48(1):179-86.
45) Sack C, Raghu G. Idiopathic pulmonary fibrosis: unmasking cryptogenic environmental factors. Eur Respir J. 2019 Feb 21;53(2):1801699.
46) Spagnolo P, Molyneaux PL, Bernardinello N, Cocconcelli E, Biondini D, Fracasso F, Tiné M, Saetta M, Maher TM, Balestro E. The Role of the Lung's Microbiome in the Pathogenesis and Progression of Idiopathic Pulmonary Fibrosis. Int J Mol Sci. 2019 Nov 10;20(22):5618.
47) Raghu G, Meyer KC. Silent gastroesophageal reflux and microaspiration in IPF: mounting evidence for anti-reflux therapy? Eur Respir J. 2012 Feb;39(2):242-5.
48) Seibold MA, Wise AL, Speer MC, et al. A common MUC5B promoter polymorphism and pulmonary fibrosis. N Engl J Med. 2011;364(16):1503–1512. doi:10.1056/NEJMoa1013660
49) Balestro E, Castelli G, Bernardinello N, Cocconcelli E, Biondini D, Fracasso F, Rea F, Saetta M, Baraldo S, Spagnolo P. CA 19-9 serum levels in patients with end-stage idiopathic pulmonary fibrosis (IPF) and other interstitial

lung diseases (ILDs): Correlation with functional decline. Chron Respir Dis. 2020 Jan-Dec;17:1479973120958428.
50) Faccioli E, Terzi S, Giraudo C, Zuin A, Modugno A, Labella F, Zambello G, Lorenzoni G, Schiavon M, Gregori D, Pasello G, Calabrese F, Dell'Amore A, Rea F. Sarcopenia as a Predictor of Short- and Long-Term Outcomes in Patients Surgically Treated for Malignant Pleural Mesothelioma. Cancers (Basel). 2022 Jul 29;14(15):3699.
51) Moon SW, Choi JS, Lee SH, Jung KS, Jung JY, Kang YA, Park MS, Kim YS, Chang J, Kim SY. Thoracic skeletal muscle quantification: low muscle mass is related with worse prognosis in idiopathic pulmonary fibrosis patients. Respir Res. 2019 Feb 15;20(1):35.
52) P.R. Tuinman, A.H. Jonkman, M. Dres, Z.H. Shi, E.C. Goligher, A. Goffi, C. de Korte, A. Demoule, L. Heunks, Respiratory muscle ultrasonography: methodology, basic and advanced principles and clinical applications in ICU and ED patients-a narrative review, Intensive Care Med. 46 (4) (2020 Apr) 594–605, https://doi.org/10.1007/s00134-019-05892-8.
53) S.S. Bolz, G.D. Rubenfeld, B.P. Kavanagh, N.D. Ferguson, Measuring diaphragm thickness with ultrasound in mechanically ventilated patients: feasibility, reproducibility, and validity, Intensive Care Med. 41 (4) (2015 Apr) 642–649, https://doi.org/10.1007/s00134-015-3687-3. Epub 2015 Feb 19. Erratum in: Intensive Care Med. 2015 Apr;41(4):734. Sebastien-Bolz, Steffen [corrected to Bolz, Steffen-Sebastien]
54) Biondini D, Cocconcelli E, Bernardinello N, Lorenzoni G, Rigobello C, Lococo S, Castelli G, Baraldo S, Cosio MG, Gregori D, Saetta M, Balestro E, Spagnolo P. Prognostic role of MUC5B rs35705950 genotype in patients with idiopathic pulmonary fibrosis (IPF) on antifibrotic treatment. Respir Res. 2021 Apr 1;22(1):98.
55) Balestro E, Cocconcelli E, Giraudo C, Polverosi R, Biondini D, Lacedonia D, Bazzan E, Mazzai L, Rizzon G, Lococo S, Turato G, Tinè M, Cosio MG, Saetta M, Spagnolo P. High-Resolution CT Change over Time in Patients with Idiopathic Pulmonary Fibrosis on Antifibrotic Treatment. J Clin Med. 2019 Sep 15;8(9):1469. doi: 10.3390/jcm8091469.
56) Baxter EW, Graham AE, Re NA, Carr IM, Robinson JI, Mackie SL, Morgan AW. Standardized protocols for differentiation of THP-1 cells to macrophages with distinct M(IFNγ+LPS), M(IL-4) and M(IL-10) phenotypes. J Immunol Methods. 2020 Mar;478:112721.
57) Cocconcelli E, Bernardinello N, Giraudo C, Castelli G, Giorgino A, Leoni D, Petrarulo S, Ferrari A, Saetta M, Cattelan A, Spagnolo P, Balestro E. Characteristics and Prognostic Factors of Pulmonary Fibrosis After COVID-19 Pneumonia. Front Med (Lausanne). 2022 Jan 31;8:823600.
58) WHO. Clinical Management of Severe Acute Respiratory Infection When Novel Coronavirus (nCoV) Infection is Suspected: Interim Guidance. (2020). Available online at: https://www.who.int/docs/default-

source/coronaviruse/clinical-management-of-novel-cov.pdf (accessed March 13, 2020).
59) Kreuter M, Bradley SJ, Lee JS, et al. Monocyte count as a prognostic biomarker in patients with idiopathic pulmonary fibrosis. Am. J. Respir. Crit. Care Med.. Published online January 12, 2021. doi:10.1164/rccm.202003-0669oc.
60) K. Kawamura, K. Ichikado, K. Anan, et al., Monocyte count and the risk for acute exacerbation of fibrosing interstitial lung disease: a retrospective cohort study, Chron. Respir. Dis. 17 (2020), https://doi.org/10.1177/1479973120909840.
61) M.K.D. Scott, K. Quinn, Q. Li, et al., Increased monocyte count as a cellular biomarker for poor outcomes in fibrotic diseases: a retrospective, multicentre cohort study, Lancet Respir. Med. 7 (6) (2019) 497–508, https://doi.org/10.1016/S2213-2600(18)30508-3.
62) D. Tan, Y. Fu, W. Tong, F. Li, Prognostic significance of lymphocyte to monocyte ratio in colorectal cancer: a meta-analysis, Int. J. Surg. 55 (2018) 128–138, https:// doi.org/10.1016/j.ijsu.2018.05.030. Jul.
63) R.J. Hu, J.Y. Ma, G. Hu, Lymphocyte-to-monocyte ratio in pancreatic cancer: prognostic significance and meta-analysis, Clin. Chim. Acta 481 (2018) 142–146, https://doi.org/10.1016/j.cca.2018.03.008. Jun.
64) T. Tham, C. Olson, J. Khaymovich, S.W. Herman, P.D. Costantino, The lymphocyteto- monocyte ratio as a prognostic indicator in head and neck cancer: a systematic review and meta-analysis, Eur. Arch. Oto-Rhino-Laryngol. 275 (7) (2018) 1663–1670, https://doi.org/10.1007/s00405-018-4972-x. Jul.
65) W. Li, G. Ma, Q. Wu, Y. Deng, Y. Liu, J. Wang, Prognostic value of lymphocyte-tomonocyte ratio among Asian lung cancer patients: a systematic review and metaanalysis, Oncotarget 8 (66) (2017) 110606–110613, https://doi.org/10.18632/ oncotarget.20574. Aug 28.
66) T.A. Wynn, K.M. Vannella, Macrophages in tissue repair, regeneration, and fibrosis, Immunity 44 (3) (2016) 450–462, https://doi.org/10.1016/j.immuni.2016.02.015.
67) Martinez FJ, Collard HR, Pardo A, Raghu G, Richeldi L, Selman M, et al. Idiopathic pulmonary fibrosis. Nat Rev Dis Primer. 20 ottobre 2017;3(1):1–19.
68) Chen X, Guo J, Yu D, Jie B, Zhou Y. Predictors of Mortality in Progressive Fibrosing Interstitial Lung Diseases. Front Pharmacol. 2021 Oct 12;12:754851. doi: 10.3389/fphar.2021.754851. PMID: 34712141; PMCID: PMC8546258.
69) Durdu H, Yurdalan SU, Ozmen I. Clinical significance of pectoralis muscle strength in elderly patients with idiopathic pulmonary fibrosis. Sarcoidosis Vasc Diffuse Lung Dis. 2022;39(1):e2022009.
70) Boccatonda, V. Decorato, G. Cocco, S. Marinari, C. Schiavone, Ultrasound evaluation of diaphragmatic mobility in patients with idiopathic lung fibrosis: a pilot study, Multidiscip Respir Med 14 (2018 Dec 14) 1, https://doi.org/10.1186/s40248-018-0159-y. PMID: 30651988; PMCID: PMC6330497.

71) A.J. Boon, C.J. Harper, L.S. Ghahfarokhi, J.A. Strommen, J.C. Watson, E. J. Sorenson, Two-dimensional ultrasound imaging of the diaphragm: quantitative values in normal subjects, Muscle Nerve 47 (2013) 884–889.
72) Moon SW, Choi JS, Lee SH, Jung KS, Jung JY, Kang YA, Park MS, Kim YS, Chang J, Kim SY. Thoracic skeletal muscle quantification: low muscle mass is related with worse prognosis in idiopathic pulmonary fibrosis patients. Respir Res. 2019 Feb 15;20(1):35.
73) Noth, I.; Zhang, Y.; Ma, S.-F.; Flores, C.; Barber, M.; Huang, Y.; Broderick, S.M.; Wade, M.S.; Hysi, P.; Scuirba, J.; et al. Genetic variants associated with idiopathic pulmonary fibrosis susceptibility and mortality: A genome-wide association study. Lancet Respir. Med. 2013, 1, 309–317.
74) Peljto, A.L.; Selman, M.; Kim, D.S.; Murphy, E.; Tucker, L.; Pardo, A.; Lee, J.S.; Ji, W.; Schwarz, M.I.; Yang, I.V.; et al. The MUC5B Promoter Polymorphism Is Associated With Idiopathic Pulmonary Fibrosis in a Mexican Cohort but Is Rare Among Asian Ancestries. Chest 2015, 147, 460–464.
75) Stock, C.J.; Conti, C.; Montero-Fernandez, Á.; Caramori, G.; Molyneaux, P.L.; George, P.M.; Kokosi, M.; Kouranos, V.; Maher, T.M.; Chua, F.; et al. Interaction between the promoter MUC5B polymorphism and mucin expression: Is there a difference according to ILD subtype? Thorax 2020, 75, 901–903.
76) Okuda, K.; Chen, G.; Subramani, D.B.; Wolf, M.; Gilmore, R.C.; Kato, T.; Radicioni, G.; Kesimer, M.; Chua, M.; Dang, H.; et al. Localization of Secretory Mucins MUC5AC and MUC5B in Normal/Healthy Human Airways. Am. J. Respir. Crit. Care Med. 2019, 199, 715–727.
77) Peljto, A.L.; Zhang, Y.; Fingerlin, T.E.; Ma, S.-F.; Garcia, J.G.N.; Richards, T.J.; Silveira, L.J.; Lindell, K.O.; Steele, M.P.; Loyd, J.; et al. Association Between the MUC5B Promoter Polymorphism and Survival in Patients With Idiopathic Pulmonary Fibrosis. JAMA 2013, 309, 2232–2239.
78) Newton, C.A.; Zhang, D.; Oldham, J.M.; Kozlitina, J.; Ma, S.-F.; Martinez, F.J.; Raghu, G.; Noth, I.; Garcia, C.K. Telomere Length and Use of Immunosuppressive Medications in Idiopathic Pulmonary Fibrosis. Am. J. Respir. Crit. Care Med. 2019, 200, 336–347.
79) Dong R, Zhang M, Hu Q, Zheng S, Soh A, Zheng Y, Yuan H. Galectin-3 as a novel biomarker for disease diagnosis and a target for therapy (Review). Int J Mol Med. 2018 Feb;41(2):599-614.
80) Boutin L, Dépret F, Gayat E, Legrand M, Chadjichristos CE. Galectin-3 in Kidney Diseases: From an Old Protein to a New Therapeutic Target. Int J Mol Sci. 2022 Mar 14;23(6):3124.
81) Larsen L, Chen HY, Saegusa J, Liu FT. Galectin-3 and the skin. J Dermatol Sci. 2011 Nov;64(2):85-91.
82) Neuman MG, Nanau RM, Oruña-Sanchez L, Coto G. Hyaluronic acid and wound healing. J Pharm Pharm Sci. 2015;18(1):53-60. doi: 10.18433/j3k89d.

83) Aggarwal A, Sempowski IP. Hyaluronic acid injections for knee osteoarthritis. Systematic review of the literature. Can Fam Physician. 2004 Feb;50:249-56.
84) Achaiah A, Rathnapala A, Pereira A, Bothwell H, Dwivedi K, Barker R, Benamore R, Hoyles RK, Iotchkova V, Ho LP. Monocyte and neutrophil levels are potentially linked to progression to IPF for patients with indeterminate UIP CT pattern. BMJ Open Respir Res. 2021 Nov;8(1):e000899.
85) S. Jimeno, P. S. Ventura, J. M. Castellano, S. I. Garcıa-Adasme, M. Miranda, P. Touza, I. Lllana, and A. L´opez-Escobar. "Prognostic implications of neutrophil-lymphocyte ratio in COVID-19". In: European journal of clinical investigation 51.1 (2021), e13404.
86) X. Yan, F. Li, X. Wang, J. Yan, F. Zhu, S. Tang, Y. Deng, H. Wang, R, Chen, Z. Yu, et al. "Neutrophil to lymphocyte ratio as prognostic and predictive factor in patients with coronavirus disease 2019: a retrospective cross-sectional study". In: Journal of medical virology 92.11 (2020), pp. 2573–2581.
87) R. Chen, L. Sang, M. Jiang, Z. Yang, N. Jia, W. Fu, J. Xie, W. Guan, W. Liang, Z. Ni, et al. "Longitudinal hematologic and immunologic variations associated with the progression of COVID-19 patients in China". In: Journal of Allergy and Clinical Immunology 146.1 (2020), pp. 89–100.
88) M. Fraiss´e, E. Logre, H. Mentec, R. Cally, G. Plantef ̀eve, and D. Contou. "Eosinophilia in critically ill COVID-19 patients: a French monocenter retrospective study". In: Critical Care 24.1 (2020), pp. 1–4.
89) Z. L. Yang, C. Chen, L. Huang, S. C. Zhou, Y. N. Hu, L. M. Xia, and Y. Li. "Fibrotic changes depicted by thin-section CT in patients with COVID-19 at the early recovery stage: preliminary experience". In: Frontiers in Medicine 7 (2020), p. 605088.
90) D. M. Toraldo, F. Satriano, R. Rollo, G. Verdastro, G. Imbriani, E. Rizzo, A. Argentiero, A. Falco, P. Ambrosino, A. Miani, et al. "COVID-19 IgG/IgM patterns, early IL-6 elevation and long-term radiological sequelae in 75 patients hospitalized due to interstitial pneumonia followed up from 3 to 12 months". In: Plos one 17.2 (2022), e0262911.
91) Y. Du, L. Tu, P. Zhu, M. Mu, R. Wang, P. Yang, X. Wang, C. Hu, R. Ping, P. Hu, et al. "Clinical features of 85 fatal cases of COVID-19 from Wuhan. A retrospective observational study". In: American journal of respiratory and critical care medicine 201.11 (2020), pp. 1372–1379.
92) Spagnolo P, Balestro E, Aliberti S, Cocconcelli E, Biondini D, Casa GD, Sverzellati N, Maher TM. Pulmonary fibrosis secondary to COVID-19: a call to arms? Lancet Respir Med. 2020 Aug;8(8):750-752. doi: 10.1016/S2213-2600(20)30222-8.
93) Baratella E, Ruaro B, Marrocchio C, Starvaggi N, Salton F, Giudici F, et al. Interstitial lung disease at high resolution CT after SARS-CoV- 2-related acute respiratory distress syndrome according to pulmonary segmental anatomy. J Clin Med. (2021) 10:3985. doi: 10.3390/jcm101 73985

94) Korkmaz I, Kele¸s F. COVID-19-Related lung involvement at different time intervals: evaluation of computed tomography images with semiquantitative scoring system and COVID-19 reporting and data system scoring. Cureus. (2021) 13:e18554. doi: 10.7759/cureus. 18554
95) Das KM, Lee EY, Singh R, Enani MA, Al Dossari K, Van Gorkom K, et al. Follow-up chest radiographic findings in patients with MERS-CoV after recovery. Indian J Radiol Imaging. 27:342–9. doi: 10.4103/ijri.IJRI_ 469_
96) British Thoracic Society. Guidance on Respiratory Follow up of Patients With a Clinico Radiological Diagnosis of COVID-19 Pneumonia. (2021). Available online at: https://britthoracic.org.uk/about-us/covid-19-information-forthe-respiratory-community/(accessed May 7, 2021).
97) Han X, Fan Y, Alwalid O, Li N, Jia X, Yuan M, et al. Sixmonth Follow-up chest CT Findings after severe COVID-19 pneumonia. Radiology. (2021) 299:E177–86. doi: 10.1148/radiol.20212 03153
98) Huang C, Huang L, Wang Y, Li X, Ren L, Gu X, et al. 6-month consequences of COVID-19 in patients discharged from hospital: a cohort study. Lancet. (2021) 397:220–32. doi: 10.1016/S0140 6736(20)3 2656-8
99) Jutant E, Meyrignac O, Beurnier A, Jaïs X, Pham T, Morin L, et al. Respiratory symptoms and radiological findings in post-acute COVID-19 syndrome. ERJ Open Res. (2022) 8:00479–2021.
100) Watanabe A, So M, Iwagami M, Fukunaga K, Takagi H, Kabata H, et al. One-year follow-up CT findings in COVID-19 patients: a systematic review and meta-analysis. Respirology. (2022) 27:605–16. doi: 10.1111/resp.14311
101) Mylvaganam R, Bailey J, Sznajder J, Sala M. Recovering from a pandemic: pulmonary fibrosis after SARS-CoV-2 infection. Eur Respir Rev. (2021) 30:210194.
102) Faverio P, Luppi F, Rebora P, D'Andrea G, Stainer A, Busnelli S, et al. One-year pulmonary impairment after severe COVID-19: a prospective, multicenter follow-up study. Respir Res. (2022) 23:65. doi: 10.1186/s12931-022-01994-y
103) Benowitz N, Goniewicz M, Halpern-Felsher B, Krishnan-Sarin S, Ling P, O'Connor R, et al. Tobacco product use and the risks of SARS-CoV-2 infection and COVID-19: current understanding and recommendations for future research. Lancet Respir Med. (2022) 10:900–15. doi: 10.1016/S2213-2600(22)00182-5
104) Baumgartner K, Samet J, Stidley C, Colby T, Waldron J. Cigarette smoking: a risk factor for idiopathic pulmonary fibrosis. Am J Respir Crit Care Med. (1997) 155:242–8.
105) Antoniou K, Hansell D, Rubens M, Marten K, Desai S, Siafakas N, et al. Idiopathic pulmonary fibrosis: outcome in relation to smoking status. Am J Respir Crit Care Med. (2008) 177:190–4.
106) Lee S, Sharma L, Kang Y, Kim S, Chandrasekharan S, Losier A, et al. Impact of cigarette smoke exposure on the lung fibroblastic response after

influenza pneumonia. Am J Respir Cell Mol Biol. (2018) 59:770–81. doi: 10.1165/rcmb.2018-0004O
107) Steinbeis F, Thibeault C, Doellinger F, Ring R, Mittermaier M, Ruwwe-Glösenkamp C, et al. Severity of respiratory failure and computed chest tomography in acute COVID-19 correlates with pulmonary function and respiratory symptoms after infection with SARS-CoV-2: an observational longitudinal study over 12 months. Respir Med. (2022) 191:106709. doi: 10.1016/j.rmed.2021.10670
108) Nathana SD, Meyer KC. IPF clinical trial design and endpoints. Curr Opin Pulm Med. (2014) 20:463–71. 25. King T Jr, Bradford W, Castro-Bernardini S, Fagan E, Glaspole I, Glassberg M, et al. A phase 3 trial of pirfenidone in patients with idiopathic pulmonary fibrosis. N Engl J Med. (2014) 370:2083–92.
109) Richeldi L, du Bois R, Raghu G, Azuma A, Brown K, Costabel U, et al. Efficacy and safety of nintedanib in idiopathic pulmonary fibrosis. N Engl J Med. (2014) 370:2071–82. doi: 10.1056/NEJMoa1402589